



Faculty of Science and Technology

## BACHELOR'S THESIS

<b>Study program/ Specialization:</b>  Mechanical Engineering and Material Science	Spring Semester 2021  Open access
<b>Writer:</b> MAHMOOD AL-DAYEKH  SIMON BELAY  AKSEL SØRAUNET	<i>Mahmood AL-Dayekh</i>  <i>Simon Belay</i>  <div style="border: 1px solid black; padding: 2px; display: inline-block;"><i>Aksel Søraunet</i></div> Writer's Signature
<b>Faculty Supervisor:</b> Hirpa Gelgele Lemu  <b>External Supervisor:</b> Jakob Trydal	
<b>Thesis title:</b>  <b>Component Design and Study of The Internal Surface Quality of Additive Manufactured Parts for a Paint Robot</b>	
<b>Credits (ECTS):</b> 20	
<b>Key Words</b> <ul style="list-style-type: none"><li>• Gear Calculation</li><li>• Additive Manufacturing</li><li>• Surface Roughness</li></ul>	Pages            90 +enclosure    55 Stavanger May 14, 2021

# Abstract

This thesis is written in collaboration with ABB. The task revolves around improving the abilities for a paint robot. The paint robot consists of several mechanical parts. The focus is to improve the payload capacity by studying the hollow wrist and reducing wastage of paint that flows through the paint system.

The first part of the thesis contains theory and literature studies of possible improvement methods. The gear coupling, that has been identified as the weakest link, and production methods for the casing of the hollow wrist and the test block. The conclusion is based on material selection, quality, environmental impact and maturity of the production method. To minimize the risk for the paint to stick to the surface, there is a need for a post processing method. Further on in the thesis several methods to improve the surface have been evaluated and considered.

The conclusion for methods to improve the paint robot based on calculations, studies and experience. The knowledge obtained from the sources are combined and adjusted to improve the current robot and solve the difficulties it is facing. It is concluded that the Powder Bed Fusion production method is the best suited option in terms of its wide material selection, great strength and maturity of the method. The finished manufactured test block is relatively rough. Abrasive Flow Machining process is considered to be the optimal method for reducing the roughness due to the geometry of the test block. The Abrasive Flow Machining process corrodes the surface and reaches the desired surface roughness. To obtain the desired payload capacity without failure in the gear coupling an expansion of the gear and substituting the material is advised. By changing the gear geometry from spur gear to helical gears results in an improvement of the bearing capacity with 16,4 %. To reach the specified goal there is a need to expand the current size of the coupling.

Mahmood AL-Dayekh

14.05.21

Simon Belag

14.05.21

Aksel Soraunet

14.05.21

# Acknowledgment

We would like to express our gratefulness to professor Hirpa G.Lemu who has been our faculty supervisor during this process. Professor Lemu has been a great mentor and contributed with knowledge, motivation and guidance throughout the process of completing the thesis.

Gratitude to Jakob Trydal who has been our external supervisor from ABB and provided us with useful information and guidance throughout this thesis. The papers we have received from Trydal and ABB has made this project possible.

We would like to acknowledge Brede Berg Øvrebø for the proof reading and spelling check.

Finally, we would like the opportunity to thank our beloved families for the support, the love and the continuous support during our studies.

# Contents

	<b>Page</b>
<b>Abstract</b>	<b>ii</b>
<b>Acknowledgement</b>	<b>iii</b>
<b>Table of Contents</b>	<b>v</b>
<b>List of Figures</b>	<b>viii</b>
<b>List of Tables</b>	<b>ix</b>
<b>List of Notations</b>	<b>xii</b>
<b>Acronyms</b>	<b>xii</b>
<b>1 Introduction</b>	<b>1</b>
1.1 Background . . . . .	2
1.2 Problem Description . . . . .	2
1.3 Limitations . . . . .	2
<b>2 Theory and Literature</b>	<b>4</b>
2.1 Strength Study . . . . .	4
2.1.1 Gear . . . . .	5



2.1.2	Gear Failures . . . . .	7
2.1.3	Gear Fatigue . . . . .	9
2.1.4	Material Selection for Gear . . . . .	11
2.2	Manufacturing . . . . .	15
2.2.1	Manufacturing Environments . . . . .	15
2.2.2	Traditional Manufacturing . . . . .	17
2.2.3	Additive Manufacturing . . . . .	21
2.2.4	Environmental Impact . . . . .	29
2.3	Methods of Improving Internal Surfaces . . . . .	31
2.3.1	Abrasive Blasting . . . . .	31
2.3.2	Abrasive Flow Machining . . . . .	32
2.4	Previous Studies of Internal Surface . . . . .	34
2.4.1	Chemical Testing . . . . .	34
2.4.2	Extrude Hone . . . . .	37
2.4.3	Abrasive Flow Machining of Laser Powder Bed-fused Parts . .	39
<b>3</b>	<b>Methodology</b>	<b>43</b>
<b>4</b>	<b>Comparing Additive Manufacturing Methods</b>	<b>44</b>
4.1	Mechanical Properties . . . . .	44
4.2	Material Selection . . . . .	46
4.3	Surface Roughness . . . . .	47
<b>5</b>	<b>Design of Test Block</b>	<b>48</b>
<b>6</b>	<b>Gear Calculations</b>	<b>53</b>
6.1	Spur Bevel Gears . . . . .	54

6.2	Spur Bevel Gear with Larger Face Width . . . . .	62
6.3	Helical Bevel Gears . . . . .	63
6.4	Emergency Stop . . . . .	65
6.5	Material Properties . . . . .	66
<b>7</b>	<b>Discussion</b>	<b>67</b>
7.1	Gear . . . . .	67
7.2	Manufacturing . . . . .	69
7.3	Surface Treatment of Test Block . . . . .	71
<b>8</b>	<b>Conclusion</b>	<b>72</b>
<b>A</b>	<b>Pre-Study Report</b>	<b>I</b>
<b>B</b>	<b>18NiCrMo5 Material</b>	<b>XVI</b>
<b>C</b>	<b>16MnCr5 Material</b>	<b>XIX</b>
<b>D</b>	<b>34CrNiMo6 Material</b>	<b>XXII</b>
<b>E</b>	<b>Technical Drawing</b>	<b>XXIX</b>
<b>F</b>	<b>Technical Drawing Block</b>	<b>XXXVII</b>
<b>G</b>	<b>Data From ABB</b>	<b>XXXIX</b>
<b>H</b>	<b>Material Standard for AM</b>	<b>XLIII</b>

# List of Figures

1.1	IRB 5510 Medium-sized paint robot . . . . .	1
2.1	Illustration of different types of gears. . . . .	6
2.2	Abrasive wear due to presence of foreign bodies between two gears. . . . .	7
2.3	Scuffing due to high rotation speed. . . . .	7
2.4	Pitting and spalling due to repeated high contact stresses. . . . .	8
2.5	Crack initiation due to high load cycles. . . . .	8
2.6	Demonstration of the influence of mean stress $\sigma_m$ on S-N fatigue behavior. . . . .	10
2.7	Yield strength, tensile strength, and Brinell hardness versus carbon concentration for plain carbon steels having micro-structures consisting of fine pearlite. . . . .	12
2.8	Photo of gears under nitriding treatment. . . . .	13
2.9	Heavily oxidised gears wheel <b>a)</b> before and <b>b)</b> after Nitriding. . . . .	14
2.10	Basic bulk deformation processes: <b>(a)</b> rolling, <b>(b)</b> forging, <b>(c)</b> extrusion, and <b>(d)</b> drawing. Relative motion in the operations is indicated by $v$ ; forces are indicated by $F$ . . . . .	18
2.11	<b>(a)</b> A cross-sectional view of the machining process. <b>(b)</b> Tool with negative rake angle; compare with positive rake angle in <b>(a)</b> . . . . .	19

---

2.12 Two forms of mould: <b>(a)</b> open mould, simply a container in the shape of the desired part; and <b>(b)</b> closed mould, in which the mould geometry is more complex and requires a gating system (passageway) leading into the cavity. . . . .	20
2.13 Illustration of powder bed fusion process. . . . .	22
2.14 Illustration of binder jetting process. . . . .	24
2.15 Illustration of metal extrusion process. . . . .	26
2.16 Abrasive flow machining process. . . . .	32
2.17 Surface morphology of the channels and their corresponding roughness profiles: <b>(a)</b> as-built, <b>(b)</b> VF, <b>(c)</b> SB+VF and <b>(d)</b> CAVE. . . . .	36
2.18 Test piece after AFM and COOLPULSE. . . . .	38
2.19 Overview of the article. . . . .	39
2.20 Illustration of test pieces. . . . .	40
2.21 The rig used to polish the samples . . . . .	40
2.22 CFD calculated fields: <b>(a)</b> medium velocity, <b>(b)</b> shear rate, <b>(c)</b> rate of deformation. . . . .	41
2.23 Graph showing $R_a$ and material removal (MR) value depending on number of passes. . . . .	42
3.1 Design tree for the Methodology . . . . .	43
4.1 The hoop stress in the pipe walls depending on the pipe diameter and the wall thickness. . . . .	46
5.1 Image of test block taken from SOLIDWORKS. . . . .	49
5.2 Image of strait internal channels at 3, 4 and 5 mm in the test block. . . . .	50
5.3 Image of bent internal channels in the test block. . . . .	51

---

5.4	Image of intersection and expanding internal channels in the test block. . . . .	52
6.1	The fifth axis of the paint robot. . . . .	53
6.2	Force components in spur gears. . . . .	55
6.3	Angle of bevel gear. This picture does not illustrates the gears in this thesis but bevel gears on a general level. . . . .	56
6.4	Overview of properties of gear. . . . .	56
6.5	Values of Lewis form factor Y for standard spur gears. . . . .	58
6.6	Graph for determining velocity factor, $K_v$ . . . . .	60
6.7	Force components in helical gears. . . . .	63
6.8	Portion of a helical rack. . . . .	64
6.9	Graph for determining geometry factor, $J$ . . . . .	64

# List of Tables

2.1	LCI data of selective laser melting (SLM) processes, 2017, Procedia Cirp . . . . .	29
2.2	Abrasive media composition and processing condition of the investigated samples . . . . .	35
2.3	Values of surface roughness after different treatment processes. . . . .	38
4.1	Mechanical properties for different production methods, all values in MPa . . . . .	45
4.2	Overview of material selection available. Values indicate number of alloys . . . . .	46
4.3	Surface Roughness ( $R_a$ ) for different production methods. All values are in $\mu\text{m}$ . . . . .	47
6.1	Overload correction factor, $K_o$ . . . . .	60
6.2	Mounting correction factor, $K_m$ . . . . .	60
6.3	Chemical composition properties. . . . .	66
6.4	Mechanical properties. . . . .	66

# List of Notations

$\alpha$	Normal Pressure Angle
$b$	Face Width of The Teeth
$\gamma$	Cone Angle
$C_p$	Elastic Coefficient
$D$	The Outer Diameter
$D_i$	The Inner Diameter
$d$	Center Reference Diameter
$F$	Pitch Line
$F_t$	Tangential Force
$I$	Geometry Factor
$J$	Geometry Factor
$K_m$	Mounting Factor
$K_o$	Overload Factor
$K_v$	Velocity/dynamic Factor
$m$	Module
$P$	Circular Pitch
$P_i$	Internal Pressure
$R_a$	Arithmetic Average Height
$s$	Wall Thickness

$\Sigma$	Shaft Angle
$\sigma$	Bending Stress
$\sigma_H$	Surface Fatigue Stress
$\sigma_\theta$	Hoop Stress
$\tau$	Torque
$\phi$	Presser Angel
$V$	Poisson's Ratio
$Y$	Lewis Factor
$\psi$	Pitch Angle
$\omega$	Angular Velocity
$Z$	Number of Teeth



# Acronyms

- AFM** Abrasive Flow Machining. i, 32, 33, 37–39, 41, 48, 50–52, 71, 72
- AM** Additive Manufacturing. 2, 15, 21–31, 37, 39, 41, 43, 44, 46–48, 69–72
- BJ** Binder Jetting. 21, 24, 25, 27, 30, 47, 69
- CA** Chemically Assisted. 34
- CAVF** Chemically Assisted Vibro-Finishing. 34, 35, 71
- CFD** Computational Fluid Dynamics. 39, 50
- CP** COOLPULSE. 37, 38, 71
- DED** Directed Energy Deposition. 21, 28, 44, 47, 69
- DMLS** Direct Metal Laser Melting. 22, 23, 25
- EBM** Electron-Beam Melting. 22, 23
- ME** Material Extrusion. 26, 27
- MIT** Massachusetts Institute of Technology. 24
- MME** Metal Material Extrusion. 21, 26, 27, 47, 69
- PBF** Powder Bed Fusion. i, 21–25, 27, 29, 30, 39, 47, 69, 72
- SB + VF** Sandblasting accompanied by vibro-finishing. 34, 35
- SEM** Scanning Electron Microscope. 35
- SLM** Selective Laser Melting. 22, 23, 29
- VF** Vibro-Finishing. 34, 35, 71

# Chapter 1

## Introduction

Industrial paint robots have been used for decades in automotive paint applications. Originally, paint robots were used to shield people from dangerous jobs and streamline the production. The dangers of having workers in a work environment such as a paint hall is the exposure to unsafe VOCs, iso-cyanides and carcinogens. Today, the paint robots are money saving giants for innovative companies. ABB Robotics designs and manufactures paint robots for companies that utilize this painting method to streamline the process of painting cars Figure 1.1[1].



*Figure 1.1: IRB 5510 Medium-sized paint robot*

## **1.1 Background**

The utilizer of the paint robot requests a higher maximum load level for the hollow wrist. The current robot has difficulties carrying the weight of various bonnet and doors for regular sized cars. The paint system of the robot consist of a complex geometry. With the production methods used today the production is challenging and requires production in several different phases. In addition it is requested an improvement of processing techniques to limit the wastage of paint that flows through the system.

## **1.2 Problem Description**

The objective of this thesis is to design a test piece, that is compatible with Additive Manufacturing, and research methods to improve the internal surface. In addition, research methods to increase the bearing capacity of the hollow wrist.

The ultimate goal is for the robot to carry a payload up to 20 kg. When the maximum load is applied to the robot, a break occurs in one of the gears. Improvements must be made for the gear for the robot to handle a higher maximum load. In this thesis, several different solutions have been discussed to find a solution to this problem.

Another challenge with paint robots is the paint that flows through the systems often sticks to the internal surface which results in wastage of paint and additional work when cleaning the pipes. Treatment and possibly another production method to smooth this layer is considered as a potential for improvement and will be studied in detail in this thesis. The production method used today is welding and machining to get the desired shape. Innovative production methods such as Additive Manufacturing are options to improve the production.

## **1.3 Limitations**

The main objectives in this thesis is to increase the capability for the current existing robots. Therefore, there are certain limitations and criteria. For the gear coupling the limitations are the physical size that cannot exceed the current design due to the lack of space. The shaft angle of the gears are 145 °. Due to this, the more complex the geometry, the more the difficulties in producing the gears.

The AM production is limited by several factors. The requirement of a certain level of strength, cost efficiency, production rate and environmental impact.

The test block for paint flow is AM produced and should fit the current paint system. For that reason the block is limited by the need for the same measurements at the connection points. Another limitation is the Covid-19 restrictions limiting the possibilities to a physical demonstration and validate the calculations made. During this project there was no access to a 3D-printer. This resulted in taking assumptions and base many of the results on previous studies.

# Chapter 2

## Theory and Literature

This chapter can be divided into three parts. The potential of strengthening the gear coupling, exploring the opportunities for innovative production methods and post processing methods to reduce the surface roughness.

The purpose of this chapter is to give a fundamental definition of the parts that are causing the challenges of this thesis and options to improve this challenges. Below, various options are described to give insight in the different methods for improving both the strength of the gear coupling and for innovative method of producing parts of the hollow wrist. Furthermore, the dangers of applying the proposed methods will be presented as well as the challenges attached to the specific method.

### 2.1 Strength Study

The important question in this section is how much torque or power a given couple of gears is transmitting without any tooth failure. There are two points in a gear where failure is most likely to occur. The contact point with the mating gear and along the pitch line at the basis of the tooth also known as the tooth root. The failure method and load capacity of a gear coupling are influenced by their angular speed [2].

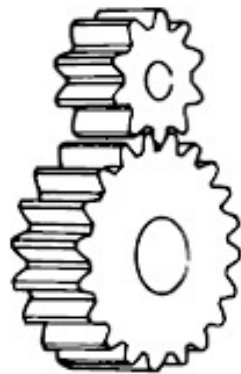
### **2.1.1 Gear**

Gear transmissions are fundamental and essential machine segments that are broadly utilized in an assortment of machines, constructions and developments. These are utilized for translation and exchange of forces and rotation in mechanical structures. Gears are also one of the most efficient ways to transfer forces between mechanical components. There are many different types of gears used in various machines. The most common types are straight-toothed, hereby referred to as spur gear, conical, worm gears, helical and spiral gears [2].

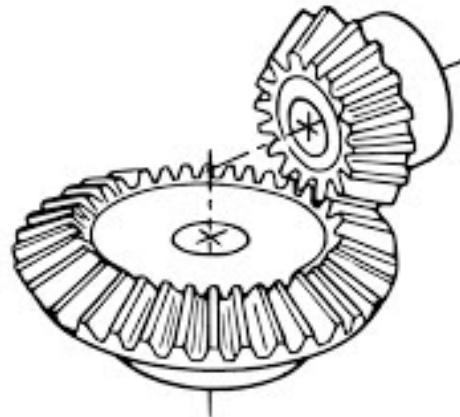
A spur gear has teeth that are parallel to the axis of rotation. These type of gears are the simplest existing forms and are less expensive in terms of production price and time. The spur gear is illustrated in Figure 2.1a

A bevel gear has teeth that are inclined usually with an angle of  $90^\circ$ . The purpose of bevel gears are to transmit forces from one direction to another. Bevel gears are widely used in cars as a differential in the drive axles, as these can transmit forces between intersecting axis. The two gears that together combine a bevel gear have a conical shape. Bevel gears are shown in Figure 2.1b.

A helical gear is one type of cylindrical gears with slanted tooth trace. The name helical comes from Helix which is a geometric figure. The difference between helical and spur gears is that the helical gear tooth has an angle relative to the axis of the gear, it than form the shape of a helix. The benefit of this type of gear is letting the teeth mesh gradually starting as points of contact and develop into line contact. Helical gears also generate less noise, and has several teeth in contact at the same time which minimize the load on a single tooth and again reduce the danger of fractures. Given that several teeth are in contact the force transition will result in a smoother process and less backlash. In addition to tangential forces, the helical gears will have axial forces [2]. The helical gears are shown in Figure 2.1c.



(a) Illustration of spur gear.



(b) Illustration of bevel gear.



(c) Illustration of helical gear.

**Figure 2.1:** Illustration of different types of gears.

There are advantages and disadvantages in the use of helical gears compared to spur gears. Given the same module and equivalent tooth width, helical gears can handle more load than spur gears because the helical gear tooth is effectively larger because it is diagonally positioned. Given that the helical gears have more teeth interacting at the same time it will also be capable of bearing a higher payload. The level of simplicity on a spur gear makes it easier and cheaper to produce than the helical gear. There are no axial forces related to the spur gear. To minimize the loss of effect to axial forces there is possibilities to insert a double helical gear. Since the axial forces are equal, the corresponding resultant force will apply in the horizontal axis direction. The double helical gear is known as a herringbone gear, which has teeth shaped as an arrowheads. The forces will work similarly in opposite directions and then cancel each other.

## 2.1.2 Gear Failures

There are multiple reasons why failure in gears occur. Listed below are the most common types of failures. Failure modes of a mechanical component are necessary knowledge when dimensioning and calculating strength to be able to prevent components from failing.

There are two main causes for gear failure, large bending stress at the root of the tooth and a large surface pressure on the tooth flank. When two gears involved consist of the same material but different diameter and number of teeth, the gear with the smallest diameter will normally fail first. This is due to the larger gear having more teeth to distribute the force on. The most common causes of failures are abrasive wear, scuffing, pitting and spalling.

Abrasive wear is one of the most common surface effects that can lead to gear failure. This happens when two gears have a lack of grease between them or in presence of foreign bodies such as dust, stone or a results of unevenness after manufacturing the parts [2]. The result of this wear is illustrated in Figure 2.2.

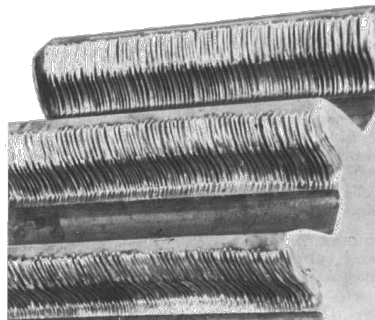


**Figure 2.2:** Abrasive wear due to presence of foreign bodies between two gears.

Scuffing is an another reason for gear failure and a form of abrasive wear that occur especially at a high rotation speed and insufficient amount of grease. This will happen under a high temperature at the contact area, than demolition, as shown in Figure 2.3, appears [2].

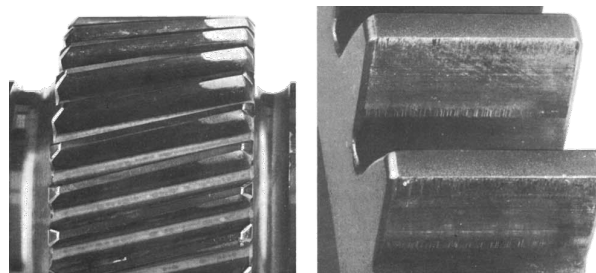


**Figure 2.3:** Scuffing due to high rotation speed.



It is normal to have a larger safety factor for bending stress than for the surface pressure. The reason for this is that the failure due to bending will be far more critical [3]. Pitting occurs when fatigue cracks are initiated on the tooth surface. This type of fatigue occurs slowly and is caused by repeated high contact stresses [2]. This is illustrated in Figure 2.4.

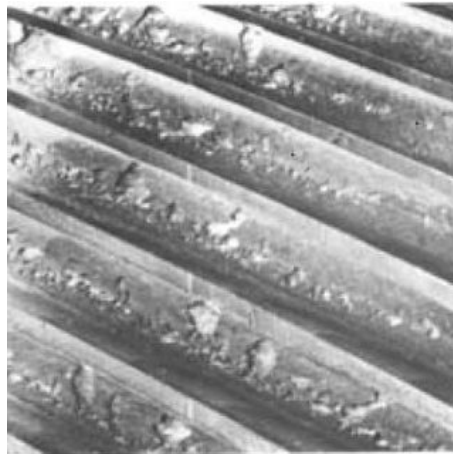


**Figure 2.4:** Pitting and spalling due to repeated high contact stresses.

Crack creation at the root of the gear as a result of cycles bending moment is also a reason for failure. It starts with a crack initiation that grows, and eventually is significantly large enough to break. The tension builds up in the transition at the root of the tooth due to stress concentrations which is often referred to as notch effects [4]. The result of a crack is illustrated in Figure 2.5.



**Figure 2.5:** Crack initiation due to high load cycles.

### 2.1.3 Gear Fatigue

Fatigue is a harm process that happens under situations of variable, cyclic loading where the material is exposed for a repetitive stress lower than the tensile strength. Due to the repetitive pressure the material will over time deform and eventually break. This situation is described by an initiation of a crack that grows to a critical size due to a high level of stress. A qualified guess is that approximately 80-90 % of all failures of machine components and structures are caused by fatigue[5].

A section of a part that has been broken because of fatigue will have a fracture at the surface with an exceptionally recognizable appearance. It is ordinarily simple to identify where the failure has begun, regularly but not generally, at an external surface.

The failure modes of fatigue can be categorized in two different modes. One of the modes is tooth root bending fatigue and the other one is contact fatigue at the tooth flank. Originally the initiation of cracks are causing fatigue failure, which start at the surface. Today it is normal to strengthen the surface of gears to prevent this. While the gear surface is strengthened the sub surface is becomes the critical point. For that reason the failure may start from a subsurface zone under the surface layer that has been hardened. This happens because the material strength at this area is much lower than its strength at the surface. Expanding and developing cracks quickly can happen because of the effect on the material by the tension continuing stress.

Push-pull and bending test are names of methods used for testing samples made out of a particular material and surface treatment. The two tests are useful to foretell bending strength of the tooth root when dimensioning a gear. The experimental element analysis results can tell that the range of the subsurface crack from the surface agrees with the depth of the maximum shear stress range. Recently, there has been some progress on the simulation of gear contact fatigue [6].

After studying the gear geometry, there are some factors that effects the bending stress that cause fatigue. The fatigue conduct of designing materials is profoundly sensitive to various factors, including mean stress level, surface effects, mathematical design and metallurgical factors just as the environment. The possibilities for increasing strength and improving the fatigue resistance of gears, are mean stress, stronger material that can have a higher quality, larger center distance between gears, larger module, larger encroachment angle, use of helical gear and wider tooth flank or wider gear [4].

The reliance of fatigue life on stress amplitude is represented on the S-N plot also called Wöhler diagram. The data originally taken for a constant mean stress  $\sigma_m$ , which is the average between the highest and lowest stress, effecting the material. Given that the diagram is indicating the fatigue life over time, it is the mean stress that is relevant for this case.

S-N curves are made by machining many identical test rods. Each individual rod is exhausted to rupture with a given stress amplitude. The next rod is exhausted with a different stress amplitude which gives a different number of cycles to rupture etc. Such data are systematized in S-N plot. The mean stress also effects the fatigue life. The effect can be represented by many S-N plot, that is registered at different  $\sigma_m$ , a standard S-N plot is shown in Figure 2.6 [7]. It is worth mentioning worthy that increasing the mean stress level results in fewer number of cycles to break. This will lead to a decrease in fatigue life [8].

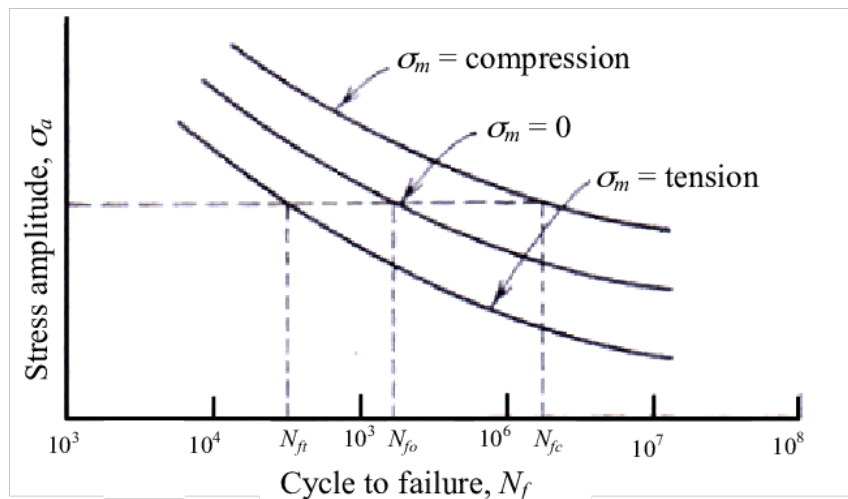


**Figure 2.6:** Demonstration of the influence of mean stress  $\sigma_m$  on S-N fatigue behavior.

For some basic loading situations, the most extreme stress inside a segment or structure happens at its surface. Most cracks prompting fatigue failure start at surface areas, explicitly at stress amplification points. The fatigue life is particularly sensitive to the condition and setup of the segment surface. Various variables impact fatigue resistance than proper management of them, will therefore prompt to refine the life of fatigue. These include design criteria just as different surface treatments [8].

#### 2.1.4 Material Selection for Gear

There are several thousand different material alloys with different characteristics. Different material types can be combined to reach the wanted properties. There are numerous of examples from where both buildings and machine components has collapsed due to lack of strength in the materials. Therefore the use of material must be selected carefully. The material with greater strength of surface hardness is prescribed, for example, steel.

The effect on the gear flank causes damage on the gear tooth. Because of this, it is important to choose a material with a high tensile strength that can withstand a large bending stress. The chosen material should have the option to apply quenching after induction hardening and annealing treatment. Such determination stresses has an effect on the object rather than the surface strength. In addition to having a larger tensile strength it is also common for materials used in gears to have a greater hardness to tolerate a high surface pressure, while at the same time being ductile enough not to fail due to large bending stresses at the root of the tooth.

It is recommended to use different materials in the gear transmissions. Similar material in contact increases the risk for micro-welding to occur, thus a higher wear rate is produced. It is then common to have the hardest material on the smallest gear, as the teeth on this will have the most load cycles and at the same time have to endure greater stress. It is also cheaper to produce the smaller gears in a material with greater hardness than large gears with greater hardness.

Steel is the most widely utilized material for the construction and development of most powerful and enduring parts, including machine parts. By reasonably changing the installation, mechanical treatment and thermal treatment producers can get an enormous scope of mechanical properties [2].

As the gear teeth are projected to high stress, it is required that the hardness and strength are sufficient. This is usually done by using different steel alloys and adding substances which enhances these properties. Case hardening is a strategy where both surface hardness, called case, and fatigue life are improved for steel alloys. This can be refined by carbonization or nitriding.

There are some major connections that are essential to the proper choice of steel structure. The carbon content will determine the hardness of the steel. However, increasing the level of hardness with carbon content is only limited to 0.7 weight percentage. This process is called carbonization. The other option to increase the strength is nitriding. In this process nitrogen is diffused onto the surface of the

components. Nitriding produces great wear impedance, high surface hardness and an increase in both the fatigue strength as well as toughness.

Through increasing the carbon content, the hardness of the material will also increase. However, this process should be controlled, as over-carbonization the material may lead to embrittlement which is highly unwanted. Moreover, the rusting properties, yield and tensile strength are affected by the increase of the carbon concentration.

Carbonization introduces additional carbon into the surface of an otherwise low-carbon steel at a raised temperature to give a greater surface hardness, changing the micro-structure of the material. A carbon rich external surface layer or case is created by diffusing the carbon atoms into the micro-structure. The impact of carbon content on hardness for Fe–C alloys is exhibited in Figure 2.7. The enhancement of the fatigue properties is a result of the increased hardness inside the case [8].

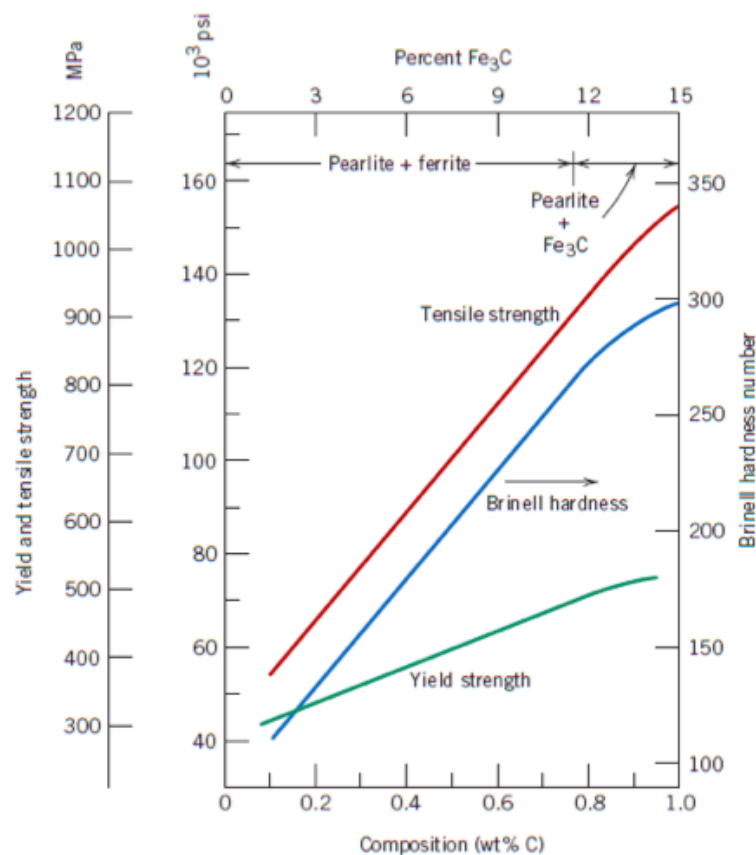


**Figure 2.7:** Yield strength, tensile strength, and Brinell hardness versus carbon concentration for plain carbon steels having micro-structures consisting of fine pearlite.

Nitriding is an advanced method for surface solidifying metallic parts to get a greater service life. Fundamentally, nitriding is a glow discharge technology combination of two gases, hydrogen and nitrogen Figure 2.8 [9]. The purpose is to insert the nitrogen atoms into the already existing surface of a metal, which is going to diffuse. This strategy has gotten progressively more popular, because of its improvement capabilities [10].

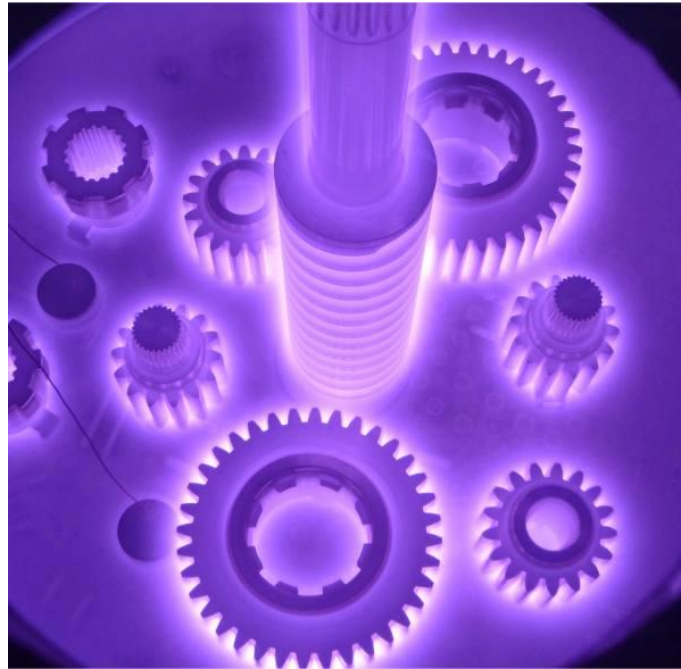


**Figure 2.8:** Photo of gears under nitriding treatment.

Nitriding is a common heat treatment for steel where the main objective is to increase of the load capacity of gears. A thin layer, called case, is created by nitriding, which is a hard surface layer. Underneath this layer a diffusion layer is created to increase the fatigue strength. The nitriding process is done on a finished manufactured gear to achieve a greater payload capacity. The finished product of the nitriding process is illustrated Figure 2.9 [11]. The payload capacity is effected by the compound layer. A drawbacks with nitriding is the risk of over-increasing the nitrogen atom leading to a reduction of the quality and increase the surface roughness of the gears. The aim of this process is to improve the gears by a chemical compositions via chemical and thermal reactions. Nitriding will results to increase the fatigue strength as well as resisting heat. The nitriding process can also produce a greater resistance to adhesive, corrosion and abrasive wear. The influence factor on the load capacity is stabling of the compound layer [12].

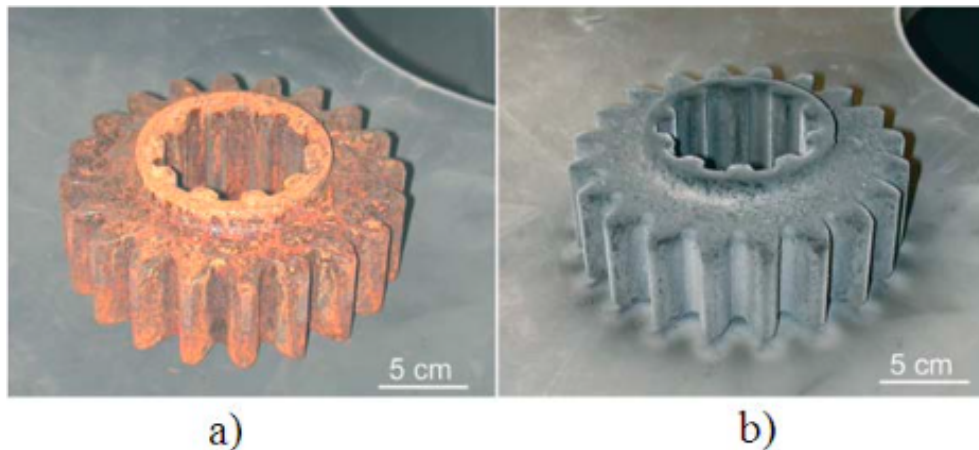


**Figure 2.9:** Heavily oxidised gears wheel **a)** before and **b)** after Nitriding.

Choosing the correct material for a part or structure requires knowledge of the load it experiences. In some cases, this will be hard or close to impossible to predict in advance. To make sure that the gear will withstand the forces they are experiencing, they are designed with a safety margin to cover the unpredictable load cases. Its common to have a safety factor of about 1,4 to 2 on normal parts, but new or unknown parts may have a safety factor of 2 - 2,5 [13].

Some of the most important factors to take into account when selecting material is the availability, hardness, harden ability, strength and toughness/ductility. Increasing the hardness is a synonym with a greater wear. The concerns following choosing a material with a high hardness or increasing the hardness is the risk of a brittle surface. The yield strength determines the load a component can be exposed to without getting plastically deformed. A plastic deformation is a permanent change in the dimensions of the finished part. The ultimate tensile strength is related to how much tensile load the material can be exposed to without breaking. The meaning of toughness is the resistance of a material to prevent crack initiations. Crack initiation can be prevented already in the selection of the material. Brittle material and surface is direct consequences of crack initiations [5].



## **2.2 Manufacturing**

The production of a mechanical component is called manufacturing. Manufacturing is the way toward changing material segments or parts to produce a complete product. The word manufacture is derived from two Latin words. Manus means hand, and factus means make. Combined they form the English phrase, made by hand. The phrase is many centuries old and is still actively used today. Some of the manufacturing processes described dates back 6000 years or more. The oldest methods are casting, hammering and grinding. In this thesis the processes are divided into two general categories. Additive- and traditional manufacturing.

Traditional manufacturing are a well known production methods with a large variety of production types within the category. When choosing a production method there are several criteria that needs to be taken into account to find the best suited option. The cost, production numbers, customization, flexibility, environmental impact and time efficiency are some of the important factors that needs to be taken into account. Additive Manufacturing, known as AM is a relatively new development and is predicted to be the main production method in the future. The production type is based on 3D-printing, and there is no actual machining in this process. A model is designed in a CAD-program (Computer Aided Design) and converted to a printer that produces the physical component. Given that AM is relatively new there are a lot of research gaps in the production method and all the features and advantages/disadvantages are yet to be discovered. The five different methods described below are primarily production methods of traditional manufacturing. AM is considered to be the sixth method which is described in a separate section [14].

### **2.2.1 Manufacturing Environments**

A manufacturing environment is a description of how a production is set up. It does not necessarily describe how the parts themselves are made, but it describes the production philosophy. A production facility will often be made to suit one of these environments, and a change in environment will involve a costly teardown and buildup. The different environments will be optimized for different production volumes. AM meanwhile will be able to suit all solid-based production without major changes and can adjust its output depending on demand. Below the five manufacturing environments are described, where repetitive, discrete and job shop all describe solid-based productions while continues and batch involve liquids and powders, etc.



### **Repetitive**

The repetitive process describes a manufacturing environment where the same product is produced continually and has often a dedicated production line. The production line is based on producing several products. The series of tasks are completed in the same sequence by either employees or robots. The production rate can fluctuate to meet demand. Given small differences in the product the production method still can be repetitive. Small variations in the product can occur to meet customer needs. If the demand becomes bigger than the production rate of the line, a setup of a new line is required. This environment commonly arises when a business has a steady stream of orders that do not vary over time [15].

### **Discrete**

The discrete process is a highly diverse environment where the parts produced can be alike or highly different. Depending on the similarities between the products the unproductive tear-down and set-up times will vary. The products are still produced on a production line, but this will be more loosely defined compared to repetitive process. Given that the production line differs in a small degree from for each product, this method is not as time efficient as the repetitive process. If the part that is to be produced are significantly different then other parts, a larger part of the production line will be required altering the setup [16].

### **Job Shops**

Job shop manufacturing are the opposite of repetitive and discrete manufacturing. In the job Shop environment, there is rarely a production line. The products are produced in smaller batches or specially made for a specific order. In this environment it is hard to justify the use of automation and therefore a big consideration is placed on how the product is produced. The number of parts produced can vary from one single product to a few dozen [16].

### **Continuous**

The continuous environment has a lot of commonality with a repetitive method. Instead of parts, it covers the production of gasses, liquids, slurries and powders. The production is continuous and can be scaled up or down depending on demand. They will often involve large production plants where many products are made at once, and the production will run continuously [16].

### **Batch**

The batch process is producing similar products to continuous processes, but instead of a continuous production, it makes a given amount, then stops and cleans the equipment. This environment is used when the demand for product may vary or it is hard to ensure that the quality meets a given specification. A good example of this is mud production for oil production [16].

## **2.2.2 Traditional Manufacturing**

Technologically, manufacturing is the use of physical power and chemicals to change the geometry, properties, or potentially the appearance of a given material to make parts or an item. Additionally, manufacturing incorporates numerous parts to make a product. The cycles to achieve product includes a mix of machinery, power, tools, and labor. Traditional manufacturing has been used for more than 60 centuries, and still widely used in many types of manufacturing. In some industries, it has been replaced by another process that called additive manufacturing, which seeks design freedom. The six main categories of traditional manufacturing are moulding, forming, joining, machining, coating and casting . All of these mentioned methods are described below.

### **Moulding**

Moulding is a manufacturing process with similar principals to casting. It involves shaping a liquid or pliable material using a rigid frame (mould). Most of the time, moulding is used to form plastic, but other substances can be used. The substance is pushed in to a closed volume where it is cooled down to the desired shape. At scale moulding will allow for cheap production of each part. The typical moulding processes are compression moulding, blow moulding and injection moulding [14].

## Forming

Forming involves applying force or pressure, resulting in a plastic deformation of the material to produce the desired shape. This method is typically used for metals. Most forming processes can be done when the metal is either above or below its re-crystallization temperature. That is known as hot working and cold working respectively. Hot working makes it easier to plastically deform the metal. While cold working causes strengthening of the material. There are four different types of manufacturing processes under forming which are forging, rolling, extrusion and wire and bar drawing [14]. All of them are illustrated in Figure 2.10.

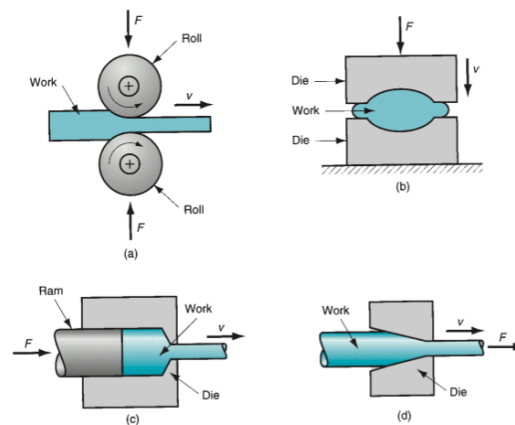


**Figure 2.10:** Basic bulk deformation processes: *(a) rolling, (b) forging, (c) extrusion, and (d) drawing. Relative motion in the operations is indicated by  $v$ ; forces are indicated by  $F$ .*

## Joining

Joining involves every production process combining two or multiple separate components into a larger assembly. It is usually combined with other manufacturing processes to make a final product. For example, machining, where joining is a secondary process. Welding, riveting, brazing, soldering and fastening (adhesive bonding) are all different types of joining processes. All these processes form a permanent bond between the parts, this joint will not easily break or separate. The term assembly generally describes the mechanical methods of fastening the pieces together [14].

## Machining

Machining is one of the most important manufacturing processes in a material removal. A sharp tool is used to remove material from a larger object, to get the required shape and size of the part. Usually, the sharp tool is turn-and-movable, and the part is stationary, as shown in Figure 2.11. It is often used for secondary shaping, when the part has already been formed using a primary process such as bulk or casting. Machining can be used for all product types, for example metal products and an extensive range of materials, including metals, plastics and wood. Examples of machining include turning, drilling and reaming [14].

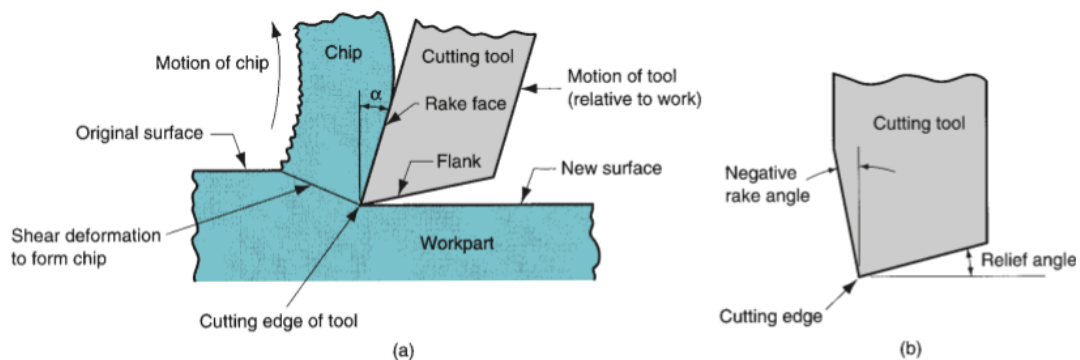


**Figure 2.11:** (a) A cross-sectional view of the machining process. (b) Tool with negative rake angle; compare with positive rake angle in (a).

## Coating

Coating is a process that involves covering the surface of the part by depositing a layer of molten metal, powder, zinc or other chemical compositions onto a surface. Coating has many functions, such as adjusting and reinforcing the surface functions instead of removing the composition of the bulk material. In addition, saving the part from rust, corrosion and other failures. Coating can be used to improve the electrical conductivity or magnetic response of the parts [14].

## Casting

Casting is a process where molten metal is poured in to a mould or cavity and cooled down to a solidified part. Casting is one of the oldest manufacturing process and dates back over 6000 years. It is often used to produce large or complex parts that otherwise would be expensive and challenging to produce.

Metal casting is divided in to two categories depending on the type of mould. These categories are expendable mould and permanent mould casting. There are many subcategories under each category including sand, die, casting and gravity casting. Figure 2.12 shows open and closed mould types [14].

Casting works by first making a replica part in another material to make the mould. The replica is then removed, then molten metal is poured in to the cavity by gravity or by high pressure. Then the part is cold down and removed from the mould. There are many factors that can influence how the result of a cast will end up [17].

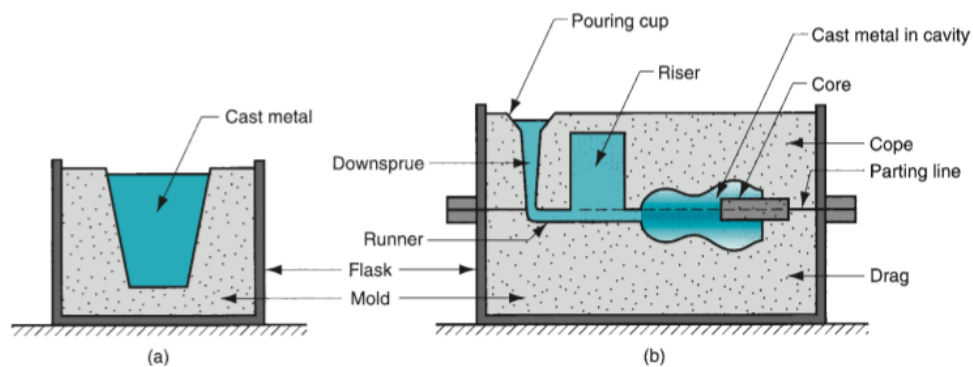


**Figure 2.12:** Two forms of mould: **(a)** open mould, simply a container in the shape of the desired part; and **(b)** closed mould, in which the mould geometry is more complex and requires a gating system (passageway) leading into the cavity.

### **2.2.3 Additive Manufacturing**

Additive manufacturing, known as 3D printing, is a relatively new development. It is a transformative approach to produce all types of physical parts. A 3D printer creates objects by adding layer-upon-layer of material. The printer can print in various types of material. The common process for printing is to use a computer to create a CAD model (Computer Aided Design) and convert the design to the printer.

One of the largest benefits of additive manufacturing is rapid prototyping. Rapid prototyping gives the opportunity to design, produce, test and adapt a part in as little time as possible. Additive manufacturing, commonly known as AM can be revolutionizing for small companies, because there is no need for a variation of expensive machinery. AM is also the most cost-efficient method to produce small batch like a job shop environment.

The degree of flexibility is also worth mentioning. A 3D printer can print anything that fits inside its volume of production. Compared to traditional manufacturing there is no need for several different pieces of equipment to produce different products. Additive manufacturing likewise gives the possibility to include several different materials in one simple object, which can give a mixture of mechanical properties. Additive manufacturing allows for easy manufacturing of hollow parts that previously would require cutting and welding to achieve.

Additive manufacturing gives the opportunity to produce a simple prototype without actually buying the equipment needed if this was to be produced in the traditional way. This will give the customer an opportunity to test the product and have a physical demonstration before actually starting to do mass production. This will also be cost-efficient for testing the market and getting feedback from customers.

AM is a large category involving several production methods. A few of the methods are widely used and some are under development. The most mature methods and the ones considered in this thesis. The following methods included are Powder Bed Fusion, Binder Jetting, Metal Material Extrusion and Directed Energy Deposition. These methods will be explored further.

## Powder Bed Fusion

Powder Bed Fusion (PBF) is a category of different methods within Additive Manufacturing which is currently leading the way for AM for industrial application. The powder based system uses a high energy source, usually a laser, to melt and fuse the powder into a part. It was invented in 1995 during a collaboration between Fraunhofer Institute, EOS and others. There are currently 15 to 20 companies in the PBF industry. The method has one of the largest material selections of any metal AM method without any special design limitations [18].

Within Powder Bed Fusion there are many manufacturing processes, including Direct Metal Laser Melting (DMLS), Selective Laser Melting (SLM) and Electron-Beam Melting (EBM). The common factor between them is as mentioned, a high powder energy source where DMLS and SLM uses a laser while EBM uses an electric beam. DMLS differ from SLM in the way where DMLS will sinter the material, while SLM will completely melt the powder and layers together. DMLS will be used to explain the process and the difference to others will be pointed out.

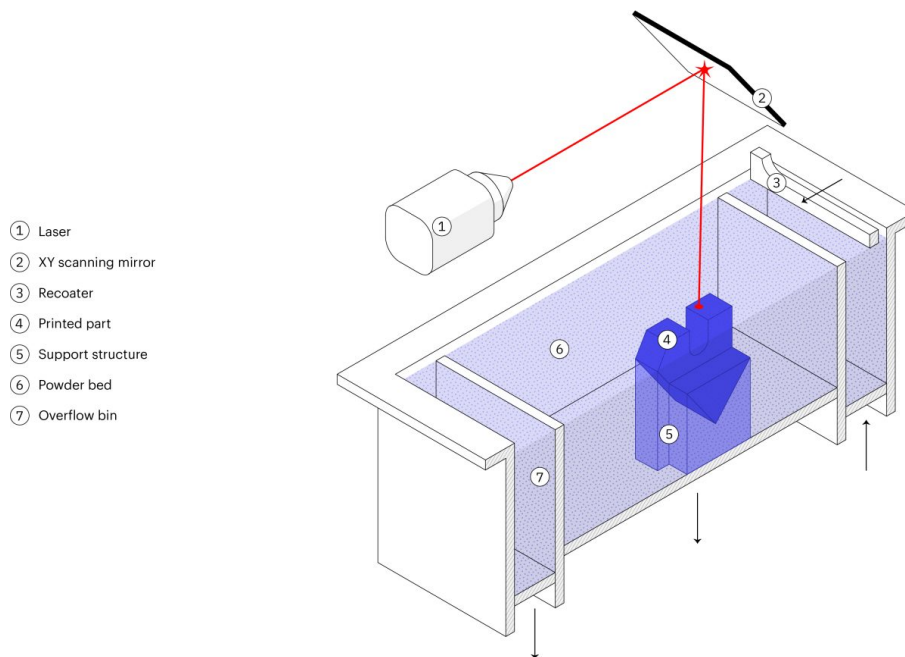


**Figure 2.13:** Illustration of powder bed fusion process.

The PBF machine consist primarily of a high-power laser, a scanning mirror, a powder spreading tool (roller), a powder supply and a build envelope which both have movable plates as seen in Figure 2.13 [19]. The printing process starts with the spreading tool pushing a layer of powder from the supply over to the build envelope before it is returned to its resting position. Then, the laser will fire the

powder by the mirror, which will redirect the laser to the given position. When the laser has sintered the whole layer, the build plate is lowered, and the powder supply is raised to an equivalent distances. This is when the spreader is used. This process goes on layer by layer until the part is finished. To reduce the chance of unwanted effects on the micro-structure, like formalization of metal oxides, the chamber will be frequently loaded with nitrogen or argon. When the part is finished the build platform is raised and the part is removed. The remaining powder is recycled and stored. The part is given a proper clean and is ready to be used. In situations where lower tolerances or lower surface roughness is required, a suitable post process is used. For SLM the process is similar apart from being produced at a higher temperature and the previous layers are also reheated. For EBM the difference is the energy source used as it used as an electron beam instead of a laser [20].

Currently within the Additive Manufacturing industry PBF and especially DMLS has the widest material selection of any production method. For example, EOS currently has more than 20 materials and over 70 processes to produce a part. Compared to most other AM method which has about 5-10 materials between all producers in total. The main benefit of this is the possibility to specialize the material to every use case and allows for more optimized designs. Another benefit is the strength characteristics of parts made by PBF. For example, a 316L stainless steel part made by EOS has an ultimate tensile strength of 590 MPa and a yield strength of 500 MPa using a DMLS process.

SLM will result in greater strength characteristics, SLM Solutions produces an ultimate tensile strength of 692-618 MPa and a yield strength of 591-541 MPa horizontal and vertical, respectively. All these data have been retrieved from Appendix H. This makes PBF stronger than other metal AM produced parts. Given these characteristics their use cases are nearly endless compared to other AM systems.

One of the biggest disadvantages of the system is the cost. The cost of these systems is at around a half a million dollars or more. This will make the method inaccessible for many companies and for prototyping phases of a project. The material cost is also fairly high and will be expensive to run. It is best suited for use cases where material strength matters. Other disadvantages include long printing time and the powder can be toxic if touched without personal protective equipment [20].

Powder Bed Fusion is one of the most attractive AM methods for production of parts due to its wide selection of material and mechanical properties. The cost is relatively high and production time is high, but their usability neglects this. PBF includes many subcategories which all have their use cases and one of the most mature metal AM methods.



## Binder Jetting

Binder Jetting, commonly known as BJ, is an AM method used to produce metal parts. It works by binding together layers of loose metal powder with an adhesive substance. This makes a green part which has to be heat treated in a furnace to remove the adhesive and melt the metal together. The part is called green because the metal is not melted together yet, and it contains a lot of adhesive. In this state the part is fragile and can easily be damaged or destroyed, therefore it is necessary to post process for the part to be useful. BJ was invented in 1993 by Massachusetts Institute of Technology (MIT) and two years later a license to Z corporation was granted and printers started to be produced shortly after. Today multiple companies are in this segment including Voxeljet, ExOne and Z Corp (part of 3D systems from 2012) which deliver different material solutions. During the latest years, most of the patents have expired which will lead to innovation in this sector[21].

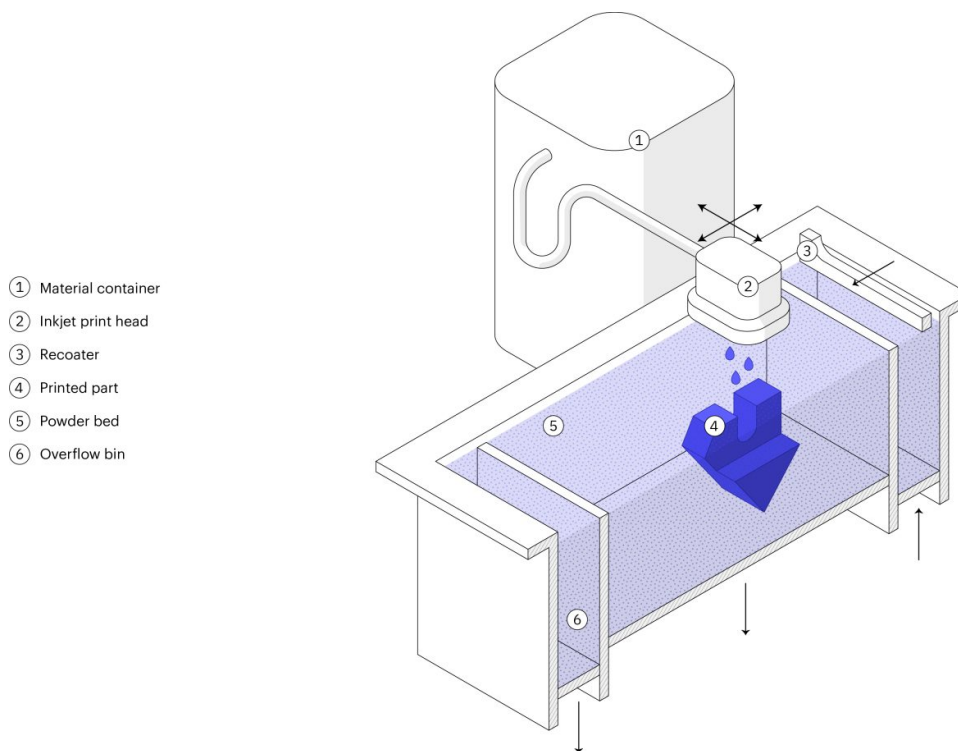


**Figure 2.14:** Illustration of binder jetting process.

Binder Jetting works in a similar fashion to PBF by also using a metal powder bed and binding powder together. The BJ machines consist primarily of a printer head, a powder spreading tool (roller), a powder supply and a build envelop which both have movable plates, as seen in Figure 2.14 [19]. The build process starts with the powder spreading by moving one layer of powder from the supply over to the envelop and moves back to its initial position to make sure the layer is flat.

Afterwards the inkjet print-head creates a 2D-pattern by jetting the liquid adhesive to the powder bed. The build envelop platform is then lowered by one layer and the powder supply is moved up the same distance and the process repeats until the part is done. The powder is then removed from the envelop and stored for later use and the green part is removed and cleaned.

Some of the biggest advantages of BJ as an AM method is the production time and lower cost of production. A large part of the process is similar to inkjet printing on paper with an addition of a new axis for the printing head and the ink is replaced by adhesive. The relatively high build rate of  $200 \text{ cm}^3/\text{min}$  for average BJ printer allows for quick creation of part. In the hardening process it's possible to have more than one part in the furnace at ones and therefore increase the production rate and reduce cost per part. The cost of a part is related to the material that is used, but for equivalent material the process is cheaper than PBF 2.2.3. The selection of material available is also fairly large allowing for better optimization for each use case. Some of these are 316 stainless steel, 718 inconel, copper and titanium. Within this selection there are both conductive and non-conductive metals which may be valuable in some use cases [21].

One of the biggest down sides of Binder Jetting is the mechanical properties. The strength of parts produced with BJ is notably lower than other parts produced with the same material. For example, stainless steel 316L produced by BJ has an ultimate tensile strength of 450 - 580 MPa and a yield strength of 140 - 220 MPa. This collected from Appendix H. Even though the ultimate tensile strength is similar to DMLS, the large difference in yield strength is notable and has to be taken into consideration when designing AM parts. Given these properties and the design freedom from AM the use cases for BJ are still many. It is an excellent way to showcase a product and being used for prototyping of new products. The method is also convenient if a high functionality is more important than raw strength.

Binder Jetting gives a cost-efficient production with a large range of material with acceptable mechanical properties. The design freedom is the same as associated with AM method. Given many companies producing BJ printers and the expiring patterns, the capability of the system is expected to increase in the coming years.

## Metal Material Extrusion

Material Extrusion (ME) is considered to be the face of 3D-printing or Additive Manufacturing. ME has taken the AM community by storm mostly due to its low cost, easy usage and large library of downloadable documents and resources. The community around ME is still continuously growing and has sparked some clever design ideas which the industry has lacked in some areas. Production in metal material is underdeveloped compared to plastics and polymers.

Metal Material Extrusion (MME) is a subcategory of the AM method Material Extrusion. The production is based on melting a part of a metal rod and placing it on the build plate, as seen in Figure 2.15 [19]. The machine consists primarily of the filament spools for both main and support filament, extrusion head, movable axis and the build platform. Depending on the printer, the build platform is either stationary or movable. The process works by heating up the extrusion head and in turn heat the filament. Then the head moves to a given position and is in contact with the build platform before laying down in the melted material. A cooling process will immediately start and settle the material on the platform. The extrude head is moved continuously to position the material until the layer is completed. Depending on the machine, either the build platform or the extrude head is moved one layer and the process is repeated. This will result in a green part which has to be post processed before use to reach the desired hardness [22].

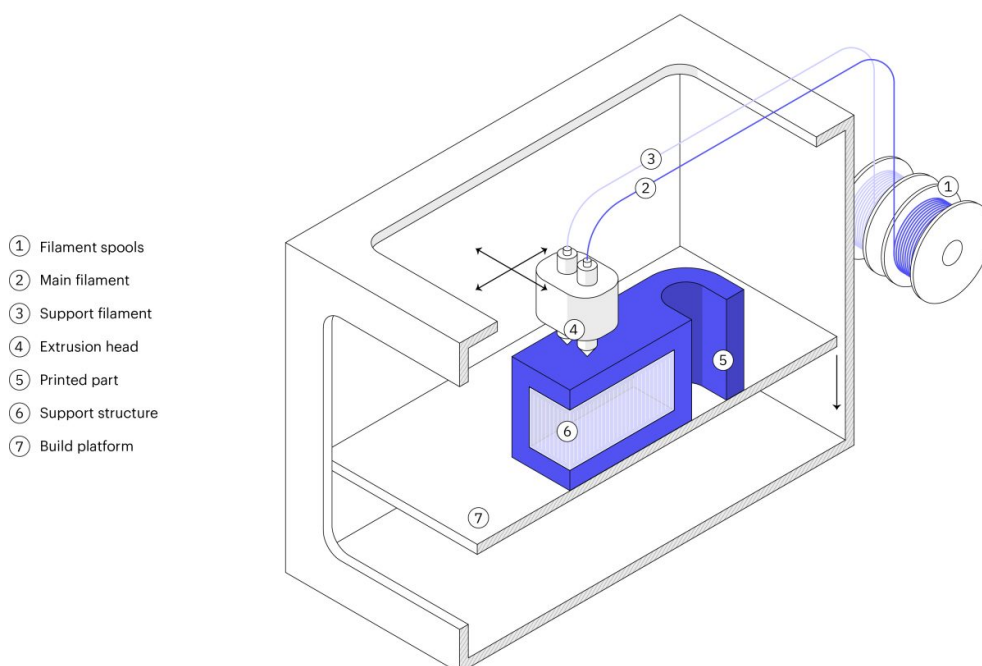


**Figure 2.15:** Illustration of metal extrusion process.

Metal Material Extrusion has a decent material selection. There is one alloy per material which limits the number of use cases for the method. currently there are about 8-9 different materials from two producers which include 316L and 17-4 stainless steel, copper, H13 steel and 625 inconel. Compared to PBF it is fairly limited and the material properties of MME are not brilliant. For example, 316L stainless steel produced by MME has an ultimate tensile strength of 533 MPa and a yield strength of 169 MPa, obtained from Appendix H.

From an economical point of view the MME is attractive for startup and prototyping. The ability of the method to produce physical prototypes without the need for a specialized production line makes it a desirable asset in a product development environment. The absence of metal powder means the machine and its surroundings will minimize the risk of contamination in comparison to BJ and PBF. On a large scale, the production level of this method may be disadvantageous primarily due to the mechanical properties. Other use cases will be job shop environment where every product is different, or small numbers of similar products [22].

Metal Material Extrusion is a contamination free and cost-efficient production method of parts and can be used everywhere from design offices to machining halls. The similarities to the current AM excitement will probably lead to advancement and accessibility. ME allow everyone from a hobbyist to a large company to step into 3D-printing and seek the benefits this brings. Strength wise it is underdeveloped compared to other methods and the smaller material selection limits the different use cases.

## Directed Energy Deposition

Directed Energy Deposition (DED) covers a range of terminology including Laser engineered net shaping, directed light fabrication, direct metal deposition and 3D laser cladding. DED is a method focusing on energy source commonly used to repair or add additional material to existing components. DED works by depositing material that has been melted onto a specified surface where it solidifies. Then, fusing materials together to form a structure. A nozzle mounted on a multi axis arm, that has the ability to move in multiple directions, allowing for variable depositions, are typically used by DED machines [23].

The chamber where the process is performed contains a reduced level of oxygen. With electron beam-based systems, the process is performed in a vacuum, while laser-based systems use a fully inert chamber when working with reactive metals. A shielding gas is also possible to use for preventing contamination during metal AM. A heat source is used to melt a powder or wire as it is deposited onto the surface of an object. Powder gives a greater accuracy in deposition while a wire is more efficient with respect to material use.

DED produces layer by layer and hardens from the melt pool to create new features. The thickness of the layers are typically 0,25 mm to 0,5 mm. Given that the material is heated the cooling time is relatively fast. The temperature reduces around 1 000-5 000 °c per second. The fast cooling time affects the final grain structure, the danger with this method is that overlapping the material can cause a re-melting. This will create a uniform but alternating micro-structure. To obtain the greater strength, steel parts can be used. This type of production is also suitable for polymers and ceramics. Almost any weldable metal can be additively manufactured using DED [24].

The DED can produce in the material LENS 316 Stainless Steel with a ultimate tensile strength of 799 MPa an yield strength of 500 MPa, collected from Appendix H. The property of elongation is 50 % [25]. The biggest advantage with DED is the ability to control the grain structure. This allows the process to be used for repair of high-quality functional parts. DED also allows for the production of relatively large parts with minimal tooling. A disadvantage with this type of production is that the product will require some post processing until it achieves the desired effect. DED can be used to fabricate parts but is generally used for repair or to add material to existing components [24].

### 2.2.4 Environmental Impact

Taking environmentally friendly considerations has become fundamental for today's companies. It is often the large companies that are responsible for the largest emissions in the world. It is therefore important that companies take action and explore new opportunities for environmentally friendly productions. Having a sustainable production is important for both the climate, and also the reputation of the company.

AM is considered to be one of the sparse production methods as it reduces wastage compared to traditional machining in the actual process. In traditional manufacturing, more raw material will be used than necessary. In comparison, some of the AM production methods will only use the amount of raw material needed in the object or store the leftovers. AM material need a specific feed stock which often needs to be pre-processed. The extra process will also result in an additional environmental impact. In a former study [26] the authors proposed a new method that can evaluate the environmental impact with a higher accuracy already in the CAD design before the actual part has been produced. The measurement is then based on electrical, fluids and material consumption. This type of method is currently unfinished, but it shows the potential of AM.

A study from 2017 has tested the average power in kW and how many kJ/kg is needed to produce an object in the material alloy 316L by the method SLM and also the resource consumption. While using PBF as production method there is required a post processing method to disconnect the parts from the build plate. To separate parts from the platform a wire erosion discharge process was used. The estimated amount of energy consumption of the removal is 142,5 MJ per build. The report also estimates the electrical discharge machining energy share up to 25 % of the total energy consumption during the manufacturing [26].

From Table 2.1 a material produced with the machine tool Concept Laser M3 Liner the average operational power equals 3,350 kW and has a density of 97 MJ/kg. The total waste powder used by SLM method will be of 20,4 % of the total powder involved [27].

**Table 2.1:** LCI data of selective laser melting (SLM) processes, 2017, Proccedia Cirp

<i>Material</i>	<i>Average operational power [kW]</i>	<i>SEC [MJ/kg]</i>	<i>Resource consumption</i>	<i>16</i>
316 L	3,350	97,0	Nitrogen: 3,5 m <sup>3</sup> /h 20,4 % waste powder	1,8

If only the finished part is taken into account, several studies show that it is more environmentally friendly using AM than traditional manufacturing. AM is currently a field where studies are limited. Because traditional manufacturing has been around for a long time, this area has been well explored. As mentioned, the potential of AM is limitless. More and more researchers consider AM as the production method that will revolutionize the industry in the future. With traditional production methods, there are countless ways to run an environmentally friendly production. The most obvious six methods are to choose a material that requires little energy to manufacture. Choose a process that minimizes the use of energy and raw material, design a part that is recyclable, design product that minimizes the use of hazardous and toxic material and focus on how the material is disposed.

AM minimizes waste of material in production compared to traditional manufacturing. When the raw material is reduced the transportation is also limited. The production is material efficient compared to machining and casting. It has less impact on the part over its life cycle, resulting in a lower carbon footprint, less embodied energy and better economic model [14].

The benefits of using AM technology through the result-oriented Product-Service Systems approach in the scale model kit industry was investigated by Nopparat and Kianian. This was done by quantifying energy consumption and raw material. The test indicated that AM has higher efficiency in the raw material usage, however the energy consumption compared to the more traditional methods are greater [27].

There is a lack of measurement of AM technology to actually conclude if there is a significant difference in the impact the AM production has on the environment. The guidelines for testing additive manufactured products are yet to come. Given the information in this chapter there is a large potential in AM technology and several aspects of the production is yet to be explored. Meaning that there is a significantly larger possibility to develop a environmentally friendly way to produce using AM method. In general, the reported specific energy values for AM unit processes are one to two orders of magnitude higher compared to conventional machining and injection moulding processes.

Due to the fine powder used in both PBF and BJ the local of the manufacturing hall is effected. This can be harmful if not handled correctly. They can oxidise and need to be stored and printed correctly to avoid changes in quality of the powder and the final product. Reasoning behind this sensitivity is their high surface area compared to their mass. The risk of inhaling and flammability means personal protective equipment it required when handled. Building and maintaining of the infrastructure, and investing in the equipment required significant investment and need to be considered carefully [28].



## 2.3 Methods of Improving Internal Surfaces

Parts produced by AM has a relatively high surface roughness. Surface roughness are irregularities in the surface inherent from the production process. The measurement of how varied a surface is or how much it deviates from a smooth surface is to be considered as the surface roughness. This is a useful measurement to determine how the surface will interact with solid objects and fluids. Depending on the application, different values of surface roughness will be tolerated or accepted. Post processing methods are useful in reducing the roughness. In some applications a certain surface roughness is required to reduce the turbulent flow in pipes. Smoother internal surfaces will reduce friction, prevent buildup of settlements in pipelines and again prevent clogging of the pipe. In this section some post processing techniques have been described.

One of the most used and widespread parameters to describe the surface roughness is  $R_a$ . The current criteria to determine how rough the surface relies on a single amplitude parameter. The unit  $R_a$  is equivalent to the parameter used for sand grain roughness,  $k_s$ . The surface roughness of an object is complicated. Studies have shown that the real surface roughness cannot be measured by a simple number. Still the most used measurement of the surface roughness relies on one number. The parameter is based on the center line average roughness and is the ultimate measurement for this thesis [29]. In this thesis the base of measuring the surface roughness is  $R_a$ . This is due to the criteria for the expected surface roughness given from the external supervisor.

Objects that have different geometric shapes require different post processing techniques to reach a certain level of  $R_a$ . There are several methods for improving the internal surface roughness. The most complex geometries containing hidden surfaces makes it challenging to treat by the most widespread methods such as abrasive blasting.

### 2.3.1 Abrasive Blasting

Abrasive blasting, known as sandblasting, is a method of increasing the surface quality. Under high pressure a stream of sand is abrasive against a surface to generate a smoother surface by shaping or removing surface contaminants. Abrasive blasting was first patented in 1870 by Benjamin Chew Tilghman. The quartz in sand was used as the corrosive element and was carried through the surface with high pressure [30].



There are various types of sandblasters, some more powerful than others. It is challenging to use a sandblaster on components with complex design. The internal surface in the pipes can be a challenging if the pipe has an angle. If a sandblaster was used in the internal surface of a pipe with the shape of the letter "L", the internal surface in the corner with the largest radius, will be relatively smoother than the corner with the smallest radius. This is why it is challenging to sandblast the internal surface of a complex geometry.

### 2.3.2 Abrasive Flow Machining

Abrasive Flow Machining (AFM) is a surface finish processing method. Both the surface finish and edge conditions of the produced parts gets treated. In Abrasive Flow Machining a chemically inactive and non-corrosive media is used. The process of this method works by moving polishing material back and forth within the part working on the internal surfaces causing erosion. The process is shown in Figure 2.16 [31]. This has a grinding effect on the part which act like form-able sandpaper. Rather than cutting away the unwanted material the abrasive particles in the media grinds it away. To achieve the required surface roughness, the material is moved through the part several times. This method of polishing allows for many different shapes and still produces a smooth surface finish.

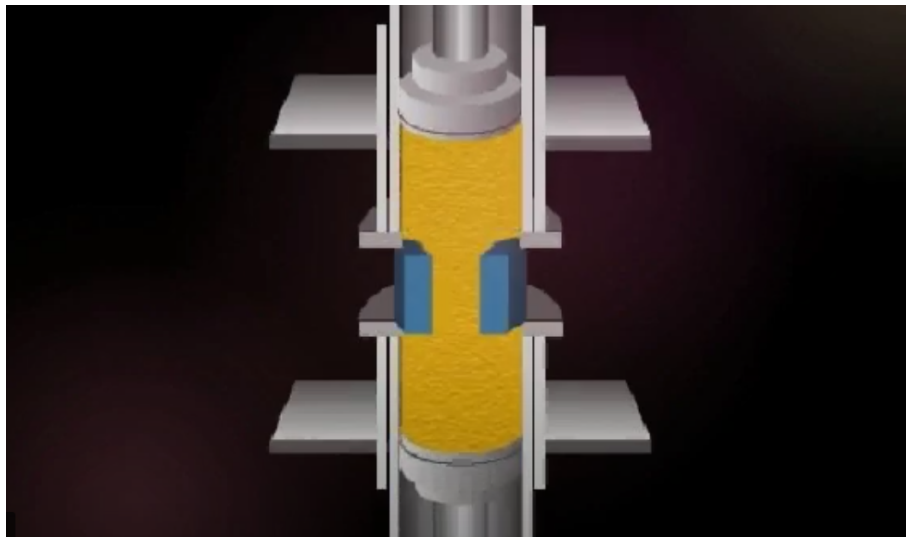


*Figure 2.16: Abrasive flow machining process.*

Abrasive Flow Machining (AFM) contains three main aspects. The following are the polishing material, the polishing program and the machine itself. All factors, such as viscosity, abrasive particle size, abrasive concentration, particle density, particle hardness and work-piece hardness have an effect on the rate of material removal.

The parameters such as media flow rate, pressure, type and volume of the media as well as media temperature can be controlled by the AFM process and will effect the material removal rate. To ensure repeatability for any application, the removal rate is both identified and monitored. It can easily be modified according to the required needs. The media can be customized for each application and material, but often the same types of media can be used on various metals. The same batch of media can be reused in many times. In addition, it can be used on different metals, without transferring the removed material between various work pieces[32].

Abrasive Flow Machining makes it possible to control the polishing program behavior. This will in return results in different results depending on the program. For example it is possible to make a program where the high mass flow rate increase the effectiveness of the material removal compared to time. It is noteworthy that different programs result in a different finish.

## 2.4 Previous Studies of Internal Surface

The surface roughness is an important measurement to determine the amount of paint flowing through the system that will be stuck on the internal surfaces of the paint system. The lower the surface roughness, the less paint will be stuck on the surface. The paint that adheres to the surface of the pipe systems is considered as waste and creates additional work when cleaning the appliance.

### 2.4.1 Chemical Testing

The test pieces have two types of shapes. One is formed as the letter L and the other as U, with different shapes and diameters. The different diameters prepared to simulate hydraulics and conformal cooling channels are 3, 5, 7, 5 and 10 mm. By following the research study, [33], four samples were printed by a Renishaw AM250 system in Maraging steel type 300 to assess post-processing techniques. There are several techniques to accomplish the required surface quality on the internal channels of pipes that has been additively manufactured. In a research study, based on the methods Vibro-Finishing (VF), Chemically Assisted (CA) and Sandblasting accompanied by vibro-finishing (SB + VF).

VF is a method used where mechanical parts is covered in liquid media and compounds (specially treated water). The vibro-finishing machine vibrates causing the mechanical components to move in a circular motion while the liquid media grinds away the irregularities until reaching the required surface roughness.

The SB + VF method is initiated by a slight sandblasting with white corundum ( $Al_2O_3$ ) under a pressure of 400 kPa. This process removes the roughness layer and is preformed prior to the vibro-finishing stage.

The final method is CAVF, the method is an expanded version of VF improved by the chemical solution containing oxalic acid, sodium nitrobenzenesulfonate, boric acid and hydrofluoric acid. The acid creates a thin brittle and spongy layer in contact with the Fe alloys. The removal of this layer is caused by the acid. The new layer has a thickness of a few nanometers and follows the surface irregularities. The cavities are less exposed and therefore the top point of the asperities is mostly polished.

All the pieces are tested in the same manner to have comparable results. The samples are placed in a Domeless machine and covered with the media corresponding to the following test. A continuous flow of water combined with corrosion inhibitors and soap are applied. After this process the samples were removed from the machine and cleaned followed by a roughness analysis. The analysis is performed deploying a standard Gaussian filter and the final value is calculated as the average of the parameters. Each test results are based on five measurements. The length of the test objects are 5,6 mm. The process name, different media, number of cycles and the total time used is listed in Table 2.2.

**Table 2.2:** Abrasive media composition and processing condition of the investigated samples

<b>Process</b>	<b>Media Composition</b>	<b>No. of VF cycles</b>	<b>Total time [h]</b>
<b>VF</b>	High density Porcelain, boron carbide	4	64
<b>SB + VF</b>	High density Porcelain, boron carbide	3	48
<b>CAVF</b>	Oxalic Acid, Sodium Nitrobenzenesulfonate, Boric Acid and Hydrofluoric Acid	2	32

The analysis of the surface roughness is made with a optical microscope (OM), a stereo microscope (SM) and a scanning electron microscope (SEM). The comparison of the results has been prepared for L-type channels with a diameter of 10 mm, according to the research study [33]. By Scanning Electron Microscope, the inside channel surface of the produced part has been examined. To more readily comprehend the distinction in these processes and according to the research study [33]. The images taken by SEM, show the surfaces of each test piece. These are shown in Figure 2.17. It has been observed that the likeness in both situations among SB + VF and VF, spatter effect is removed and achieved a similar roughness profile in both cases. CAVF produces the smoothest surface and a  $R_a$  value as low as of 0,7  $\mu\text{m}$ . According to roughness profile and SEM morphology.

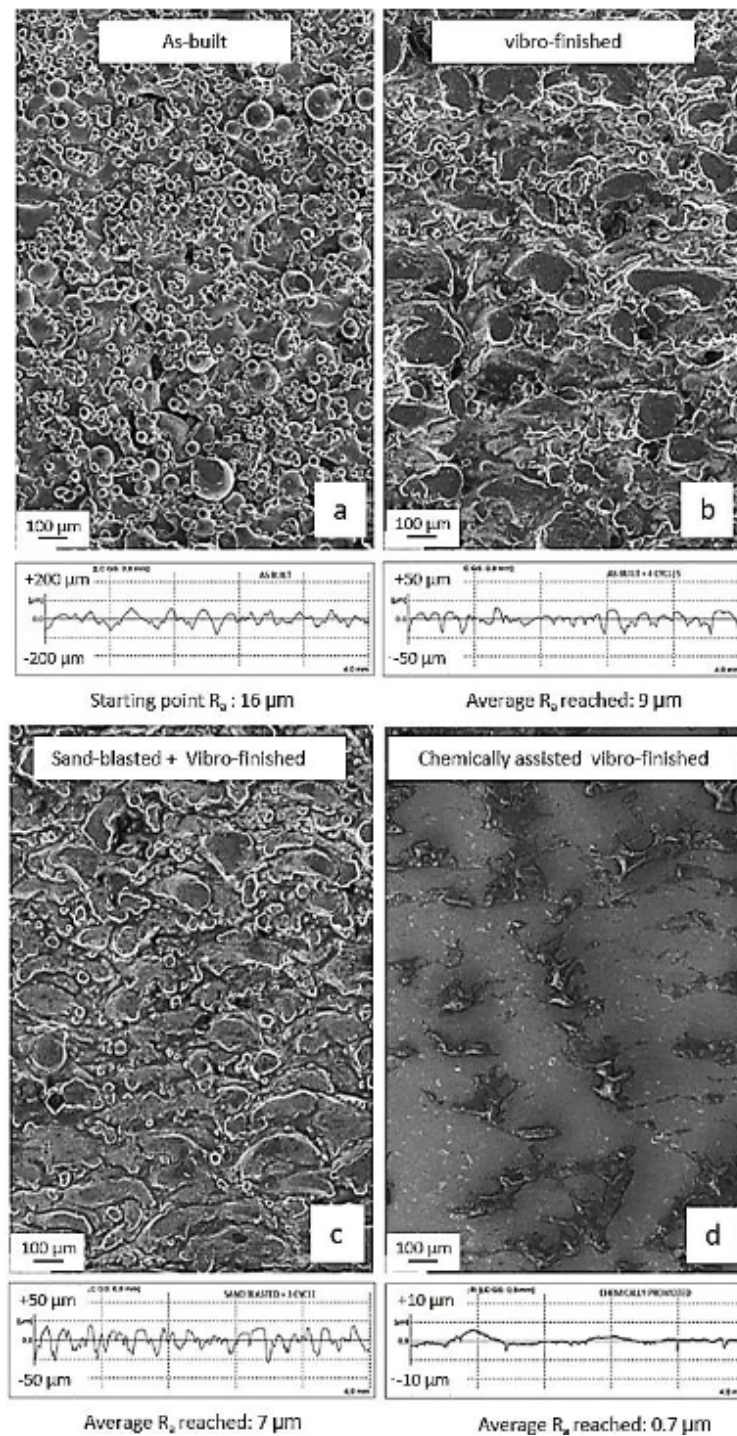


**Figure 2.17:** Surface morphology of the channels and their corresponding roughness profiles: (a) as-built, (b) VF, (c) SB+VF and (d) CAVE

## 2.4.2 Extrude Hone

One of the solutions based on the AFM method is made by Extrude Hone. The process is performed in a closed system where no material leave the chamber in the operation and the risk of contamination is eliminated. It is also possible to apply pressure in the chamber as the system is closed. The process works by attaching the object to the machine and closing the chamber. The system is then filled with the abrasive media. After pressure is applied in the chamber the machine starts pushing the media back and forth working on the surface of the part.

Depending on the part and the targeted finish, this is done in a specified manner. Variables such as flow rate, the travel of the media and number of repetitions need to be specified to achieve the desired surface roughness. The media can also be specialized to the given use case by finding the correct hardness and size of the grains.

From one of Extrude Hone own marketing materials [34] the processes have been described on how it works together with an AM produced part. The COOLPULSE (CP) and Abrasive Flow Machining (AFM) technologies have been evaluated. CP is a surface treatment method where the object is placed into a machine where a chemical solution is added. The solution will corrosive the surface, resulting in a smoother finish. The parts are produced by an EOS M 290 printer by using the material of EOS NickelAlloy IN718 and IN718 Performance (40  $\mu\text{m}$ ) process. Prior to the surface treatment process the supports of the object are removed.

The three different methods processed, resulted in a significantly smoother surface for the object. The methods are AFM, COOLPULSE and both of them combined. The visualisation of the surface finish is illustrated in Figure 2.18 [34]. The given research study [34] gives the values presented in Table 2.3. The COOLPULSE was used to attain a results of arithmetic average height  $R_a = 1,6 \mu\text{m}$  on the external surface as well as pre-finishing interaction to the AFM vanes polishing on the internal section.



**Table 2.3:** Values of surface roughness after different treatment processes.

	<i>AM</i>	<i>CP</i>	<i>AFM</i>	<i>CP &amp; AFM</i>
<b><i>R<sub>a</sub> Blade</i></b> <b><i>[μm]</i></b>	5-8	0,6	0,18	0,19
<b><i>R<sub>a</sub> External</i></b> <b><i>[μm]</i></b>	5-12	1,6		1,6
<b><i>Process Time</i></b> <b><i>[min]</i></b>		23	54	50
<b><i>Removal</i></b> <b><i>[μm]</i></b>		130	80	125

All the three processes CP, AFM and the combination have different advantages. CP manufactures a high material evacuation rates, permits surface finishing on both the internal and external surface and high structure precision at the same time. AFM, conveys a very high-quality surface finish. By combining them successfully results in an uniform and stable quality surface. According to the research study [34] the combination of COOLPULSE & AFM was used on the internal surface, and for the external surface simply COOLPULSE process was used [34].



**Figure 2.18:** Test piece after AFM and COOLPULSE.

### 2.4.3 Abrasive Flow Machining of Laser Powder Bed-fused Parts

In a research paper [35] researchers explore different ways to predict the results from Abrasive Flow Machining of a AM produced parts. The paper presents a combined numerical and experimental approach to predict the result after AFM process and evaluate both the surface roughness and the amount of material removed. Figure 2.19 show a overview of everything included in the paper.

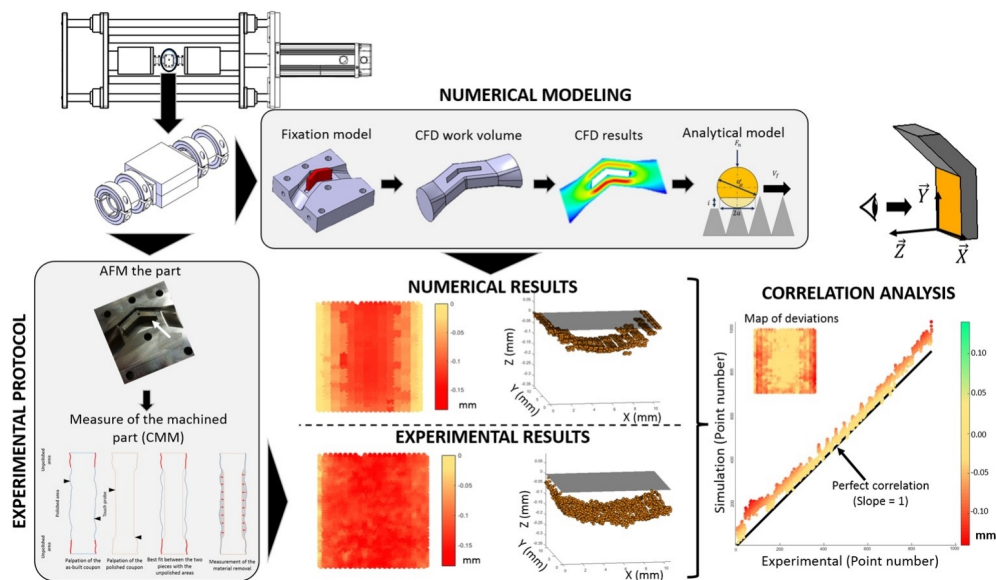


Figure 2.19: Overview of the article.

The experiment involves numerical analysis and physical experiment. The numerical analysis is based around a material removal model which describe the amount of material removed for each pass. A Computational Fluid Dynamics analysis done based on the Navier-Stokes equations for continuity and momentum. To validate the calculated results a physical experiment is preformed involving AFM of AM produced metal pieces using a abrasive medium and two pistons. The piece itself is placed inside a pipe channel.

The test pieces is made of Ti-6Al-4 V Titanium in a EOS M 280 printer which uses a PBF technique. Mechanical properties of the material is ultimate tensile strength equaling 1050 MPa and yield strength equaling 945 MPa, the material is also available for different printers. The EOS M 280 is subsided by the M 290. M 290 builds on the same principles as its predecessor and deliver similar results. The test pieces has a rectangular shape with a bend of 45 °, 4 mm thick, 15 mm wide and approximately 25,6 mm high. Figure 2.20 show a visualisation of the test pieces. The pieces are placed in a channel which is identical to the shape of the test pieces. The channel has an opening to remove and swap test pieces.



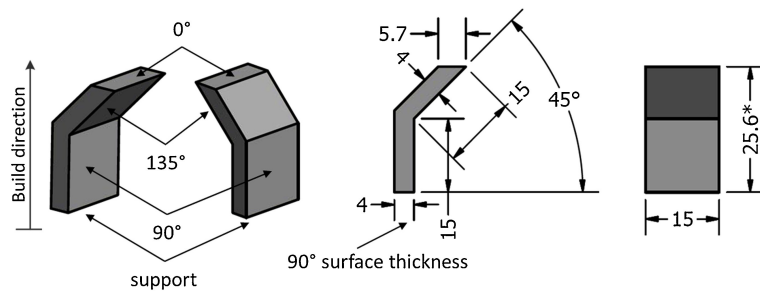


Figure 2.20: Illustration of test pieces.

An abrasive medium is used to reduce the surface roughness and is delivered by Extrude Hone LLC. The medium is called LMV-24BCE and grinds the surface and reduce the surface roughness by acting as moldable sand paper. To move the medium two pistons mounted on a movable assembly is pushed by an actuator so the medium is moved while the test piece is held stationary. The assembly is moved 60 mm each direction resulting in 120 mm for each pass at a speed of  $V = 0,0164$  m/s. During the process the pieces is measured at different interval of passes. The records are compared to the predicted values from the mathematical model. A visualisation is illustrated in Figure 2.21.

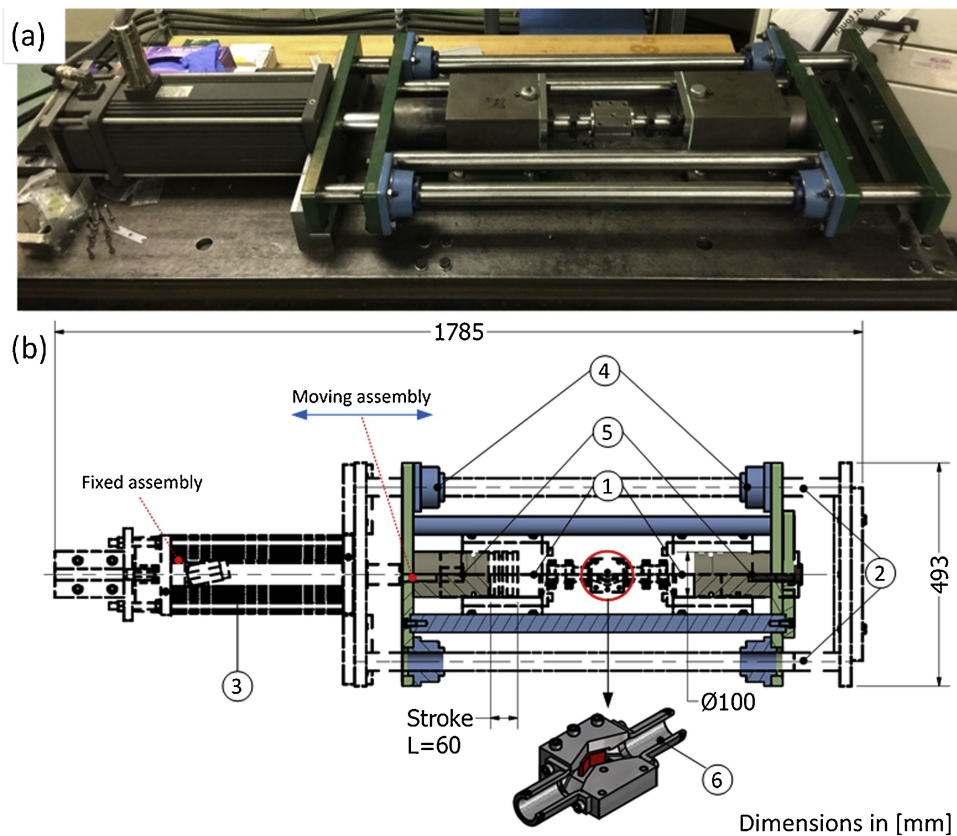
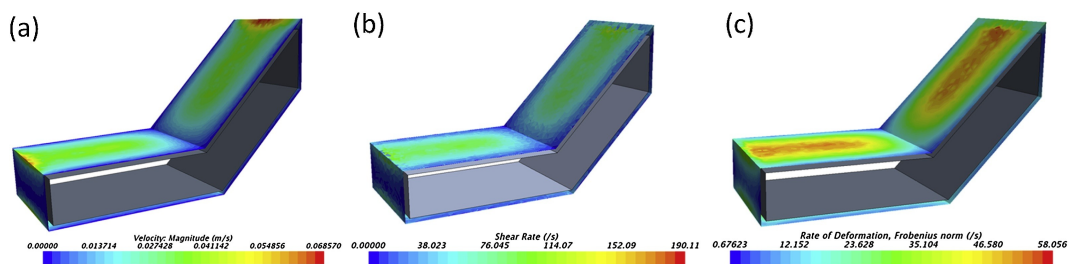


Figure 2.21: The rig used to polish the samples

Build orientation of a AM parts has a big impact on properties. For this experiment the piece has three different side orientation at 90°, 45° and 135°. The angles are taken between the bottom line of the part, and build plane showed in Figure 2.20. The differences in build orientation will result is each side having different surface roughness.

In addition to the physical testing, simulations is preformed. The simulation evaluates how the abrasive grains move over the surface. Figure 2.22 shows the medium velocity, shear rate and rate of deformation. It is possible to see the factors change drastically in the corner.



**Figure 2.22:** CFD calculated fields: (a) medium velocity, (b) shear rate, (c) rate of deformation.

The results of the paper are based on the experimental data collected from treating the part with AFM. Both Surface roughness and the amount of removed material is recorded at different intervals. Each surface is recorded and the results are plotted in Figure 2.23. The left y-axis represent the surface roughness in  $R_a$  and the right y-axis represent the material removed in mm. The graph shows that the 135° have a higher value than the others and will require more passes to reach the the desired values.

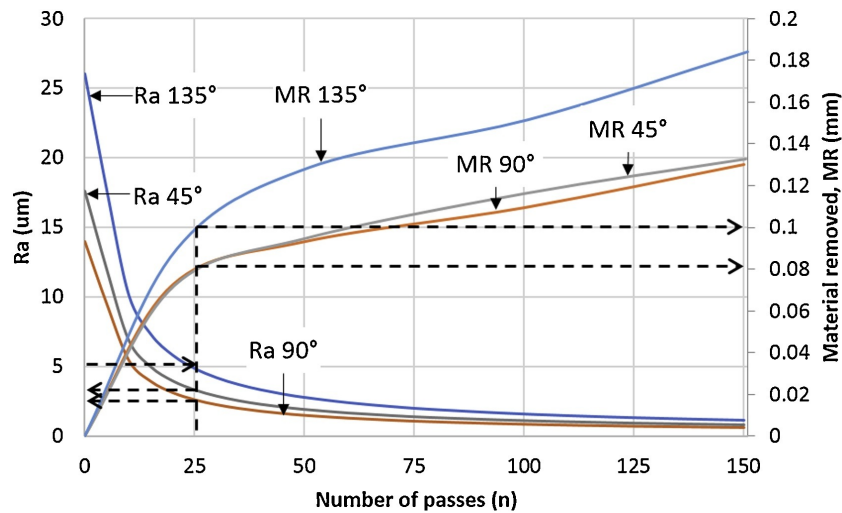


**Figure 2.23:** Graph showing  $R_a$  and material removal (MR) value depending on number of passes.

Depending on the build direction it requires approximately 50 to 100 passes to achieve the desired  $R_a$  value. Figure 2.23 illustrates what this equates to in material removed in mm. Both build direction of  $90^\circ$  and  $45^\circ$  is fairly close in roughness and material removal, while the results of the  $135^\circ$  build direction is rougher. Depending on the material of the part and the composition of the abrasive medium the results may vary [35].

# Chapter 3

## Methodology

Literature and formulas are obtained to provide sufficient basis for identifying the most common reasons for failure, and calculating the effect different gear geometries have on the force distribution. The solutions suggested to prevent failure are based on literature study, previous reports and calculations. The information obtained is processed to suit the specified case. The production method for Additive Manufacturing and surface roughness is solely based on literature study. The information in theory is tweaked into fitting the case of ABB. To be able to validate the methods obtained from the literature study there is a need for a test piece. The test piece is made in Solid Works containing different shapes and criteria set by ABB. Figure 3.1 show a summary of the methodology.

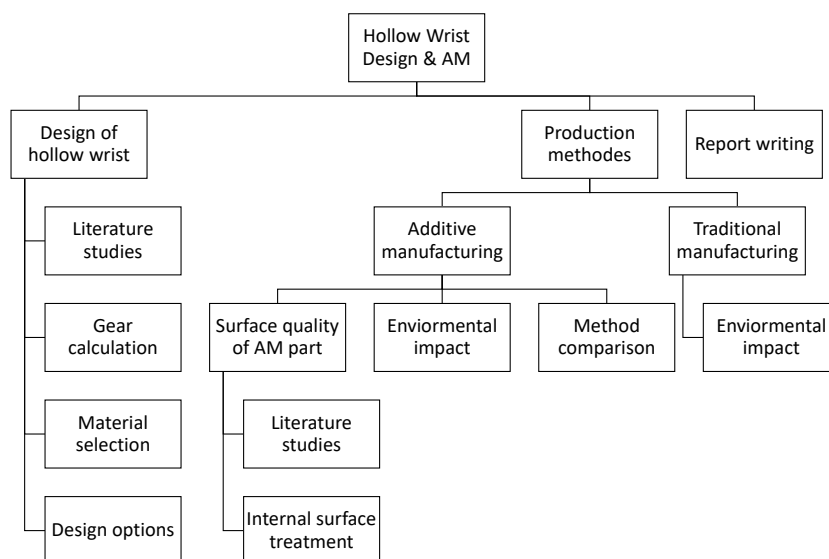


*Figure 3.1: Design tree for the Methodology*

# Chapter 4

## Comparing Additive Manufacturing Methods

Within Additive Manufacturing there are different manufacturing methods that use different processes to reach the same goal. How they work and operate are described in Subsection 2.2.3. To evaluate the methods it is valuable to determine the available use cases. Determining their expected mechanical properties, material selection and expected surface roughness allows for selecting the best-suited solution. For this comparison between the methods, the material 316L stainless steel is used. The material is selected due to great mechanical properties and its broad availability for most production methods. There is no 316L alloy for Directed Energy Deposition available, and the 316 alloy is used in the comparison. To have a comparison to non AM method casting data for Sverdrup Steel is used. Data sheets are available in Appendix H.

### 4.1 Mechanical Properties

The mechanical properties are important as they describe how parts will react to external interactions. For example, external mounting forces or pressures from paint channels. In Table 4.1 the different production methods are compared against each other by mechanical properties. Vertical direction will often be weaker than its horizontal counterpart due to the layer-based production of AM.

**Table 4.1:** Mechanical properties for different production methods, all values in MPa

<b>Material</b>	<b>Tensile Horizontal [MPa]</b>	<b>Tensile Vertical [MPa]</b>	<b>Yield Horizontal [MPa]</b>	<b>Yield Vertical [MPa]</b>
<b>Casting</b>	520 - 670	520 - 670	220	220
<b>PBF</b>	640	540	530	470
<b>BJ</b>	450 - 580	450 - 520	140 - 220	140 - 220
<b>MME</b>	533	533	169	169
<b>DED</b>	799	799	500	500

The property data show how the strength differs between methods for the same material. Greater strength will allow for a wider application of the same material. Selecting other material than 316L stainless results in different strength characteristics at the cost of weight or price. Selecting material require knowledge of the relevant loads.

The main loading the paint block experience will be the pressure from the paint channels. The current paint system is capable of withstanding 20 bars of pressure, equivalent to 2 MPa. To ensure that the block can handle this load, the required wall thickness needs to be calculated for different diameters. From Barlow's formula the pressure is defined as:

$$P_i = \frac{2\sigma_\theta s}{D} \Rightarrow \sigma_\theta = \frac{P_i(D_i + 2s)}{2s} \quad (4.1)$$

Where:

- $P_i$ : Internal pressure
- $\sigma_\theta$ : Hoop stress
- $D$ : The outer diameter of pipe
- $s$ : Wall thickness
- $D_i$ : The inner diameter of pipe ( $I = D - 2s$ )

If the pressure is set to 2 MPa it is possible to find the stress depending on the wall thickness and the pipe diameter. In Figure 4.1 the horizontal axis gives the wall thickness and the vertical axis gives the internal diameter of the pipes. The values are calculated in excel using Equation 4.1 and with a pressure set to 2 MPa.

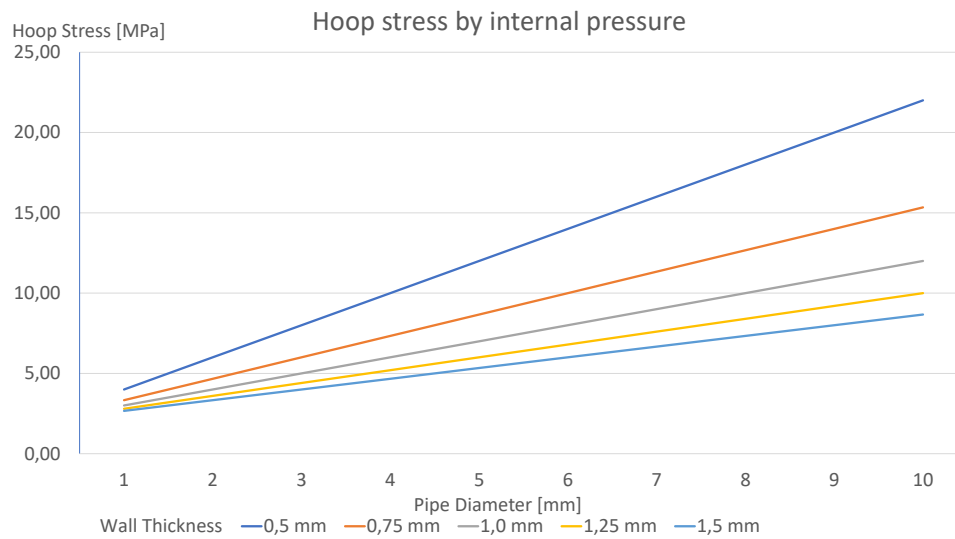


**Figure 4.1:** The hoop stress in the pipe walls depending on the pipe diameter and the wall thickness.

It will be feasible to predict that the wall thickness of the pipe channels will be at least be 1 mm and with the paint block using 3 mm to 5 mm channels, minimum yield strength of 10 MPa makes most material suitable. The material used today, which are aluminium and POM, is well within the required strength.

## 4.2 Material Selection

A wide material selection is valuable for any production method, including Additive Manufacturing. The material selection within the different AM methods are mixed. Most methods provide at least one alloy within each material category for example stainless steel, copper, titanium, aluminium. Material selection within each given category may range from one alloy to dozens of alloys.

In Table 4.2 there is an overview of the alloy selection available for each AM method from these manufactures [36] [37] [38] [39] [40] [41] [42] [43] [44] [45] [46].

**Table 4.2:** Overview of material selection available. Values indicate number of alloys

Material selection	Aluminium	Case steel	Stainless Steel	Copper	Tool steel	Titanium
<b>PBF</b>	12	4	18	7	11	12
<b>BJ</b>	1	3	10	3	8	2
<b>MME</b>	-	-	3	2	4	-
<b>DED</b>	1	2	9	2	4	4

The table shows that PBF has the largest available material selection with many alloys of each. BJ has a similar selection of material, but less alloy of each while MME has few materials available with few alloys. BJ do not have either aluminum, case hardening steel or titanium in its material selection. DED cover each material category listed but has only a few alloys of each. Availability for non listed materials have a similar distribution for each method with large selection for PBF and BJ, small selection for DED and sparse selection for MME.

### 4.3 Surface Roughness

When a part is produced there are different expectations of the surface roughness depending on the method. The surface roughness will have an effect on witch use cases the parts have. The Table 4.3 shows the average expected  $R_a$  values from different AM production methods with 316L stainless steel.

**Table 4.3:** Surface Roughness ( $R_a$ ) for different production methods. All values are in  $\mu m$

Production method	Surface roughness [ $\mu m$ ]
<b>PBF</b>	10 - 15
<b>BJ</b>	3 - 12
<b>MME</b>	-
<b>DED</b>	12 - 25

In Table 4.3 the values are collected from Appendix H. There are no results available MME, but given a similar sintering process as BJ it is possible to expect similar results at best. BJ can produce parts with the lowest  $R_a$  values of the AM methods. PBF and DED will produce parts with greater values. The requirement for the paint block is a  $R_a$  value between 0,8 to 1,6  $\mu m$  to minimize paint buildup in pipes. None of the method can provide the required surface roughness and after treatment is then required. Methods of improving the surface quality are available in Section 2.4.



## Chapter 5

### Design of Test Block

To test the surface treatment processes there is a need of a test block with internal channels of different shapes and diameters. To obtain the complex geometries required is challenging to manufacture with traditional production methods. Additive Manufacturing on the other hand overcomes these challenges. The downside by AM is the internal surface roughness. To have an efficient paint flow without risking wastage of paint a post process is required, for example Abrasive Flow Machining. Underneath is a design proposal of a block to test AFM effectiveness on different geometries. The block is of a cubic shape with four fastening brackets at the bottom. It has circular internal channels with entrances in the front and back, as well as on the top. The channels are of different shapes and dimensions. The design was made by using SOLIDWORKS, a 3D CAD application, and is showed in Figure 5.1 below. The piece is designed to be easy to produce by AM and tested afterwards. At the end of each channel there are standard pipe connector used in paint block, allowing for easy testing and integration to existing systems. A Technical drawing with dimensions can be found in Appendix F.

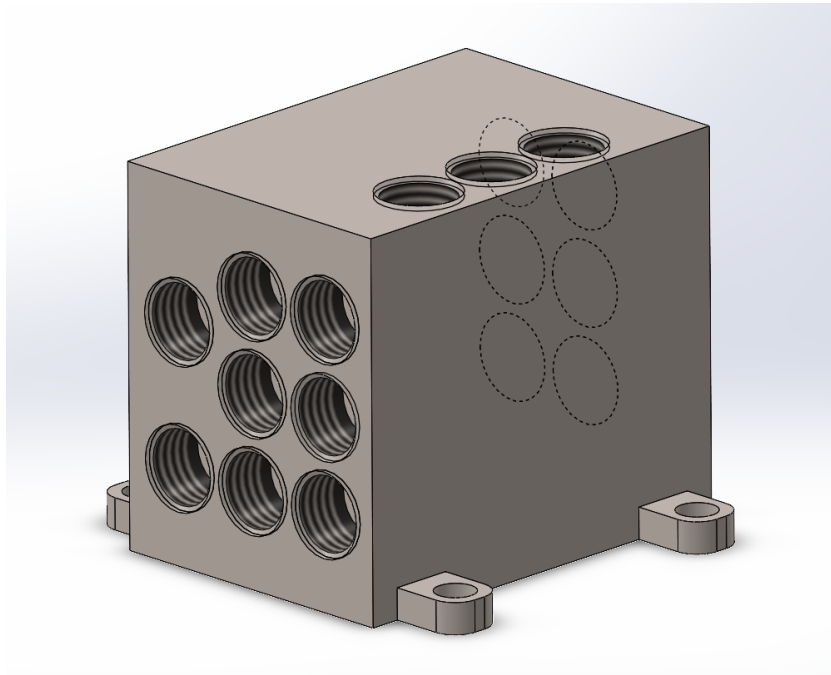


*Figure 5.1: Image of test block taken from SOLIDWORKS.*

The part is made to cover most cases where the reduction process of surface roughness is challenging. There are three straight channels in different dimensions, one 'Y' shaped intersection, one channel with a dimension transition and three different bends. The diameters ranges form 3 to 5 mm and represents the dimensions commonly needed in paint block.

In one section of the test piece there are three straight channels. There length is about 50 mm between the connectors and there diameters which are at 3, 4 and 5 mm, respectfully. This can be viewed in Figure 5.2. These channels has two main objectives, one is to prove the possibility to achieve the required  $R_a$  values and the other one is to make an estimation of how much material is removed. To achieve the desired  $R_a$  value the abrasive medium and the polishing program need to be refined. From the research paper described in Subsection 2.4.3 the data for the material removal is shown in Figure 2.23. Given that the selection of material and abrasive medium is different the values will not be the same. By testing three different dimensions close to the wanted sizes it possible to adjust the values of the equation to these results which can be used for future design.

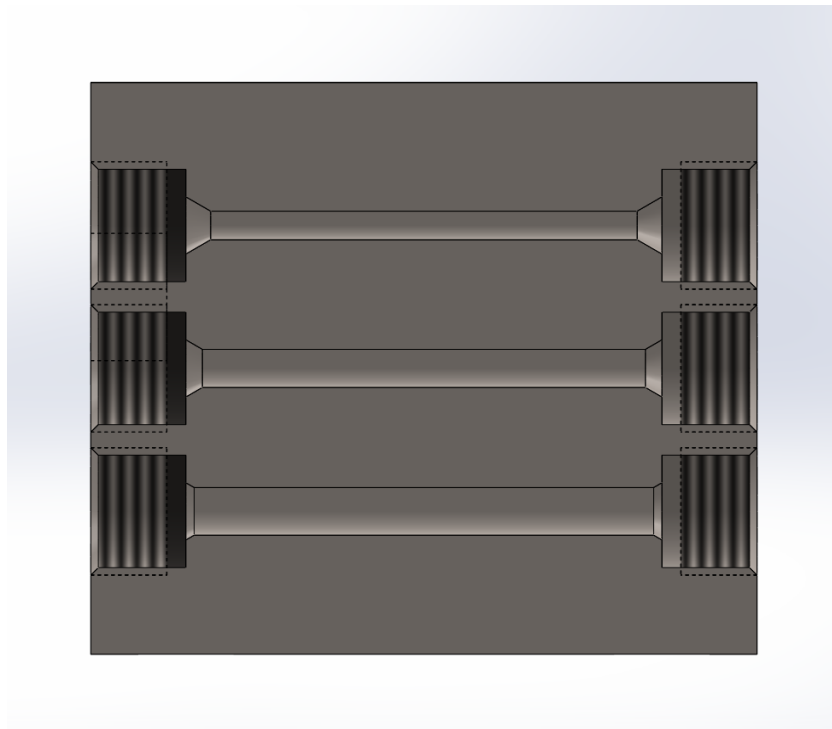


**Figure 5.2:** Image of strait internal channels at 3, 4 and 5 mm in the test block.

One of the biggest concerns related to AFM is the effect of turns and bends have on the internal surfaces. In a pipe bend the pressure distribution is uneven, with pressure being higher in the outer wall than the inner wall [47]. The effectiveness of AFM are linked to the pressure of each grain in the fluid [35]. From earlier experiments the results presented that the outer bend is more polished than desired and the inner bend is less polished. CFD of a pipe bend shows that the inner bend has negative pressure value [47]. For the medium, which has a high viscosity, the case is similar for disparity on polishing.

The three channels have different geometries. One is a 90° bend without and curvature, second one has a bend with a radius of 10 mm and the third is a combination of 2 beds of 45°, with a distance of 21 mm without curvature. This geometry is illustrated in figure Figure 5.3. The first one represent the worst case scenario of a corner, and will most likely not achieve the specified  $R_a$  values. The reason for the inclusion is that there will not be any problems with any bends and this will not be a limiting factor in the design of future parts if this potentially sorts out in the future. The second bend represent a fairly common bend and should results in a acceptable results. If the design of the test block where to expand in the future and include more profiles, a similar shape with different radius's is advised. The reason for this is the development of a similar mathematical models, as proposed for straight paths, would be helpful. The third path represents a solution which

---

may work out well. In many pipeline situation  $2 \times 45^\circ$  is used to reduce the amount of turbulence created together with decreasing the amount of stresses in the pipe-walls. This solution represent an interesting middle ground and can potentially be used in the short term before the AFM process is tuned enough for  $90^\circ$  bends.

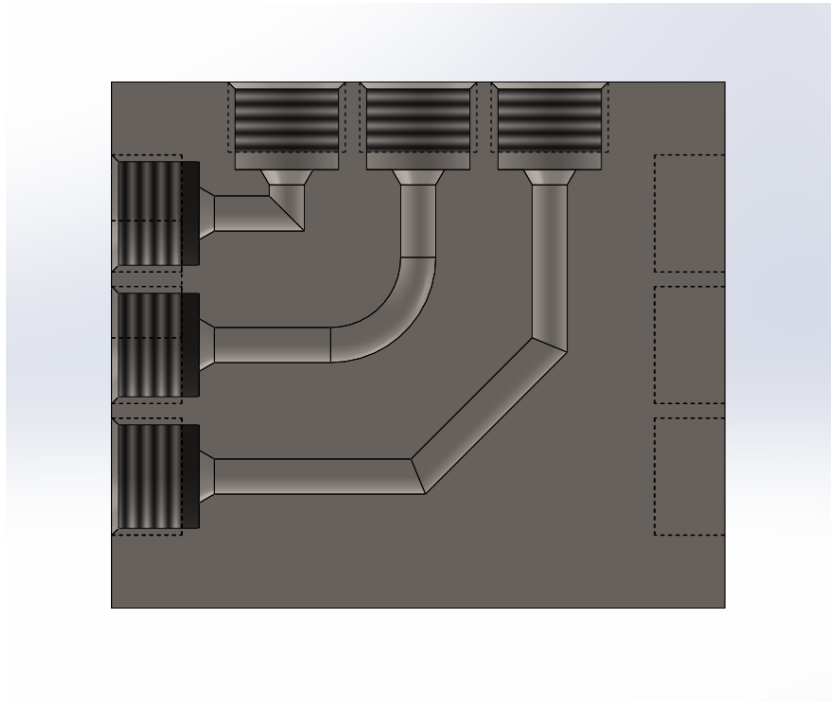


**Figure 5.3:** Image of bent internal channels in the test block.

The option of combining channels in a paint block is preferred, for example having one inlet for paint and one for solvent allowing cleaning of the system. In the block there is a 'Y' shaped intersection as seen in Figure 5.4. All diameters are equal at 4 mm resulting in doubling of the volume flow rate. This is due to the inlet and outlet volume rate must be equivalent. The fluid is incompressible both in production and operation. How the speed ratio between the inlets and the outlet will effect the surface is valuable. Depending on the result, increasing or decreasing the volume rate during AFM for the hole system may be considered. The amount of material grinded away in different parts of the intersection should also be noted. For example, the inner portion of the intersection point is likely to get eroded away, while the corners will soften out.

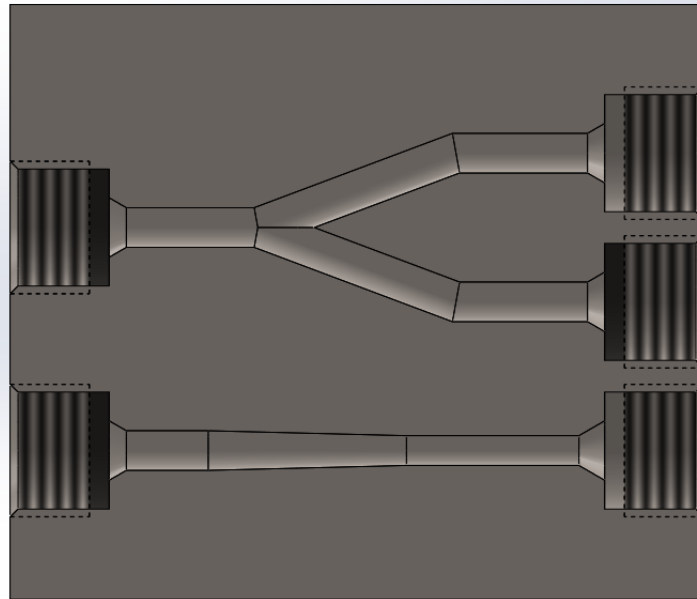


**Figure 5.4:** Image of intersection and expanding internal channels in the test block.

A change in the diameter of a pipe will be useful in many cases. This is represented in the straight channel below the 'Y' channel in Figure 5.4. The diameter changes from 4 mm to 3 mm is gradually changed over a distance of 20 mm. This represent a gradual change in diameter and should therefore not interfere with the flow. The speed of the medium will increase, due to the pressure increasing, while the volume flow rate is constant. The speed will increase by a factor of 1,778 which been calculated by Equation 5.1. Since this does not change the amount of abrasive medium that passed through the system, unlike the 'Y' section, it will be valuable to see if the effect is similar or not.

$$f = \frac{\pi \times r_A^2}{\pi \times r_B^2} \quad (5.1)$$

As a summary the block includes many different channels of different shapes and sizes. All of the challenges have a purpose and combined covers most geometries considered in a paint block. The test results of the surface of the block produced by AFM will be able to determined the design limitation to the system for make a functional and reliable part.

# Chapter 6

## Gear Calculations

The task is based on increasing the strength of gear five and six as shown in Figure 6.1 on the fifth axis given in Appendix G. The consumers have requested a higher payload capability that the robot can bear. Currently the mentioned gears are having difficulties managing the preferred weight of 20 kg. Therefore the calculation of gear tooth bending stress and the surface fatigue strength are fundamental to calculate to increase its payload capacity. The original technical drawing of the coupling of the gear set shown in Appendix E shows a shaft angle of  $145^\circ$ . With permission from the external supervisor the angle is set to  $90^\circ$  for the constants factors. This assumption is made to make the calculations manageable. There has also been made a qualified guess where there was a lack of information.

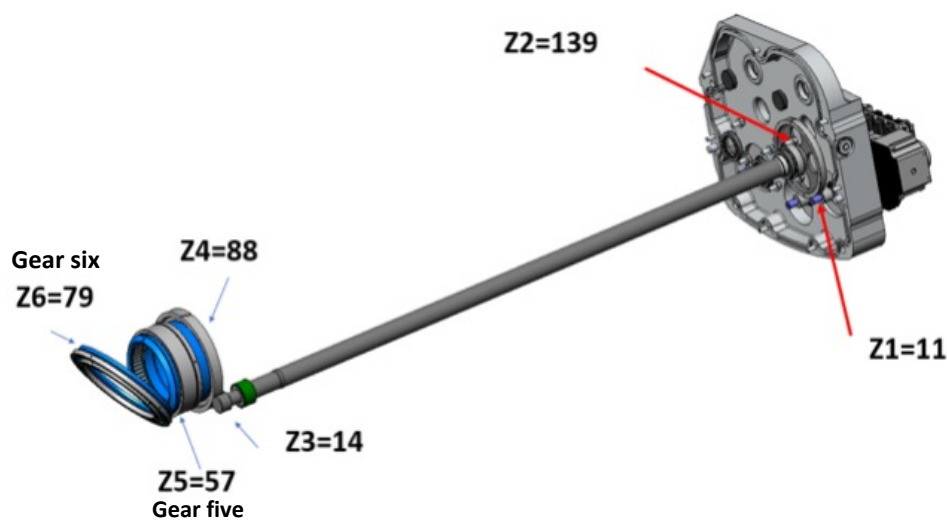


*Figure 6.1: The fifth axis of the paint robot.*

## 6.1 Spur Bevel Gears

The calculation shows how much the current gear number five and six can withstand in the normal operation.

- **Geometry and Nomenclature:**

$m$  is defined as the module for a gear and is given by the pitch diameter divided by the number of teeth as shown in Equation 6.1. Two gears having different diameter can mesh properly given that they have the same relationship between pitch diameter and number of teeth.

$$m = \frac{d}{Z} \quad (6.1)$$

For the fifth gear the pitch diameter equals to 114 mm and number for teeth,  $Z$ , equals 57. This will give the following module with respect to Equation 6.1. Given that the module must be the same for the gears to mesh properly the module for both the fifth and sixth gears must be equal.

$$m = 2 \text{ mm/teeth}$$

A small module means that there is many teeth around the circumference of the gear. It follows that if the module increases, the teeth size will also increase resulting in fewer teeth around the circumference on the gear.

As illustrated Appendix E the normal pressure angle is  $20^\circ$ . "The pressure angle known as  $\alpha$ , of a gear is defined as the angle formed by the radial line and the line tangent to the profile at the pitch point" [48]. A small  $\alpha$  provides a smoother transmission and less noise, while a larger  $\alpha$  provides the advantage of being able to transfer more load.

When two teeth come in contact, there is a force between them which is called a tangential force defined as  $F_t$  that works at the contact point of the two gears. The reaction forces applies to the same identical spot (Figure 6.2). The tangential force is a result of an applied torque in one gear and a counter torque on the other gear.

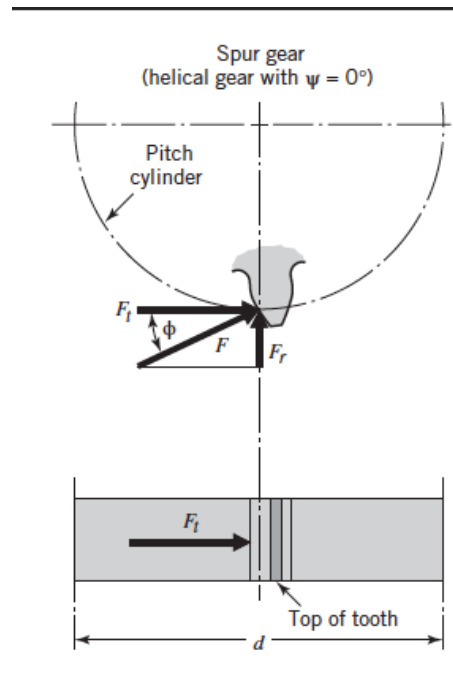


**Figure 6.2:** Force components in spur gears.

The fifth axis system contains four shaft. Gear number 2 and 3 shear the same shaft while gear 4 and 5 shear the same shaft. The initial maximum torque ( $\tau$ ) from the fifth axis system is 2,90023 N m as shown in Appendix G. The equation below will give the transmitted forces to the fifth and sixth gear.

$$\tau_B = \tau_A \times \frac{Z_B}{Z_A} \quad (6.2)$$

All gears mounted to the same shaft will have the same torque. According to 6.2 This will give the following for the second and third gear.

$$\tau_2 = \tau_3 = \tau_1 \times \frac{Z_2}{Z_1} \Rightarrow \tau_2 = \tau_3 = 2,90023 \times \frac{139}{11} \approx 36,7 \text{ N m}$$

By further calculations the transmitted torque to the fourth and fifth gears will equal the following.

$$\tau_4 = \tau_5 = \tau_3 \times \frac{Z_4}{Z_3} \Rightarrow \tau_4 = \tau_5 = 36,6484 \times \frac{88}{14} \approx 230,4 \text{ N m}$$

The tangential force between the fifth and sixth gears depends on the pitch cone angles  $\gamma$ .



The shaft angle is known as  $\Sigma$ , which is the sum of both pitch cone angles of gear five and six as defined in Figure 6.3.

$$\Sigma = \gamma_5 + \gamma_6 \tag{6.3}$$

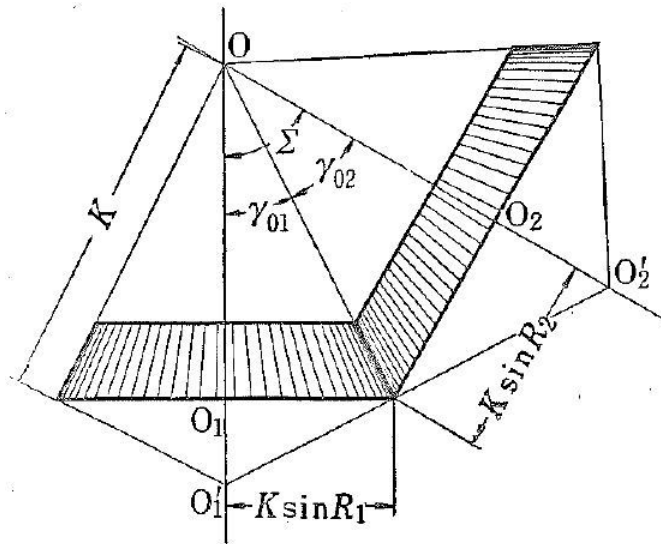


**Figure 6.3:** Angle of bevel gear. This picture does not illustrates the gears in this thesis but bevel gears on a general level.

$\gamma_5 = 45,33^\circ$  and  $\gamma_6 = 99,67^\circ$  obtained from Appendix E.

$$\Sigma = 45,33 + 99,67 = 145^\circ$$

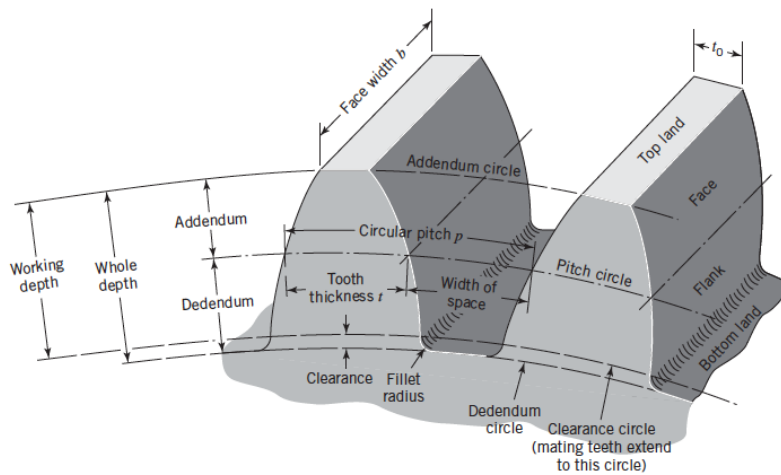


**Figure 6.4:** Overview of properties of gear.

The center reference diameter as shown in Figure 6.4 is given by the relationship:

$$d_m = d - b \times \sin \gamma \quad (6.4)$$

Where  $b$  is the face width of the teeth as shown in Figure 6.4, which is 10 mm according to Appendix E.

For the fifth gear:

$$d_5 = 114 \text{ mm}$$

$$b = 10 \text{ mm}$$

$$d_{m_5} = d_5 - b \times \sin(\gamma_6) = 106,88 \text{ mm}$$

For the sixth gear:

$$d_6 = 158 \text{ mm}$$

$$b = 10 \text{ mm}$$

$$d_{m_6} = d_6 - b \times \sin(\gamma_6) = 148,142 \text{ mm}$$

Now the tangential force between the fifth and sixth gears is given by the following equation:

$$F_t = \frac{\tau}{\frac{d_m}{2}} \quad (6.5)$$

$$F_t = \frac{\tau_5}{\frac{d_{m5}}{2}} \Rightarrow \frac{230,3611}{\frac{106,88 \times 10^{-3}}{2}} = 4310,649 \text{ N}$$

- **Gear-Tooth-Bending Stress(Lewis Equation):**

The originally perceived test of gear-tooth stresses was introduced by Wilfred Lewis in 1892 to the Philadelphia Engineers Club [2]. It is still widely used for calculating the bending stress at the teeth on gears. Bending stress equation for spur gears are giving by:

$$\sigma = \frac{F_t}{m \times b \times Y} \quad (6.6)$$

Where:

$Y$  is the Lewis form factor based on diametral pitch or module.  $Y$  is a function based on the tooth shape and is found by using Figure 6.5, it change with the gear teeth number. From Figure 6.5 the Lewis form factor is 0,41.

Lewis made the following assumptions for calculating the gear tooth bending stress.

1. All load is applied as point load at the end of the tooth.
2. Radial component of the load  $F_r$  gives little contribution to the transferred power and can be neglected.
3. The load is evenly distributed outward throughout the width of the tooth.
4. Frictional forces from slide friction between the teeth are neglected.
5. Neglect stress concentrations at the transition in the bottom of the tooth.

In addition, if the material is elastic, isotropic or homogeneous, the surface roughness can be neglected.

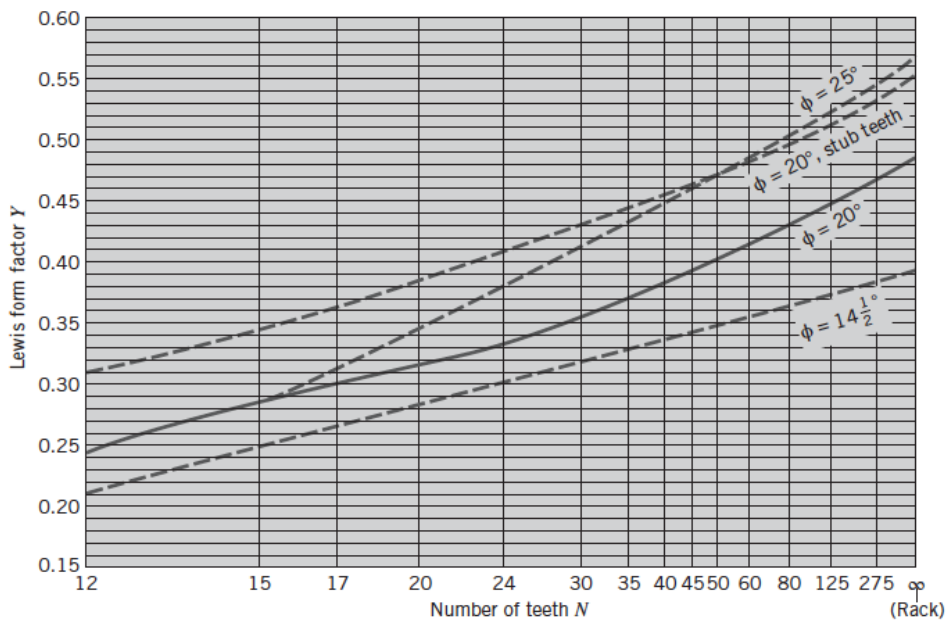


Figure 6.5: Values of Lewis form factor  $Y$  for standard spur gears.

Using Equation 6.6 the level of stress the original gear is exposed for can be calculated.  $F_t$  is previously calculated to 4 310,649 N.

$$\sigma = 525,689 \text{ MPa}$$

• **Gear-Tooth Surface Fatigue Analysis :**

Mechanical behavior of machine elements as gears are influenced by the interaction between contact elements and surfaces. Mechanical parts interacting are exposed to contact fatigue. Contact fatigue is a result of changes in the microstructure that leads to a crack under the influence of time-dependent rolling contact load. The fatigue process can be categorised to the initiation of micro-cracks due to local accumulation of dislocations, high stresses at local

points, plastic deformation around in-homogeneous inclusions or other imperfections in or under the contact surface; crack propagation, which causes permanent damage to a mechanical element. In this section the crack initiation due to bending stress will be focused on.

Fatigue strength is the highest stress a material can withstand for a given number of cycles. Equation 6.7 gives the values of gear tooth surface fatigue [2].

$$\sigma_H = C_p \times \sqrt{\frac{F_t}{b \times d_p \times I} \times K_v \times K_o \times K_m} \quad (6.7)$$

Where:

- $C_p$ : Elastic Coefficient:  $C_p = 0,564 \times \sqrt{\frac{1}{\frac{1-V_5^2}{E_5} + \frac{1-V_6^2}{E_6}}} = 188,62 \sqrt{\text{MPa}}$

Where  $E$  is the elastic modulus of material to each gear  $E_5 = 200$  GPa,  $E_6 = 210$  GPa, according to Appendix B and Appendix C respectively. The difference in elasticity modulus is due to the two gears containing different material.

$V$  is the Poisson's ratio for steel  $V = 0,29$  according to both Appendix B and Appendix C

- $I$ : Geometry factor:  $I = \frac{\sin \phi \times \cos \phi}{2} \times \frac{R}{R+1} = 0,0615$

Where  $R = \frac{d_5}{d_6}$  and  $\phi = 20^\circ$

- $d_5$ : Reference diameter
- $K_v$ : Velocity/dynamic factor, as shown in Figure 6.6
- $K_o$ : Overload factor, as shown in Table 6.1
- $K_m$ : Mounting factor, as shown in Table 6.2

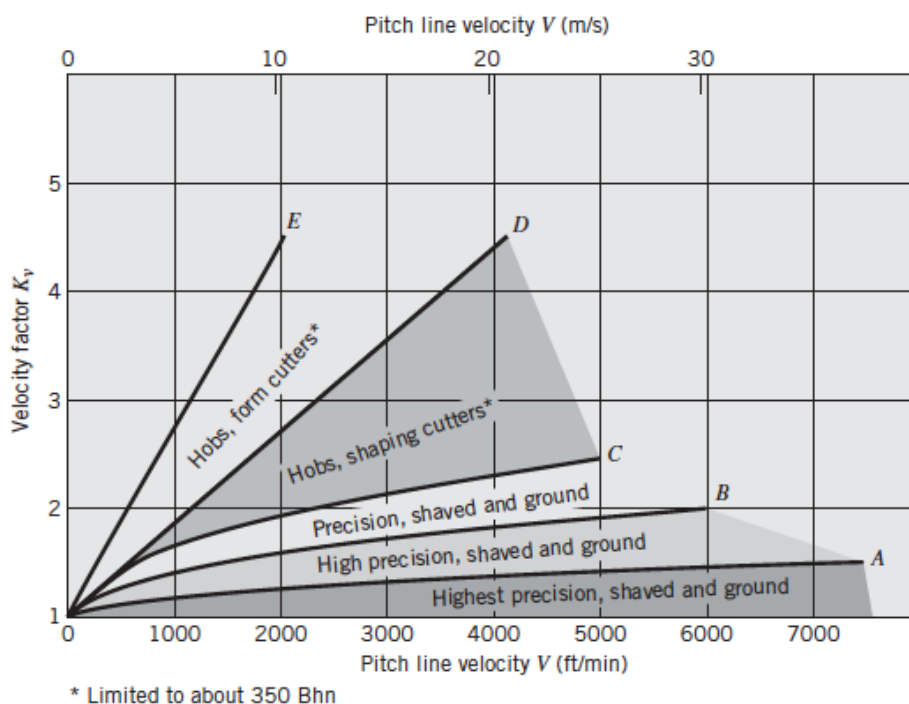


Figure 6.6: Graph for determining velocity factor,  $K_v$

Table 6.1: Overload correction factor,  $K_o$

Source of Power	Uniform	Moderate Shock	Heavy Shock
Uniform	1,00	1,25	1,75
Light shock	1,25	1,50	2,00
Medium Shock	1,50	1,75	2,25

Table 6.2: Mounting correction factor,  $K_m$

Characteristics of Support	0 - 2	6	9	16
Accurate mounting, small bearing clearances, minimum deflection, precision gear	1,3	1,4	1,5	1,8
Less rigid mountings, less accurate gears, contact across the full face	1,6	1,7	1,8	2,2
Accuracy and mounting such that less than full-face contact exists	over 2,2	over 2,2	over 2,2	over 2,2

$K_o$  is selected under the assumption that the source of power working on the gears are uniform. The assumption is based on the smooth operation of the paint robot and carefulness while opening doors and bonnets of cars.

$$K_o = 1$$

$K_m$  is a result of accurate mounting, small bearings clearances minimum deflection, precision gear. This approximation was made based on general understanding of the characteristics of support.

$$K_m = 1,3$$

The pitch line velocity of the gear is 0,48269 m/s. This is found by converting the angular velocity  $\omega$ , of axis five from degrees per second to radians per second.

$$350^\circ/s \approx 6,11 \text{ rad/s}$$

Then multiplied with the radius  $r$  of the sixth gear in meters.

Given that the precision of the gear is not specified the midpoint of graph C and D are used giving an velocity or dynamic factor of 1 [2].

$$K_v = 1$$

The velocity of the axis 4, 5 and 6 are 465 °/s, 350 °/s and 535 °/s, respectively Inserting all the values in Equation 6.7. The gear tooth surface fatigue will equal:

$$\sigma_H = 1686,32 \text{ MPa}$$

According to Equation 6.7 the value of the gear tooth surface fatigue calculated greater then the yield strength. The value should be smaller than the bending stress. This is due to the fatigue being a harm process over time. Given that the surface fatigue is as high as calculated the gear will immediately break, as understood from Subsection 2.1.2 of gear fatigue.

The factors  $K_v$ ,  $K_o$  and  $K_m$  selected based on estimation with permission from the external supervisor. There are some concerns regarding the geometry factor  $I$ . The value calculated is relatively low and is the main reason due to the high surface fatigue.

## 6.2 Spur Bevel Gear with Larger Face Width

If the payload capacity was to be increased to 20 kg with no change in the shape or material for the gears the calculations below show which dimensions that are needed to change and how much.

- **Tangential Force:**

The ratio between the two loads are  $r = \frac{20 \text{ kg}}{13 \text{ kg}} = 1,538$ . Then, from Equation 6.5 the new tangential force is found :

$$F_{t(20 \text{ kg})} = r \times F_t = 6631.77 \text{ N}$$

- **Bending Stress:**

The new bending stress is calculated by Equation 6.6:

$$\sigma_{(20 \text{ kg})} = \frac{F_{t(20 \text{ kg})}}{m \times b \times Y} = 808,752 \text{ MPa}$$

To withstand 20 kg the face width needs to be increased. The  $\sigma_{(20 \text{ kg})}$  is further used to calculate the needed face width.

After deriving the Equation 6.6 the following equation is given.

$$b = \frac{F_{t(20 \text{ kg})}}{m \times Y \times \sigma_{(13 \text{ kg})}} \quad (6.8)$$

The maximum bending stress for spur bevel gears when it withstand 13 kg is  $\sigma = 525,689 \text{ MPa}$ , therefore, by keeping the maximum bending stress constant and by using Equation 6.8, the new face width can be calculated.

$$b = \frac{6631,752}{2 \times 0,41 \times 525,689} = 15,384 \text{ mm}$$

Gears with face width of 15,38 mm can give the opportunity to increase the payload capacity up to 20 kg.

A consequence of increasing the face width of a spur bevel gear is that simultaneously the diameter of the entire gear couple will also increase.

## 6.3 Helical Bevel Gears

- **Geometry and Nomenclature:**

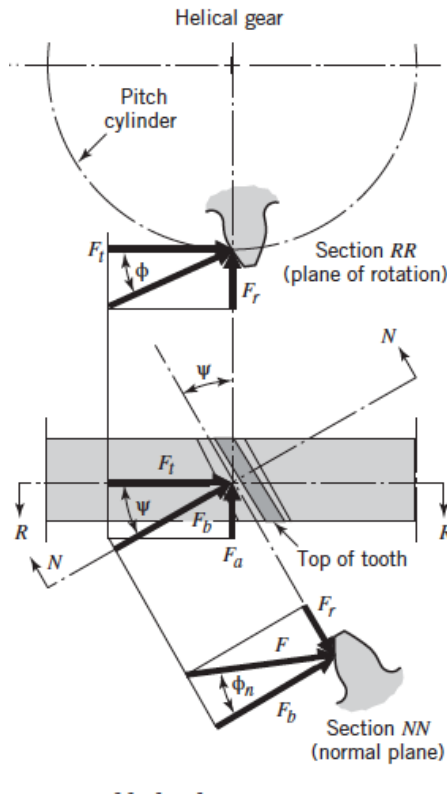


**Figure 6.7:** Force components in helical gears.

The helix angle, known as  $\psi$ , is always measured on the cylindrical pitch surface. The values of  $\psi$  are not standardized but commonly range among  $15^\circ$  and  $30^\circ$ . Higher values tend to give smoother operations. Helical gears exist as right- and left handed, defined the same as for screw thread.

Figure 6.7 illustrates that the circular pitch ( $p$ ) and pressure angle ( $\phi$ ) are measured in the axis of rotation, as for spur bevel gears. In addition to ( $p$ ) and ( $\phi$ ) the figure also shows  $\psi$  to the teeth. Pitch diameter is defined as the number of teeth per unite of pitch diameter;

$$P = \frac{N}{d} \tag{6.9}$$

Using Equation 6.9, the following can be calculated

$$P = \frac{79}{158} = \frac{57}{114} = 0,5 \text{ teeth/mm}$$



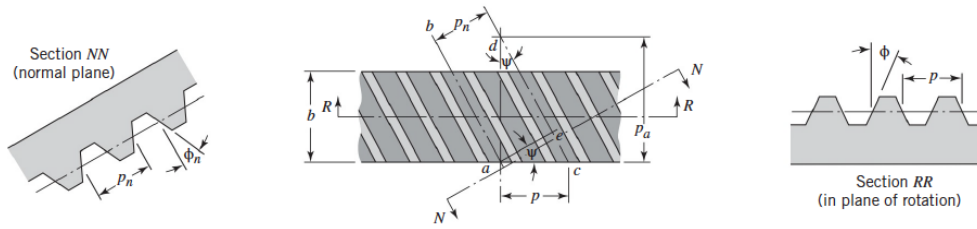


Figure 6.8: Portion of a helical rack.

By keeping the face width  $b$  constant at 10 mm as shown in Figure 6.8 and choosing a helix angle of  $30^\circ$  then by using trigonometric ratio to calculate the pitch line (tooth length,  $F$ ):

$$\cos \psi = \frac{\text{adj}}{\text{hyp}} \tag{6.10}$$

$$\text{hyp} p_1 = \frac{5}{\cos 30^\circ} = \frac{10\sqrt{3}}{3} \text{ mm} \rightarrow \text{hyp} = 2 \times \frac{10\sqrt{3}}{3} = \frac{20\sqrt{3}}{3} \text{ mm}$$

• **Gear-Tooth-Bending Stress(Lewis Equation):**

The bending stress equation for straight helix gear teeth is given by:

$$\sigma = \frac{F_t(20kg) \times P}{F \times J} \times K_v \times K_o \times (0,93 \times K_m) \tag{6.11}$$

The constant of 0,93 is introduced in the Equation 6.11. This is because the mounting condition has a lower sensitivity for helical gears.

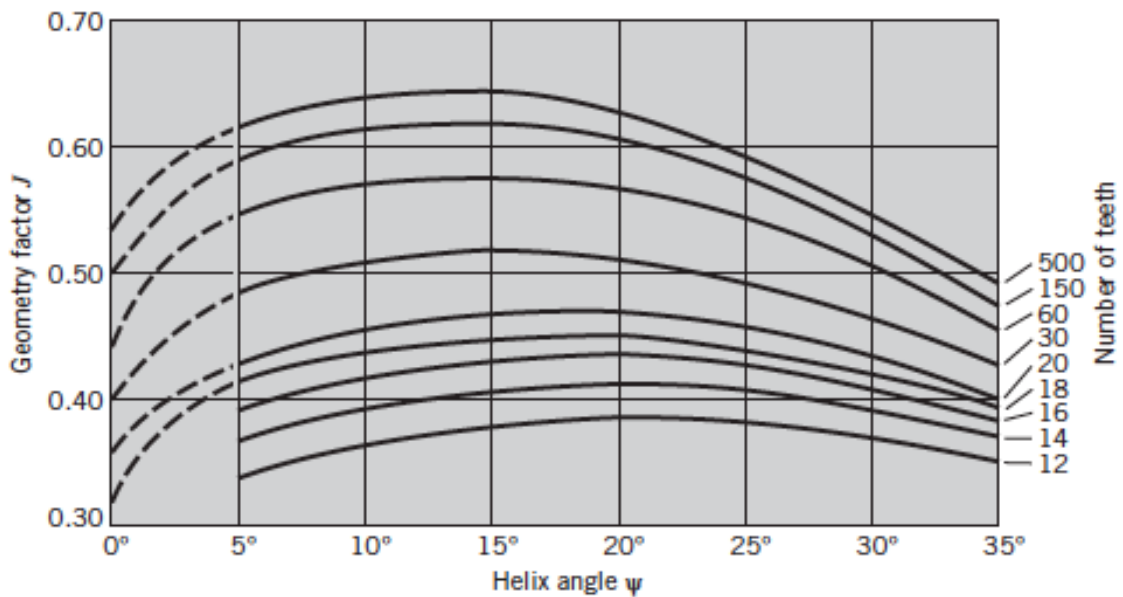


Figure 6.9: Graph for determining geometry factor,  $J$

Where:

- J: Spur gear geometry factor, as shown in Figure 6.9, (Shaft angle 90°)
- P: is circular pitch.
- F: is the pitch line.

$$P = 0,5$$

$$J = 0,5$$

$$F = \frac{20 \times \sqrt{3}}{3} \text{ mm}$$

The calculation below shows the gear tooth bending stress for helical gear with loading of 20 kg results in

$$\sigma = 694,363 \text{ MPa}$$

## 6.4 Emergency Stop

Emergency stop will effect the bending stress. Due to the emergency stop not being cyclic, there is a risk for the gear to break. In case of emergency stop the forces acting on the gears will be multiplied with the ratio that can be found by

$$R = \frac{\tau_{\text{Emergency stop}}}{\tau_{\text{Normal operation}}} \Rightarrow \frac{6,14602}{2,90023} = 2,119 \quad (6.12)$$

The value for the torque is obtained from Appendix G.

After calculating the tangential force in the case of emergency stop, the rest of the calculation will be the same as above, accept some of the factors that should be chosen correctly according to the information that have been changed for this case. The value for the overload factor,  $K_o$  from Table 6.1, changes as the source of power is no longer uniform. The new value is based on a heavy shock and set to 2,25. The  $K_o$  factor will again increases the value of surface fatigue stress.

## 6.5 Material Properties

**Table 6.3:** Chemical composition properties.

<i>Material</i>	<i>C%</i>	<i>Si%</i>	<i>Mn%</i>	<i>P% Max</i>	<i>S% Max</i>	<i>Cr%</i>	<i>Ni%</i>
<b>16MnCr5</b>	0,14-0,19	0,40	1,00-1,30	0,035	0,035	0,80-1,10	
<b>18NiCrMo55</b>	0,15-0,21	0,15-0,40	0,60-0,035	0,035	0,035	0,70-1,00	1,20-1,50
<b>34CrNiMo6</b>	0,30-0,38	0,40 max	0,5-0,8	0,025	0,035	1,3-1,7	1,3-1,7

**Table 6.4:** Mechanical properties.

<i>Material</i>	<i>Thickness t [mm]</i>	<i>Yield strength Re [N/mm<sup>2</sup>]</i>	<i>Tensile strength Rm [N/mm<sup>2</sup>]</i>	<i>Elongation A [%]</i>	<i>Hardness HB [N/mm<sup>2</sup>]</i>
<b>16MnCr5</b>	<11	735	1030-1070	min. 8	311-394
<b>18NiCrMo55</b>	<11	980	1230-1520	min. 8	≤240
<b>34CrNiMo6</b>	<8	min. 1000	1200 –1400	min. 9	360

EN 34CrNiMo6 Steel is a good suggestion for material to produce the gears used in the hollow wrist in. This is because the material has great strength, toughness and a good harden-ability. This types of steel is resistance stable to overheating. The ability of welding is less impressive due to the temper brittleness. To release the stress after the weld process, the steel needs a high temperature heating [49].

Table 6.3 and Table 6.4 show the chemical composition and properties respectively for three types of materials, the data is retrieved form the Appendix B, Appendix C and Appendix D. 16MnCr5 and 18NiCrMo55 are the materials used today for gears five and six respectively, on the fifth axis. Both materials has a low carbon contents between 0,14 to 0,21 percent. As it has been mentioned before, by increasing the carbon contents the material will be stronger and by choosing 34CrNiMo6 as an alternative material for both gears with 0,3 to 0,38 percent carbon contents will the strength of the gears are increased which results to an increase the payload capacity.

# Chapter 7

## Discussion

In this thesis several improvement methods for the paint robot has been studied. The payload capacity is attempted increased by various methods, as well as the production method of mechanical parts. The roughness value  $R_a$  is attempted lowered for the paint system to minimize the risk of paint loss. By combining information, data and specification from ABB, the solutions are produced to fit their specific use case.

### 7.1 Gear

By keeping the gear as a spur bevel gear, the calculations in Chapter 6 resulted in an increase of the face width of 5,384 mm for the hollow wrist to bear 20 kg of payload capacity. The new dimension of the gear is found by a form factor from the current design. Given that the calculations are based on measurements of the current hollow wrist the safety factor is already included. The scaling factor calculated from the wanted payload capacity compared to current payload capacity includes the safety factor.

Given the shaft angle of the gears, increasing the face width will also result in increasing the diameter. This will lead to the domino effect where the mating gear module will need to be changed. Taking into account the complex geometry of the hollow wrist the total wrist needs to be re-designed in order to make space for the new dimensioned gears, if this is desired.

The helical gear has, as mentioned in Subsection 2.1.1, obvious advantages and disadvantages. The axial forces in the gears results in efficiency loss. There are today no standards and no companies producing helical gear with a shaft angle of 145°. If this idea was chosen it must be specially ordered and produced. Changing the gear format from spur bevel gear to helical bevel gear will result in reducing the bending stress effecting the gear with 114,389 MPa. Given that the gear is exposed to 808,752 MPa while bearing 20 kg with spur bevel gear, the bending stress is reduced with 16,4 %. This will result in an increase in bearing capacity of approximately 2,14 kg.

The processes focused on for improving both the surface hardness and the fatigue life for any steel alloys by carburizing or nitriding. Carburizing is a process to increase the hardness by increasing the carbon content of the steel. This process is very sensitive and should be conducted carefully and under control. Over carburizing of the material may lead to embrittlement which is highly unwanted. Increasing the carbon concentration will influence the rusting properties together with yield and tensile strength.

Nitriding is a sophisticated technique for hardening the surface of metallic sections. The case of the gear is strengthen by this process while the downside is the risk of over increasing the nitrogen atoms. This will result in a reduction of the quality by making the material brittle and too hard, resulting in a reduction in the ductility. The reduction in ductility may lead to fracture due to the shock the gear is exposed for in touch with the mating gear. This will minimize the smoothness in transition of forces between the teeth. This combined with the brittle surface increases the risk of crack initiation. Nitriding has several benefit for producing a stronger material. It is a cost efficient method to improve capabilities, therefore this strategy has been popular. Increasing the hardness of the gear coupling is fundamental to achieve the desired properties for bearing the payload that is requested. Another option that has been discussed is the material selection and processing the gears.

*18NiCrMo55* has a relatively high tensile and yield strength. To reduce the risk for micro-welding the two gears should consist of different material. From the materials presented in Table 6.4, the *15MnCr5* material should be substituted with *34CrNiMo6*. The material contains greater tensile and yield strength and therefore has the ability to withstand a larger bending stress. In terms of this use case the material is recommended. In general there is a drawback regarding the weakness of welding. In this process the welding application is not in use and therefore not relevant. To increase the tensile further the material is also prone to both carburizing and nitriding.

## 7.2 Manufacturing

The comparison of traditional manufacturing with AM shows advantages and disadvantages with both the methods. Traditional manufacturing uses old and well tested methods which makes the results highly predictable with a well understood economical model combined with a large supply network. While AM is a relatively new development which is more immature expensive and less predictable given the lack of testing. The different methods has, as described in the theory, still a large potential. Today AM is used producing parts that are impossible or difficult to produce in other ways. It is also cost beneficial to use AM while the production volume is relatively low and the part consists of complex geometry with internal channels.

AM has several different production methods, such as Metal Material Extrusion, Powder Bed Fusion, Binder Jetting and Directed Energy Deposition. All of them were previously evaluated against specific parameters in Chapter 4. DED is primarily meant to add features to existing parts, therefore it is not suitable to producing the block. The rest of the methods are all capable of producing the desired part, but each method has different challenges.

BJ has a decent material selection available with several mechanical properties to a still high, but lower cost than PBF. It is a powder based system and has every disadvantages related to it, as described in Subsection 2.2.4 including material handling. There is a large competition within the industry and given that the patents are expiring the capabilities of these methods are expected to increase.

PBF is the other powder based system. PBF is further developed than BJ. The material selection of PBF is the widest of all AM methods and can print a few dozen different materials with the best mechanical properties within AM. The biggest problem is the cost for both the machine and material which is relatively high.

MME is currently most feasible as a rapid prototyping method and can be a useful tool to visualise parts in a development. The limited material selection with decent mechanical properties makes it difficult to recommend for a full scale production. Not to mention the lack of any aluminium alloy available.

Binder Jetting and Powder Bed Fusion are viable options that both need to be considered. Today AM can not compete against traditional manufacturing on small and standardised parts as rings, bolts, bearing, pins and simple circular parts. This is due to both the price being lower for traditional printing method and the lack of benefits of an AM production. AM is not suitable for gear design as it requires a

lot of precision which this method does not provide. The structural casing of the hollow wrist is suitable for AM together with the test piece. The casing is currently casted before the machining process to reach the desired specifications which leads to a lot of material loss. This can be optimized by, for instance, first printing the casing, then machining it to the wanted tolerance. It could also potentially have thinner walls with a pattern to keep the strength and reduce weight. The weight-saving will result in a minor increase in payload capacity. Similar patterns are used in rocket farings. This is often done by expensive machining. Doing the same with AM does not increase the build time and will save weight and in addition give valuable experience on how to effectively use the method and how future project can implement.

Chapter 5 describes the possibility of proposing a design for a test block, to ensure the proposed post treatment process is feasible and will provide the desired results. The block itself can be produced by AM in any desired metal composition by most printing processes. The main focus has been put on 316L stainless steel due to a lot of knowledge and previous studies being available. Aluminium and POM is used in current designs and as seen in Section 4.1 equivalent materials should be strong enough. During the design of the block the most important channels and shapes are carefully chosen. The amount of channels used were important, and there are arguments to both increase and decrease the amount. By having multiple channels the results will become more accurate and cover more cases. On the other hand, the process of testing will require more time. The case for removing channels is harder to justify. Removing one channel would not reduce the size of the block and the data then lost is greater than the cost saved. The design of the block itself seems to be of a good compromise but the selection of material and medium is harder.

From the environmental point of view the AM production method will reduce the need of raw material in production. As previously discussed in Subsection 2.2.4, several studies conclude with the fact that there are not enough information to conclude with either that AM is more or less environmental friendly. ABB has a long history and a rich heritage of technology innovation. AM is innovative and has the potential to be the new green production method.

## 7.3 Surface Treatment of Test Block

Abrasive blasting is an cheap and excellent method of improving the external surface of any rough part. The method has some difficulties while working on internal surfaces with complex geometries such has the test block. By abrasively blasting the internal surfaces of the test block the surface will become uneven. The method struggles with channels containing bends where the inner wall will be less smooth due to the high pressure and the sand following the outer bend. From the studies of chemically assisted vibrator finish and combination of them together, described in Subsection 2.4.1, valuable information is attained. Both VF and CAVF are methods that has the ability to remove the spatter effect and achieves almost alike roughness values. Figure 2.17 shows how  $R_a$  value of each of the processes developed reaches the lowest roughness. The report proves, the best process is the chemically assisted vibro-finishing, allowing it to reach the desired results of the roughness value.

Abrasive Flow Machining Extrude Hone are interesting methods. AFM and COOLPULSE are variants of electropolishing. The tests are performed by Extrude Hone and includes both methods. The CP requires a part to be placed within the channels that are to be polished. This may be challenging to execute for some internal channels consisting of bends with an angle such as a  $90^\circ$ . Even excluding the CP method, the part tested is short and straight in shape which is resulting in the best case scenario for the method. AFM works best in the entrance of straight channels and struggles with bends. This solution is encouraging and should be considered, but exporting similar results for different shapes is to be optimistic.

A more realistic and potentially more relevant study is the one made by AFM, described in Subsection 2.4.3. This study has a focus at a bent part and show data for multiple tests after a given amount of passes. The importance of build-direction of a AM part is whats interesting and how this will effect the results. To achieve a surface roughness with an  $R_a$  value of  $0.8 - 1.6 \mu\text{m}$ , the number of passes needed is in the range of 50 to 100 with the right abrasive medium according to this method.



# Chapter 8

## Conclusion

The change of the gear geometry, from spur bevel gear to helical bevel gear, increases the payload capacity with 2,14 kg. To reach the desired payload capacity which is 20 kg the best suited option is to increase the size of the gear coupling. If the gear size is increased to have a face width of 15,384 mm it would be able to handle the requested load without changing the geometry or material it consists of. For this to be processed there is a need for expanding the hollow wrist to make space for the new coupling.

For the production method by AM the Powder Bed Fusion has the widest material selection with great material properties. The method is also the most developed and mature. A disadvantage for the PBF system is the cost. The test block produced by PBF will have a rough surface and require a post processing methods to reach the criteria set by ABB. One of the benefits of using AM to create both the test block and the casing is the opportunity to produce parts that previously where impossible to produce in one piece. It is recommended to produce the test block in aluminium. This is due to the pressure the test block is exposed for is relatively low and aluminium is the cheapest material to produce in which also meets the criteria set.

To avoid paint sticking to the surfaces of the test block a post processing method is required. From the discussed options, the Abrasive Flow Machining provides the most predictable results and can be adjusted to each use case. The test block consists of channels with different radii and bends which makes the AFM the best suited option.

# Bibliography

- [1] ABB, “Irb 5510, medium-sized paint robot.” <https://new.abb.com/products/robotics/industrial-robots/irb-5510>, 2020.
- [2] J. . Marshek, *Fundenmentals of machine component design*. Sixth edition, Wiley, 2017.
- [3] A. G. M. Association, *A Rational procedure for the Preliminary Design of Minimum Volume Gears*. American Gear Manufacturers Association, 1992.
- [4] M. Bjornes, “Analyse og redesign av gir og girhus for elektromotor,” Master’s thesis, NTNU, 2015.
- [5] T. Stålvalsguide, “Steel selection guide,” 2012. <https://www.google.com/url?sa=t&rct=j&q=&esrc=s&source=web&cd=&ved=2ahUKEwiphv21g4DwAhXR-yoKHRhWBp8QFjAAegQIBBAD&url=https%3A%2F%2Fssabwebsitecdn.azureedge.net%2F-%2Fmedia%2Ffiles%2Ftibnor%2Fbrochures-and-datasheets%2Fsweden%2Fspecialstal%2Fsteel-selection-guide.pdf%3Fm%3D20190409113319&usg=AOvVaw2FwhicSXjhflxwMupvBIw5>.
- [6] M. Savolainen and A. Lehtovaara, “An approach to investigating subsurface fatigue in a rolling/sliding contact,” *International Journal of Fatigue*, vol. 117, pp. 180–188, 2018.
- [7] K. A. Zakaria, S. Abdullah, and M. Ghazali, “A review of the loading sequence effects on the fatigue life behaviour of metallic materials,” *Journal of Engineering Science and Technology Review*, vol. 9, pp. 189–200, 10 2016.
- [8] W. D. Callister and D. G. Rethwisch, *Materials science and engineering*, vol. 5 of *ninth edition*. John wiley & sons NY, 2014.
- [9] D. Pye, “Nitriding of gears.” <https://themonty.com/nitriding-of-gears-by-david-pye/>. (accessed May 9, 2021).

- [10] K.-M. Winter, J. Kalucki, and D. Koshel, "Process technologies for thermochemical surface engineering," in *Thermochemical surface engineering of steels*, pp. 141–206, Elsevier, 2015. <https://www.sciencedirect.com/topics/engineering/plasma-nitriding>.
- [11] A. Szilágyiné Biró, "Active screen plasma nitriding state of the art," *Conference Series*, vol. 7, pp. 103–114, 01 2014.
- [12] J. Koenig, S. Hoja, T. Tobie, F. Hoffmann, and K. Stahl, "Increasing the load carrying capacity of highly loaded gears by nitriding," in *MATEC Web of Conferences*, vol. 287, p. 02001, EDP Sciences, 2019.
- [13] "Safety factor." [https://www.engineeringtoolbox.com/factors-safety-fos-d\\_1624.html](https://www.engineeringtoolbox.com/factors-safety-fos-d_1624.html). (accessed May 9, 2021).
- [14] M. Groover, *Fundamentals-of-Modern-Manufacturing-4Th-Edition-By-Mikell-P-Groover*. fourth edition, John Wiley & Sons, InC, 2010. <https://aluminium-guide.com/wp-content/uploads/2019/04/fundamentals-of-modern-manufacturing-4th-edition-by-mikell-p-groover.pdf>.
- [15] S. Bragg, "Repetitive manufacturing definition," *AccountingTools*, December 2020. <https://www.accountingtools.com/articles/2017/7/27/repetitive-manufacturing>.
- [16] B. L. Goldense, "The five types of manufacturing processes," *Machine Design*, vol. 87, p. Page 88, 09 2015.
- [17] "Metal casting." <https://engineeringproductdesign.com/knowledge-base/metal-casting/>, 2021. (accessed May 9, 2021).
- [18] C. Silbernagel, "Additive manufacturing 101-5: What is powder bed fusion?," *Canada Makes*, May 2018. <http://canadamakes.ca/what-is-powder-bed-fusion/> (accessed May 9, 2021).
- [19] "Metal 3d printing." <https://www.3dhubs.com/guides/metal-3d-printing/>. (accessed Feb 12, 2021).
- [20] R. Castells, "Dmls vs slm 3d printing for metal manufacturing," *Element*, Jun 2016. <https://www.element.com/nucleus/2016/06/29/dmls-vs-slm-3d-printing-for-metal-manufacturing>.
- [21] M. Ziaee and N. B. Crane, "Binder jetting: A review of process, materials, and methods," *Additive Manufacturing*, vol. 28, pp. 781–801, 2019. <https://www.sciencedirect.com/science/article/pii/S2214860418310078>.

- [22] S. Terry, I. Fidan, and K. Tantawi, "Preliminary investigation into metal-material extrusion," *Progress in Additive Manufacturing*, vol. 6, no. 1, pp. 133–141, 2021.
- [23] L. Dale, "About additive manufacturing, directed energy deposition," *Loughborough University*, 2021. <https://www.lboro.ac.uk/research/amrg/about/the7categoriesofadditivemanufacturing/directedenergydeposition/> (accessed May 9, 2021).
- [24] "What is directed energy deposition (ded)?" <https://www.twi-global.com/technical-knowledge/faqs/directed-energy-deposition>, 2021. (accessed May 9, 2021).
- [25] "Lens material." [https://optomec.com/3d-printed-metals/lens-materials/?fbclid=IwAR39YFqBIckbzofRj\\_W2tuyuSsLvBsTz9Mc2560IL5oibAMq4sq8wR5Pq1o](https://optomec.com/3d-printed-metals/lens-materials/?fbclid=IwAR39YFqBIckbzofRj_W2tuyuSsLvBsTz9Mc2560IL5oibAMq4sq8wR5Pq1o), 2020. (accessed May 9, 2021).
- [26] F. Le Bourhis, O. Kerbrat, J.-Y. Hascoet, and P. Mognol, "Sustainable manufacturing: evaluation and modeling of environmental impacts in additive manufacturing," *The International Journal of Advanced Manufacturing Technology*, vol. 69, no. 9-12, pp. 1927–1939, 2013.
- [27] K. Kellens, R. Mertens, D. Paraskevas, W. Dewulf, and J. R. Dufloy, "Environmental impact of additive manufacturing processes: does am contribute to a more sustainable way of part manufacturing?," *Procedia Cirp*, vol. 61, pp. 582–587, 2017.
- [28] A. Huckstepp, "Powder bed fusion (pbf)." <https://www.digitalalloys.com/blog/powder-bed-fusion/>. (accessed May 11, 2021).
- [29] J. P. Davim, "A note on the determination of optimal cutting conditions for surface finish obtained in turning using design of experiments," *Journal of materials processing technology*, vol. 116, no. 2-3, pp. 305–308, 2001.
- [30] J. Cassidy, "More than scratching the surface," *The Pennsylvania State University*, 2010.
- [31] "Abrasive flow machining (afm)." <https://www.youtube.com/watch?v=-t3vvjRhicI&t=1s>. (accessed May 9, 2021).
- [32] "Abrasive flow machining (afm)." <https://extrudehone.com/products/abrasive-flow-machining-afm/>. (accessed May 9, 2021).

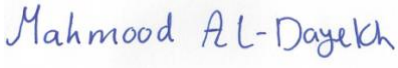


- [33] M. Hamidi, A. Falzetti, A. Redaelli, N. Lecis, A. Giussani, L. Sala, and M. Vedani, "Finishing of internal and external surfaces produced by powder bed fusion," in *Joint Special Interest Group meeting between euspen and ASPE Dimensional Accuracy and Surface Finish in Additive Manufacturing*, pp. 1–3, GBR, 2017.
- [34] P. M. at Extrude Hone; Robert Binder & Business Development Manager Turbomachinery; Lukas Fuchs, "Extrude hone's coolpulse and afm enable cost-effective surface finishes," *EOS GmbH*, 2018.
- [35] C. Bouland, V. Urlea, K. Beaubier, M. Samoilenko, and V. Brailovski, "Abrasive flow machining of laser powder bed-fused parts: numerical modeling and experimental validation," *Journal of Materials Processing Technology*, vol. 273, p. 116262, 2019.
- [36] "Metal materials." <https://www.3dsystems.com/materials/metal>, 2021. (accessed Mar 18, 2021).
- [37] "Materials engineered to perform." <https://www.desktopmetal.com/materials>, 2020. (accessed Mar 18, 2021).
- [38] "Materials for 3d printing." <https://digitalmetal.tech/materials/>, 2021. (accessed Mar 18, 2021).
- [39] "Dmls materials for additive manufacturing of metal parts." <https://www.eos.info/en/additive-manufacturing/3d-printing-metal/dmls-metal-materials>, 2021. (accessed Mar 18, 2021).
- [40] "Metal 3d printers - materials & binders." <https://www.exone.com/en-US/3d-printing-materials-and-binders/metal-materials-binders>, 2021. (accessed Mar 18, 2021).
- [41] "Powders." <https://www.ge.com/additive/powders-overview>, 2021. (accessed Mar 18, 2021).
- [42] "3d printing materials." <https://markforged.com/materials/>, 2021. (accessed Mar 18, 2021).
- [43] "Lens materials." <https://optomec.com/3d-printed-metals/lens-materials/>, 2020. (accessed Mar 18, 2021).
- [44] "Metal powders supply." <https://www.renishaw.com/en/metal-powders-supply--31458>, 2021. (accessed Mar 18, 2021).
- [45] "Electron beam additive manufacturing (ebam®)." <https://www.sciaky.com/additive-manufacturing/electron-beam-additive-manufacturing-technology>, 2021. (accessed Mar 18, 2021).

- [46] “Materials.” <https://www.slm-solutions.com/products-and-solutions/powders/>, 2021. (accessed Mar 18, 2021).
- [47] P. Dutta, S. K. Saha, and N. Nandi, “Computational study of turbulent flow in pipe bends,” *International Journal of Applied Engineering Research*, vol. 10, no. 11, p. 2015, 2015.
- [48] B. Dengel, “Under pressure,” 2017. <https://gearsolutions.com/departments/tooth-tips-under-pressure/>.
- [49] “En din 34crnimo6 | 1.6582 | 4337 engineering steel,” 2020. <http://www.astmsteel.com/product/34crnimo6-steel/>.

# **Appendix A**

## **Pre-Study Report**

## PRE-STUDY REPORT for BACHELOR THESIS

Study program/Specialization: Bachelor's Degree Program, Specialization in mechanical engineering and Materials Science	Spring semester, 2021  Open / Restricted access
Writer:  MAHMOOD AL-DAYEKH  SIMON BELAY  AKSEL SØRAUNET	  
Faculty supervisor: <i>Hirpa G. Lemu, UiS</i>  External advisor: <i>Jakob Trydal, ABB AS</i>	
Thesis title:  <b>Component Design and study of additive manufactured parts for a paint robot</b>	
Credits (ECTS): 20	
Keywords:  Design and Calculations Production method Cost analysis Environmental inspection Additive manufacturing	Pages: 12  Stavanger, UIS, 29.01.2021.



# Pre-study report ABB spring 2021

Mahmood Al-Dayekh, Simon Belay, Aksel Søråunet

May 14, 2021

# Preface

This is a pre-study report for the bachelor thesis for "Component Design and study of additive manufactured parts for a paint robot" in mechanical engineering. The thesis will be written by Mahmood Al-Dayekh, Simon Belay and Aksel Søråunet and will be completed in May 2021 at the University of Stavanger.

The milestones for the thesis will be presented in this report along with the Gantt chart that gives a guideline for the complete thesis.

The thesis is written in collaboration with ABB Bryne. ABB is a leading global technology company that energizes the transformation of society and industry to achieve a more productive, sustainable future. ABB Bryne is part of ABB's robotic branch and focuses on making paint robots design for the automotive industry and other applications [1].

# Contents

<b>1</b>	<b>Introduction</b>	<b>1</b>
1.1	Background . . . . .	1
1.2	Primary Goals . . . . .	2
<b>2</b>	<b>Thesis overview</b>	<b>3</b>
2.1	Design and calculation . . . . .	3
2.2	Production method . . . . .	3
2.3	Cost analysis . . . . .	4
2.4	Environmental inspection . . . . .	4
2.5	Additive manufacturing . . . . .	4
<b>3</b>	<b>Limitations</b>	<b>5</b>
3.1	Design limitations . . . . .	5
3.2	IP 54 Regulations . . . . .	5
3.3	Financial limitations . . . . .	5
3.4	Environmental limitations . . . . .	6
3.5	Time Limitations . . . . .	6
<b>4</b>	<b>Planning</b>	<b>7</b>
4.1	Gantt chart . . . . .	7
	<b>References</b>	<b>10</b>

# Chapter 1

## Introduction

### 1.1 Background

ABB is a leading global technology company that energizes the transformation of society and industry to achieve a more productive, sustainable future. By connecting software to its electrification, robotics, automation and motion portfolio, ABB pushes the boundaries of technology to drive performance to new levels. With a history of excellence stretching back more than 130 years, ABB's success is driven by about 110,000 talented employees in over 100 countries) [1].

One of their branches is at Bryne, where ABB has a project to develop robot IRB-5510. This paint robot provides a shorter cycle time, process optimization, and digital platform to ensure premium paint quality and up-time. IRB 5510 is equipped with ABB's hollow wrist technology. This high-precision hollow wrist features a straight design that eliminates wear and tear on the paint- and air-supply hoses, increasing overall reliability. The wrist supports 140-degree rotation in any direction, making IRB 5510 one of the most versatile and easy-to-program paint robots in its class [2].

## **1.2 Primary Goals**

The primary goal of the thesis is to explore the existing ABB Hollow Wrist and evaluate alternative ways to produce it. Including additive manufacturing, cost- and environmental analysis. The wrist must keep its reach, and keep or increase its payload capacity. It should meet the same IP54 rating as current design. The wrist must have the same level of surface quality to bearings and evaluate different ways to achieve this.

Additive manufacturing of metal components has in recent years become more accessible on the market. This method of production gives immense flexibility when designing and complexity of parts that was previously unthinkable. Therefore, exploring ways to produce some, or all, components this way can be beneficial.

# Chapter 2

## Thesis overview

The thesis will contain several categories. Design and calculation, production method, cost analysis, environmental inspection and additive manufacturing are the most comprehensive chapters. For this pre-study report only the mentioned categories will be discussed. The design process and calculations are dependent on each other. Therefore, those two processes will be discussed in the same section only for this pre-study report.

### 2.1 Design and calculation

ABB is currently using a Hollow Wrist that has a payload capability with a maximum of 15 kg. Usually ABB focuses on two different strength characteristics of their robots. Fatigue fracture during normal operation, as well as yield strength at emergency stop or any mechanical stop on the robot.

### 2.2 Production method

The main focus of the thesis is to explore different production methods and evaluate the impact these changes has on the system. This include methods such as casting, machining, additive manufacturing and comparison to current method. Post processing is usually required and it is important to see the effect on the quality of the product, time spent and the cost associated with these methods.

## 2.3 Cost analysis

To ensure that a product is viable for an economic standpoint it is necessary to take the cost of the product in to consideration. Therefore a cost analysis is a good method to evaluate different solutions. It is important to take both running cost together with the upfront investment in to consideration and analyse it for a long term solution.

## 2.4 Environmental inspection

Sustainability is currently one of the most important topics of the world. Therefore it is more important than ever to ensure that new products does not contribute to this ever growing problem. By selecting environmental friendly products and production methods it is possible to limit the environmental footprint of the part, and this will play a big part in the thesis.

## 2.5 Additive manufacturing

Additive manufacturing, commonly known as 3D printing, is a principally different way of producing parts compared to traditional methods.

Additive manufacturing is a process of making three dimensional solid objects. The creation of a 3D printed object is achieved using additive processes. In an additive process an object is created by laying down successive layers of material until the object is created. Each of these layers can be seen as a thinly sliced cross-section of the object [3].

Additive manufacturing provides the opportunity to produce designs that would not previously be possible with traditional machining. The technology also makes it possible to engineer customized product characteristics, such as optimized heat conductance or resistance and high strength or stiffness.

Two basic factors that can effect the cost and the quick growth of additive manufacturing are the amount and the type of material being used, additionally to the printing process and printing time. Other than these factors, the only cost related to edit or change an existing design is the time required to alter its digital 3D model [4].

# Chapter 3

## Limitations

### 3.1 Design limitations

The hollow wrist is a part used by many of ABB robots. In this thesis the connection between the wrist and robot is given. Therefore the connection will be maintained so the new part can be retrofitted on existing robots. The outer connection will be retained to please the customers expectations. Its also a goal to keep the same overall size, but small changes may accrue. For many reasons including software tweaks the length of the wrist should be the same.

### 3.2 IP 54 Regulations

The IP 54 regulation includes the protection of the wrist. It states that the gasket should protect the part from dust and heavy flushing from all angles. The main reason for this is that the equipment must be protected against liquids and dust that can have a harmful effect on the machine. The machine operates in an environment where there is a lot of airborne dust and paint that is flammable. IP 54 is therefore a necessary security measure to protect both people and machines [5].

### 3.3 Financial limitations

Money is an important factor while designing new parts. It is not a given budget for the project but the goal is to produce at the cheapest possible price but at the same time try to satisfy the criteria such as functionality, viability and environmental friendliness.



## **3.4 Environmental limitations**

ABB is restructuring society and industry to achieve a more productive and sustainable future. The focus on a sustainable future is interesting and a modern day issue. Therefore, the environmentally friendly aspects of production and material selection are important [1].

Environmentally friendly measures often challenge the financial budget. Therefore, in the thesis, a careful assessment will be made of the advantages and disadvantages of the environmentally friendly measures and these will be assessed against each other.

## **3.5 Time Limitations**

The thesis will be handed in the 15 of May 2020. Therefore time management is an important factor. The Gantt chart is an estimate of time distribution. For this reason, extra time has been added in the Gantt chart as challenges and unforeseen events are expected. Read more about this in chapter 4.

# Chapter 4

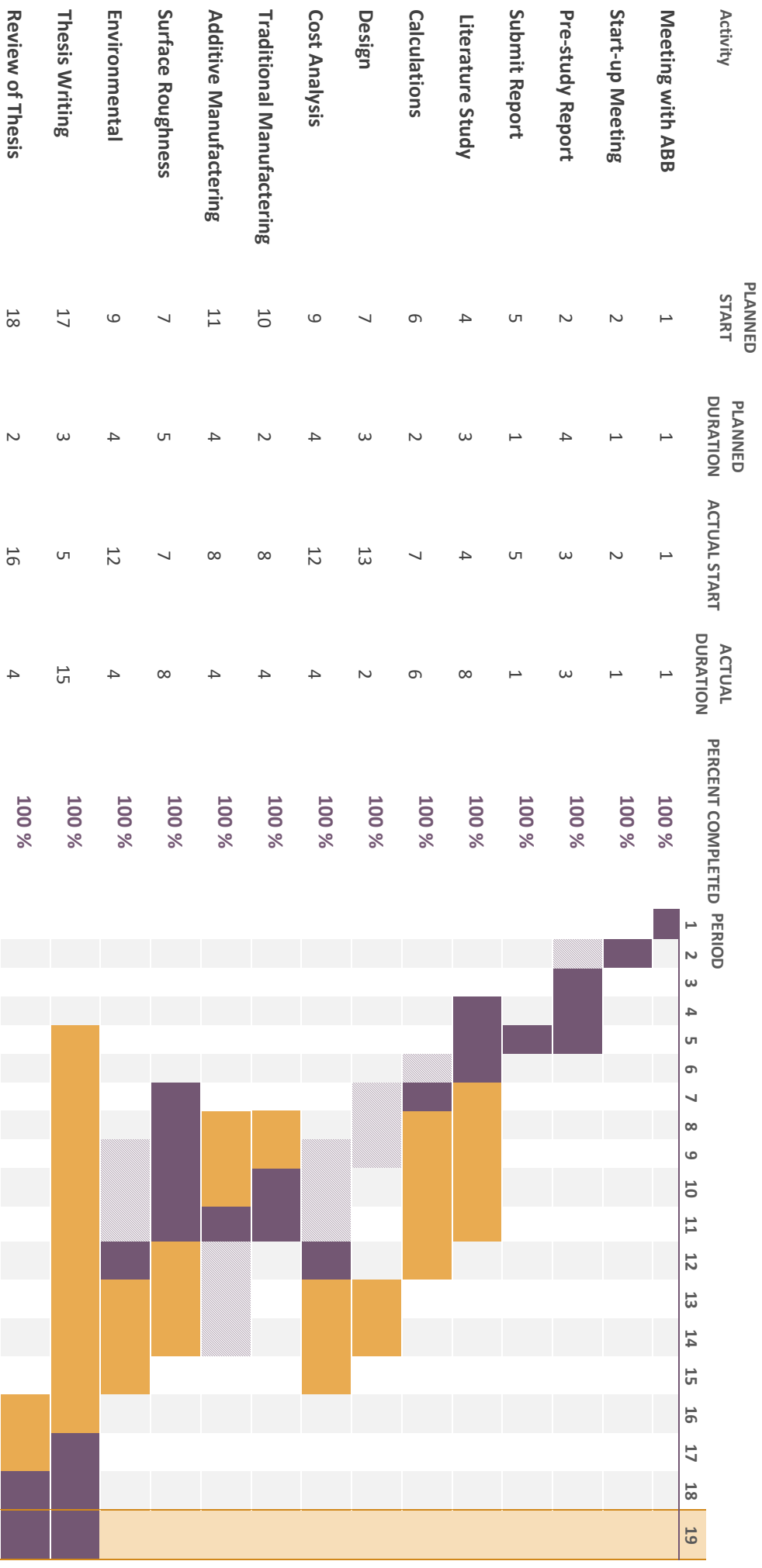
## Planning

### 4.1 Gantt chart

Planning is the first management function. It involves guiding to what needs to be done and when it is supposed to be done. Having a plan helps to find the activities required to achieve a desired goal. It is the main activity to achieve wanted results.

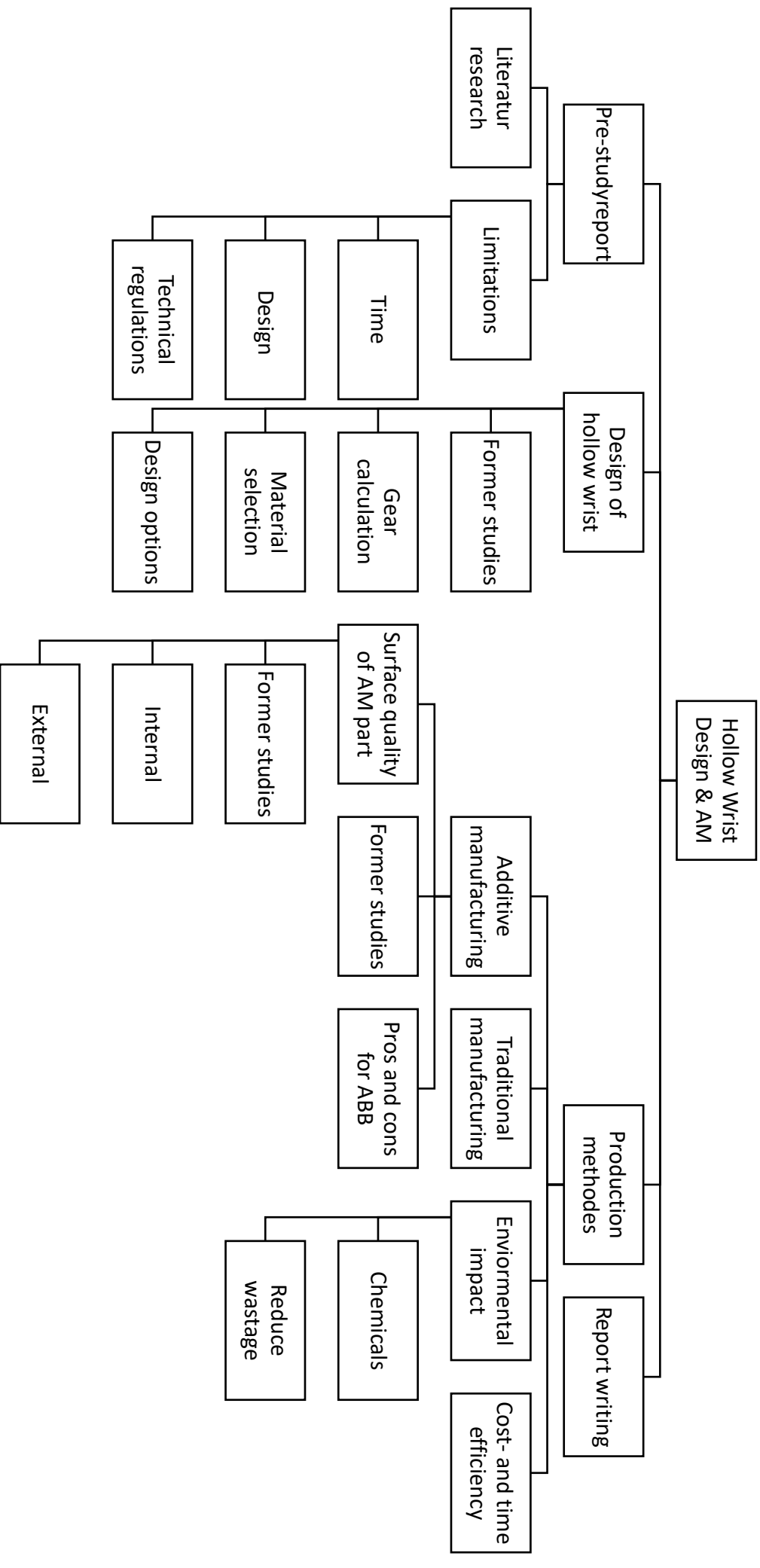
To not deviate from the thesis a Gantt chart is produced to give a certain guideline in terms of time. It gives the authors realization of time distribution and an orientation relative to the goals that have been set. The Gantt chart is located in Figure ??.

# Project planning



Period highlighting: 19

- Actual (beyond the plan)
- % Completed (beyond the plan)
- Planned duration
- Actual start
- % Completed



# References

- [1] ABB-Company, *About us*, 2020. [Online]. Available: <https://global.abb/group/en/about>.
- [2] ———, *Irb 5510, medium-sized paint robot*, 2020. [Online]. Available: <https://new.abb.com/products/robotics/industrial-robots/irb-5510>.
- [3] S. en Dehue, *Am*, 2021. [Online]. Available: <https://3dprinting.com/what-is-3d-printing/>.
- [4] ABB-Review, *Additive manufacturing*, Jan. 2020. [Online]. Available: <https://new.abb.com/news/detail/56908/additive-manufacturing>.
- [5] Richard-Coombes, *Ip ratings explained: Ingress protection and what it means for your packaging*, Oct. 2020. [Online]. Available: <https://www.gwp.co.uk/guides/ip-ratings-explained/>.

# **Appendix B**

## **18NiCrMo5 Material**

## Corrispondenze

SIAU	DIN	W.N.	AFNOR	BS	AISI/SAE
K2D	-	-	(18NCD6)	(815M17)	-

## Composizione

C	Mn	Si	Cr	Ni	Mo	P e S
.15÷.21	.60÷.90	.15÷.40	.70÷1.00	1.20÷1.50	.15÷.25	≤ .035

## Temperature per la lavorazione a caldo ed il trattamento termico

Punti critici	Fucinatura	Normalizzazione	Ricottura subcritica	Ricottura isoterma	Tempra 1° 2°	Rinvenimento di distensione
Ac1 730					840÷870	
Ac3 815	1100÷900	850÷900	650÷700	850÷900 ↓ 650x2h	810÷830	160÷200
Ms 360					olio	
Ms 180						

## Caratteristiche meccaniche

Stato	Saggio Ø mm.	Re min. N/mm <sup>2</sup>	Rm N/mm <sup>2</sup>	A min. %	KCU min. J	Durezze HB allo stato	
Temprato e disteso	11	980	1230÷1520	8	30	Ricotto lavorabile	≤ 240
	30	735	980÷1270	9	32,5	Ricotto isoterma	149÷207
	63	635	830÷1130	10	35	Ricotto sferoidale	≤ 207

## Temprabilità

HRC / % Martensite		Diametro temprabile mm.	
90%	70%	olio	acqua
43	35	50	-

## Temprabilità Jominy

Distanza dall'estremità temprata	Durezza Rockwell	
mm.	HRc min	HRc max
1,5	39	49
3	38	48,5
5	36	48
7	34	46,5
9	31	45
11	29	43,5
13	27	41
15	25,5	40
20	23	37
25	21	35,5
30	20,5	34,5
35	20	33,5
40		33
45		32,5
50		32

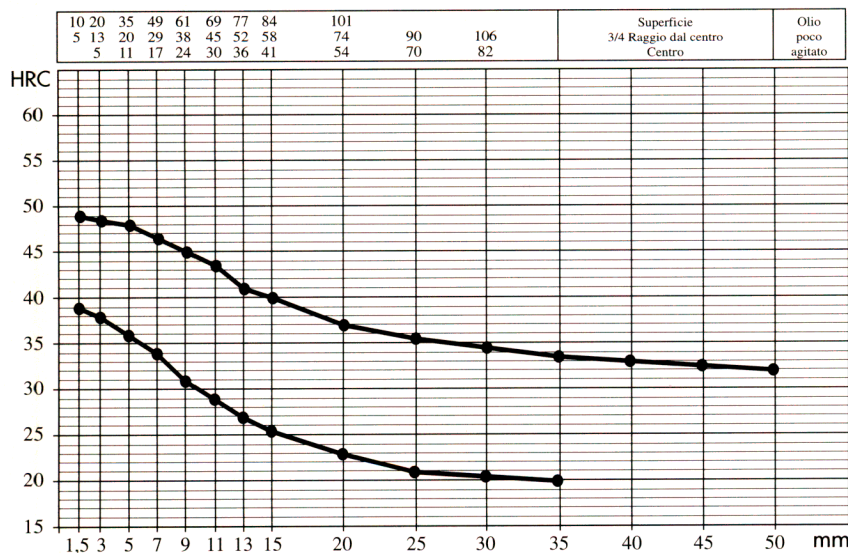
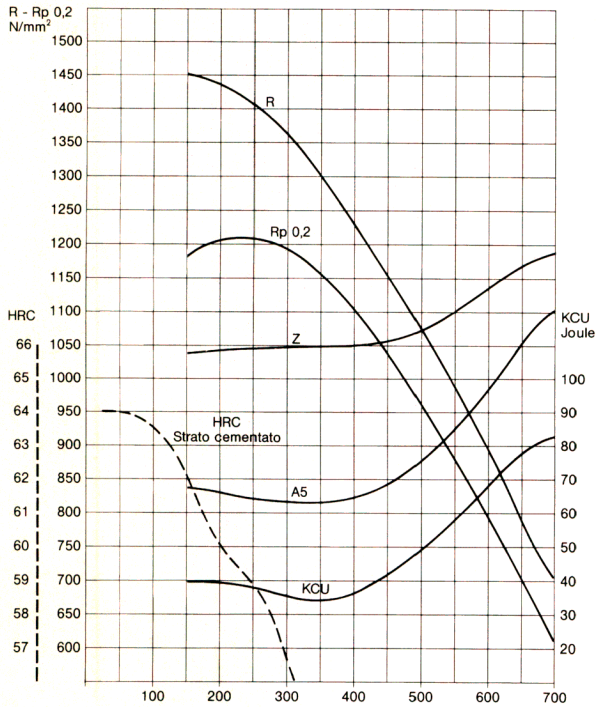


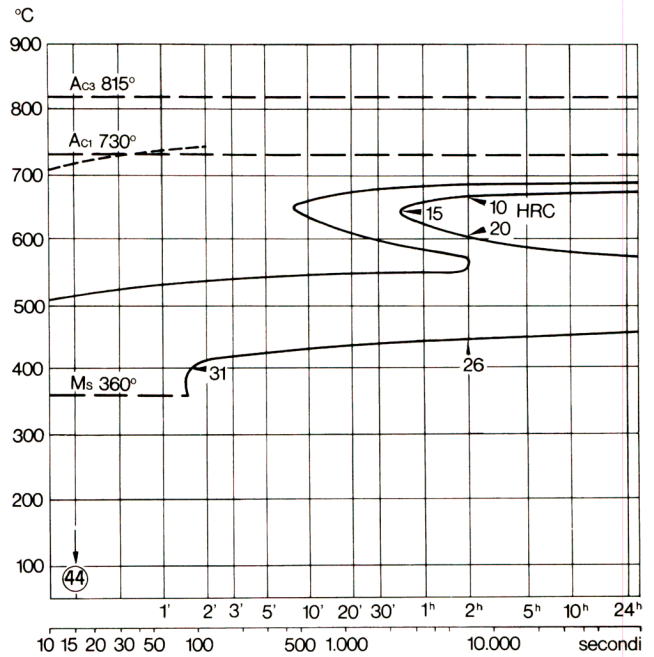
Diagramma di rinvenimento



Temperatura di rinvenimento °C

Trattamento: su Ø 11 mm Tempra: 850 °C olio Rinvenimento per 2 ore

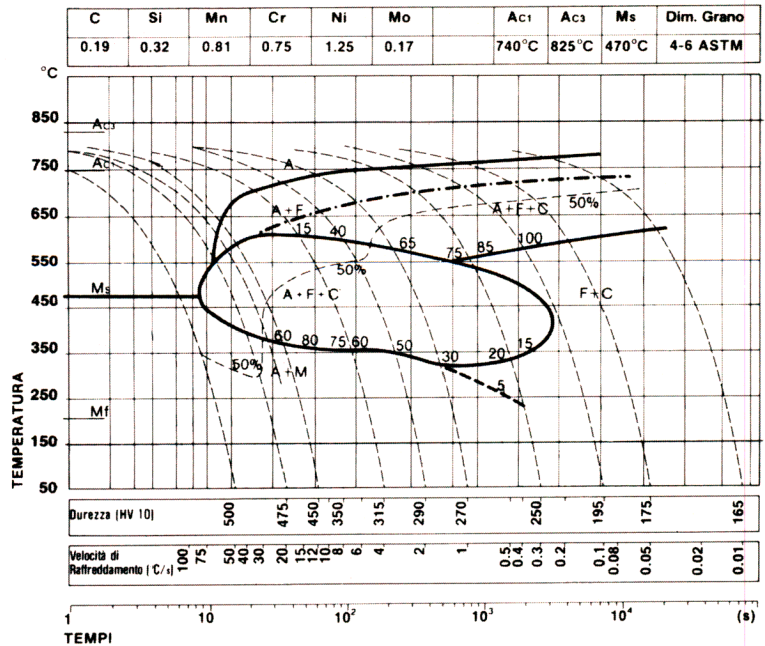
Diagramma T.T.T.



Quadro: 10 mm

Austenizzazione: 850 °C

Diagramma C.C.T.



Dimensione Provisi  
Ø=2 L=12

Trattamento Termico Precedente  
Ric. 650°C

Austenizzazione  
850°C



## **Appendix C**

### **16MnCr5 Material**

<b>Quality</b>	<b>16MnCr5</b>	<i>Technical card</i>
According to standards	<b>EN 10084: 2008</b>	<i>Lucefin Group</i>
Number	<b>1.7131</b>	

### Chemical composition

C%	Si%	Mn%	P%	S%	Cr%	
0,14-0,19	0,40	1,00-1,30	0,025	0,035	0,80-1,10	Product deviations are allowed
± 0.02	+ 0.03	± 0.05	+ 0.005	+ 0.005	± 0.05	
16MnCr5 n° 1.7139 S% 0.020-0.040 product deviation ± 0.005%						
On request, this steel grade can be supplied with addition of lead (Pb) 0.15-0.35%						

### Temperature °C

Hot-forming	Normalizing	Core hardening	Carbonitriding	Carburizing	Hardening carburizing surf.	Tempering
1150-850	880 air (HB 138-187)	860-900 oil-polymer salt bath	750-930 gas	880-980	810-840 oil polymer salt bath (160-250 °C)	150 200
Soft annealing	Isothermal annealing	Spheroidizing	End quench hardenability	Pre-heating welding	Stress-relieving after welding	
750-770 cooling 15 °C/h until 680, pause, then cooling to 400, pause, then air (HB max 207)	870 furnace cooling to 650, then air (HB 156-207)	730-750 furnace cooling 50 °C/h to 680, pause, cooling to 400 then air (HB 140-187)	870 water	welding must be carried out on the annealed state and before carburizing 150-350 <b>Ac1</b> <b>Ac3</b> 740      840	600 furnace cooling <b>Ms</b> * core <b>**</b> carburizing surface 400* 200**	
Transformation annealing +FP	950-1000 quick cooling to 630-650, 3 h holding, then air (HB 140-187)			As-rolled	<b>Stress-relieving</b> 600-620 (HB max 230)	

### Mechanical and physical properties

**Hot-rolled** values obtained on test blanks after **core hardening** + stress-relieving UNI 7846: 1978. Use only as reference

size mm test blanks	Testing at room temperature (longitudinal)					
	<b>R</b>	<b>Rp 0.2</b>	<b>A%</b>	<b>C%</b>	<b>Kcu</b>	<b>HB</b>
11	N/mm <sup>2</sup> 1030-1370	N/mm <sup>2</sup> min. 735	min. 8	min. 8	J min. 25	311-394
30	740-1030	490	9	9	25	224-311 for information only
63	640-930	440	10	10	25	198-278 for information only

Hot-rolled natural state. **Lucefin** experience

size mm	<b>R</b>	<b>Rp 0.2</b>	<b>A%</b>	<b>C%</b>	<b>Kcu</b>	<b>HB</b>
from 10 to 100	N/mm <sup>2</sup> 560-720	N/mm <sup>2</sup> min. 350	min. 15	min. 25	J min. 25	max 207

**Table of tempering** values at room temperature on rounds of Ø 10 mm after quenching at 870 °C in oil

<b>HB</b>	390	385	385	385	385	381	376	362	348	319	286	240	213	200
<b>HRC</b>	42	41.5	41.5	41.5	41.5	41	40.5	39	37.5	34	30	22.5		
<b>R</b> N/mm <sup>2</sup>	1340	1335	1330	1330	1320	1300	1260	1210	1150	1050	950	800	700	650
<b>Rp 0.2</b> N/mm <sup>2</sup>	1020	1060	1110	1140	1145	1140	1110	1070	1010	930	830	710	620	560
<b>A</b> %	12.0	12.5	12.5	12.5	12.0	12.0	12.5	13.0	14.0	15.5	17.5	20.0	23.0	25.5
<b>C</b> %	52.0	52.0	53.0	54.0	55.0	57.0	59.0	61.0	63.0	64.0	68.0	72.0	75.0	
<b>Kv</b> J	42	46	46	45	42	40	42	62	90	124	135	155	180	194
<b>HRC carburizing surface</b>	64	63	62	60.5	59	57								
Tempering at °C	<b>50</b>	<b>100</b>	<b>150</b>	<b>200</b>	<b>250</b>	<b>300</b>	<b>350</b>	<b>400</b>	<b>450</b>	<b>500</b>	<b>550</b>	<b>600</b>	<b>650</b>	<b>700</b>

<b>16MnCrS5</b> 1.7139 EN 10277-4: 2008		<i>Lucefin Group</i>			
size mm	Soft annealing +A +SH <b>Peeled-reeled, ground +SL</b>	Soft annealing +A +C <b>Cold-drawn</b>	Heat treatment +FP +SH for pearlite / ferrite structure <b>Peeled-reeled, ground</b>	Heat treatment +FP +C for pearlite / ferrite structure <b>Cold-drawn</b>	
from	to	<b>HB max</b>	<b>HB max</b>	<b>HB</b>	
5 a)	10		260		
10	16		250		
16	40	207	245	140-187	
40	63	207	240	140-187	
63	100	207	240	140-187	

a) for thickness < 5 mm, hardness values should be agreed before order placement

<b>Forged UNI 8550: 1984. Use only as reference</b>										
size mm		Testing at room temperature								
from	to	<b>R</b>	<b>Rp 0.2</b>	<b>A% L</b>	<b>A% T</b>	<b>A% Q</b>	<b>Kcu L</b>	<b>Kcu T</b>	<b>Kv L</b>	<b>HB</b>
		N/mm <sup>2</sup>	N/mm <sup>2</sup> min	min	min	min	J min	J min	J min	for inform.
	11	1030-1375	735	8			25			311-395
11	25	785-1080	540	9			30			234-327
25	50	685-930	490	10			30			209-278

Mechanical properties obtained on test blanks after core hardening + stress-relieving

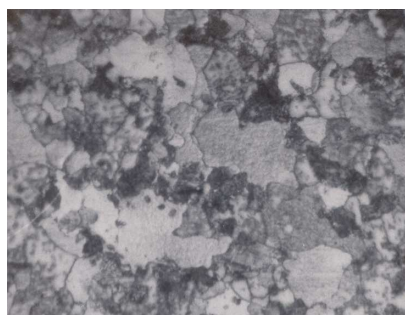
L = longitudinal T = tangential Q = radial

<b>EN 10084: 2008 Jominy test HRC</b> grain size G 5 min.																
mm distance from quenched extremity																
	1.5	3	5	7	9	11	13	15	20	25	30	35	40	45	50	H
<b>min</b>	39	36	31	28	24	21										normal
<b>max</b>	47	46	44	41	39	37	35	33	31	30	29	28	27			
<b>min</b>	42	39	35	32	29	26	24	22	20							HH
<b>max</b>	47	46	44	41	39	37	35	33	31	30	29	28	27			
<b>min</b>	39	36	31	28	24	21										HL
<b>max</b>	44	43	40	37	34	32	30	28	26	25	24	23	22			

Temperature Testing at °C	Mod. of elasticity GPa		Thermal expansion			
	E long.	G tang.	10 <sup>-6</sup> • K <sup>-1</sup>			
<b>20</b>	210	80				
<b>100</b>					11.1	
<b>200</b>					12.1	
<b>300</b>					12.9	
<b>400</b>					13.5	
<b>500</b>					13.9	
<b>600</b>						

Specific heat capacity J/(Kg•K)	Density Kg/dm <sup>3</sup>	Thermal conductivity W/(m•K)	Specific electric resist. Ohm•mm <sup>2</sup> /m	Electrical conductivity Siemens•m/mm <sup>2</sup>
460	7.85	41	0.16	6.25

EUROPE EN	ITALY UNI	CHINA GB	GERMANY DIN	FRANCE AFNOR	U.K. B.S.	RUSSIA GOST	USA AISI/SAE
16MnCr5	16MnCr5	15CrMn	16MnCr5	16MC		16HG	5115



Structure of hot-rolled annealed steel (+A)  
and subsequently cold-drawn (+C)

x1000

# **Appendix D**

## **34CrNiMo6 Material**

## 34CrNiMo6 All

### General Information

34CrNiMo6 is a quenching and tempering steel with high strength, high toughness and good hardenability. Used for large axles, machine components, tools and high strength fasteners.

The steel can be induction hardened and it is weldable under certain conditions. Through hardenability to appr. 100 mm diameter bar with oil quenching.

356D - Standard steel variant

356Q - IQ (isotropic quality) variant.

6499 - low sulphur variant of 34CrNiMo6 Suitable for fasteners according to ISO 989 Grade 10.9 up to 90 mm bar diameter

6498 - A variant of the old swedish standard SS 2541

6502 - M-steel variant of 34CrNiMo6

SB9205 - A variant of 34CrNiMo6

### **IQ-Steel®**

IQ-Steel® is an isotropic quality ultra clean steel optimized for high fatigue strength under multi axial loading.

For additional Heat Treatment Data, please visit the Heat Treatment Guide

### Similar designations

34CrNiMo6M, SS2541, MoCN315, MoCN315M, 1.6582, 35NCD6, 816M40, 817M40, 35NiCrMo6, SNCM447, 30Ch2N2MA, F.1272, 40NiCrMo7, 4337, 4340, 92541, VSQT34CrNiMo6, VSQT34CrNiMo6/700, VSQT34CrNiMo6/800, VSQT34CrNiMo6/900, SS2541, EN24, 1.6582, EN 10083-3, SS142541

## Chemical composition

Variant	Cast	Di		C %	Si %	Mn %	P %	S %	Cr %	Ni %	Mo %	V %	Al %
356D	IC		Min	0.32	0.20	0.70	-	0.020	1.35	1.30	0.20	-	-
			Max	0.38	0.35	0.80	0.025	0.030	1.60	1.60	0.30	0.100	-
356Q	IC		Min	0.32	0.15	0.65	-	-	1.30	1.30	0.20	-	-
			Max	0.38	0.35	0.80	0.025	0.002	1.60	1.60	0.30	0.100	-
6499	CC	8.81	Min	0.30	0.15	0.50	-	-	1.40	1.40	0.15	-	-
			Max	0.38	0.40	0.80	0.015	0.015	1.70	1.70	0.30	-	-
6502, MoCN 315 M	CC		Min	0.30	-	0.50	-	0.015	1.30	1.30	0.15	-	-
			Max	0.38	0.40	0.80	0.025	0.035	1.70	1.70	0.30	-	-
6498	CC	7.91	Min	0.32	0.10	0.50	-	0.020	1.30	1.30	0.15	-	-
			Max	0.39	0.40	0.80	0.035	0.035	1.70	1.70	0.30	-	-
SB9205	CC		Min	0.36	0.15	0.50	0.000	0.000	1.30	1.30	0.20	-	0.015
			Max	0.38	0.40	0.70	0.025	0.012	1.40	1.70	0.30	-	0.040
34CrNiMo6 EN ISO 683-2	Std		Min	0.30	0.10	0.50	0.000	0.000	1.30	1.30	0.15	-	-
			Max	0.38	0.40	0.80	0.025	0.035	1.70	1.70	0.30	-	-

## Mechanical Properties

Variant	Condition	Format	Dimension [mm]	Yield strength min [MPa]	Tensile strength [MPa]	Elongation A <sub>5</sub> [%]	Reduction of area Z <sub>min</sub> [%]	Hardness	Impact (ISO-V) strength <sub>min</sub>
356D	+SA	Round bar	< 190	-	-	-	-	200 HB typical	-
	+QT	Round bar	< 50	900	1000 typical	10	45	360 HB typical	20 °C 140 J (long)
		Round bar	50 < 100	800	900 typical	10	45	330 HB typical	20 °C 115 J (long)
		Round bar	100 < 200	700	800 typical	10	45	300 HB typical	-
		Round bar	> 200	600	700 typical	10	45	270 HB typical	-
		Round bar	< 150	-	-	-	-	285 HB typical	20 °C 90 J (long)
	+Q	Round bar	< 100	1200	1500 typical	7	25	50 HRC typical	-
356Q	+SA	Round bar	< 190	-	-	-	-	200 HB typical	-
	+QT	Round bar	< 50	900	1000 typical	10	45	360 HB typical	20 °C 140 J (long)
		Round bar	50 < 100	800	900 typical	10	45	330 HB typical	20 °C 115 J (long)
		Round bar	100 < 200	700	800 typical	10	45	300 HB typical	-
		Round bar	> 200	600	700 typical	10	45	270 HB typical	-
		Round bar	< 150	-	-	-	-	285 HB typical	20 °C 90 J (long)
	+Q	Round bar	< 100	1200	1500 typical	7	25	50 HRC typical	-
6499	+AR	Round bar	25 < 160	-	-	-	-	< 380 HB	-
	+A	Round bar	25 < 160	-	-	-	-	< 248 HB	-
	+QT	Round bar	25 < 40	900*	1100-1300	10	45	320-380 HB	20 °C 45 J (long)
		Round bar	40 < 100	800*	1000-1200	11	50	300-350 HB	20 °C 45 J (long)
		Round bar	100 < 160	700*	900-1100	12	55	270-320 HB	20 °C 45 J (long)
6502, MbCN 315 M	+AR	Round bar	25 < 160	-	-	-	-	< 380 HB	-
	+A	Round bar	25 < 160	-	-	-	-	< 248 HB	-
	+QT	Round bar	25 < 40	900*	1100-1300	10	45	320-380 HB	20 °C 45 J (long)
		Round bar	40 < 100	800*	1000-1200	11	50	300-350 HB	20 °C 45 J (long)
		Round bar	100 < 160	700*	900-1100	12	55	270-320 HB	20 °C 45 J (long)
6498	+AR	Round bar	25 < 160	-	-	-	-	< 380 HB	-
	+A	Round bar	25 < 160	-	-	-	-	< 248 HB	-
	+QT	Round bar	25 < 40	900*	1100-1300	10	45	320-380 HB	20 °C 45 J (long)
		Round bar	40 < 100	800*	1000-1200	11	50	300-350 HB	20 °C 45 J (long)
		Round bar	25 < 160	700*	900-1050	12	55	270-325 HB	-20 °C 27 J (long)

RP0.2 \* R<sub>eh</sub>, \*\* R<sub>el</sub>

## Transformation temperatures

	Temperature °C
MS	315
AC1	725
AC3	785

## Heat treatment recommendations

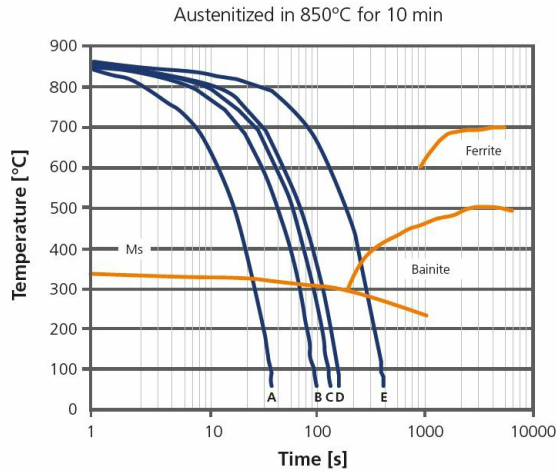
Treatment	Condition	Temperature cycle	Cooling/quenching
Hot forging	+AR	880-1050°C	In air
Soft annealing	+A	650-700°C	Slowly (15°C/h) until 600°C
Stress relieve annealing	+SRA	450-650°C (appr. 50°C under tempering temperature)	In air
Hardening	+Q	820-850°C	Quenching in oil
Tempering	+T	540-680°C	In air



## Hardenability

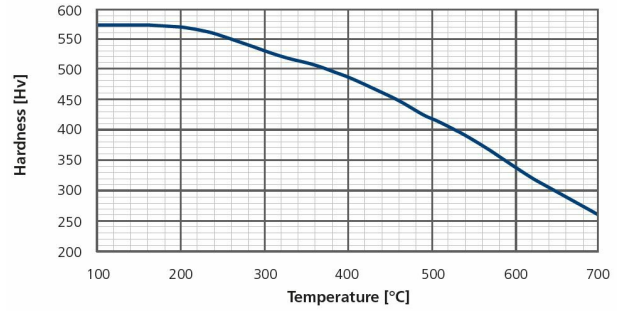
Jominy hardenability of Ovako 356D. Valid also for Ovako 356Q. Average value with +/-standard deviation.

## CCT - Ovako356D and Ovako356Q



	A	B	C	D	E
$t_{8-5}$ [s]	15	38	50	60	150
HV <sub>30</sub>	615	610	610	605	580

## Tempering response - Ovako356D and Ovako356Q



## Other properties (typical values)

## Steel cleanliness

Micro inclusions - Ovako356D								Macro inclusions - Ovako356D		
Applied standard	ASTME45							Applied standard	ISO 3763 (Blue fracture)	
Sampling	ASTMA295							Sampling	Statistical testing on billets	
Maximum average limits	A		B		C		D		Limits	< 5 mm/dm <sup>2</sup>
	Th	He	Th	He	Th	He	Th	He		
2.0	1.5	0.8	0.1	0	0	0.5	0.4			

## Steel cleanliness

Micro inclusions - Ovako356Q								Macro inclusions - Ovako356Q	
Applied standard	DIN 50602 K1							Applied standard	10 MHz UST (Ovako internal standard)
Sampling	Six random samples from final product dimension							Sampling	Statistical testing on billets
Limits	The limit is dimension dependent. The average rating of six samples should not exceed the limits given in the graph							Limits	< 10 defects/dm <sup>3</sup> > 0,2 mm FBH

Youngs module (GPa)	Poisson's ratio (-)	Shear module (GPa)	Density (kg/m <sup>3</sup> )
210	0.3	80	7800
Average CTE 20-300°C (µm/m°K)	Specific heat capacity 50/100°C (J/kg°K)	Thermal conductivity Ambient temperature (W/m°K)	Electrical resistivity Ambient temperature (µΩm)
12	460 - 480	40 - 45	0.20 - 0.25

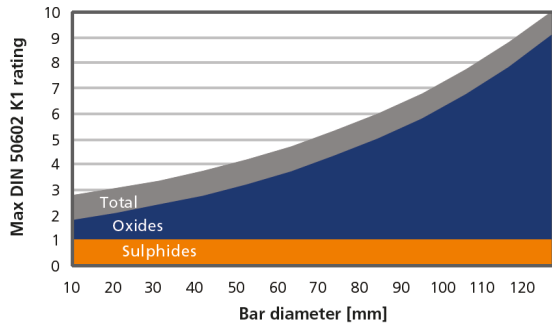
## Contact us

Would you like to know more about our offers? Don't hesitate to contact us:

Via e-mail: [info@ovako.com](mailto:info@ovako.com)

**IQ**

**Inclusion limits IQ-processed steel**



Via telephone: +46 8 622 1300

For more detailed information please visit <http://www.ovako.com/en/Contact-Ovako/>

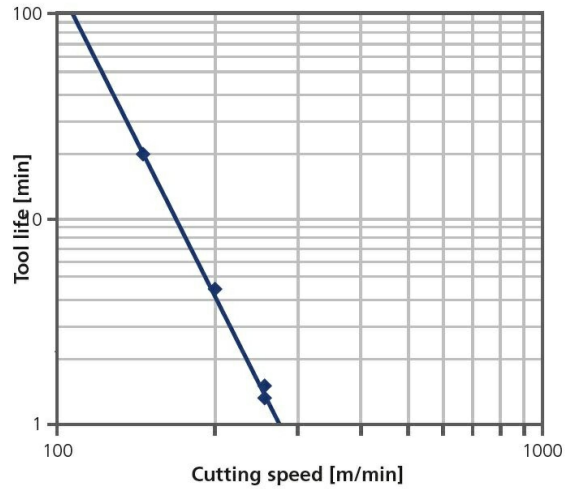
**Disclaimer**

The information in this document is for illustrative purposes only. The data and examples are only general recommendations and not a warranty or a guarantee. The suitability of a product for a specific application can be confirmed only by Ovako once given the actual conditions. The purchaser of an Ovako product has the responsibility to ascertain and control the applicability of the products before using them. Continuous development may necessitate changes in technical

**Machinability**

Test condition:	Q&T 310 HV
Test procedure:	ISO 3685
Insert:	SNMA 120408 P15
Tool holder:	CSRNL
Feed rate:	0.4 mm/r
Cutting depth:	2.5 mm
Wear criteria:	vB <sub>mean</sub> 0.3mm

**Machinability - Ovako 356D**  
According to ISO 3685



**Tensile strength at elevated temperatures - Ovako356D**

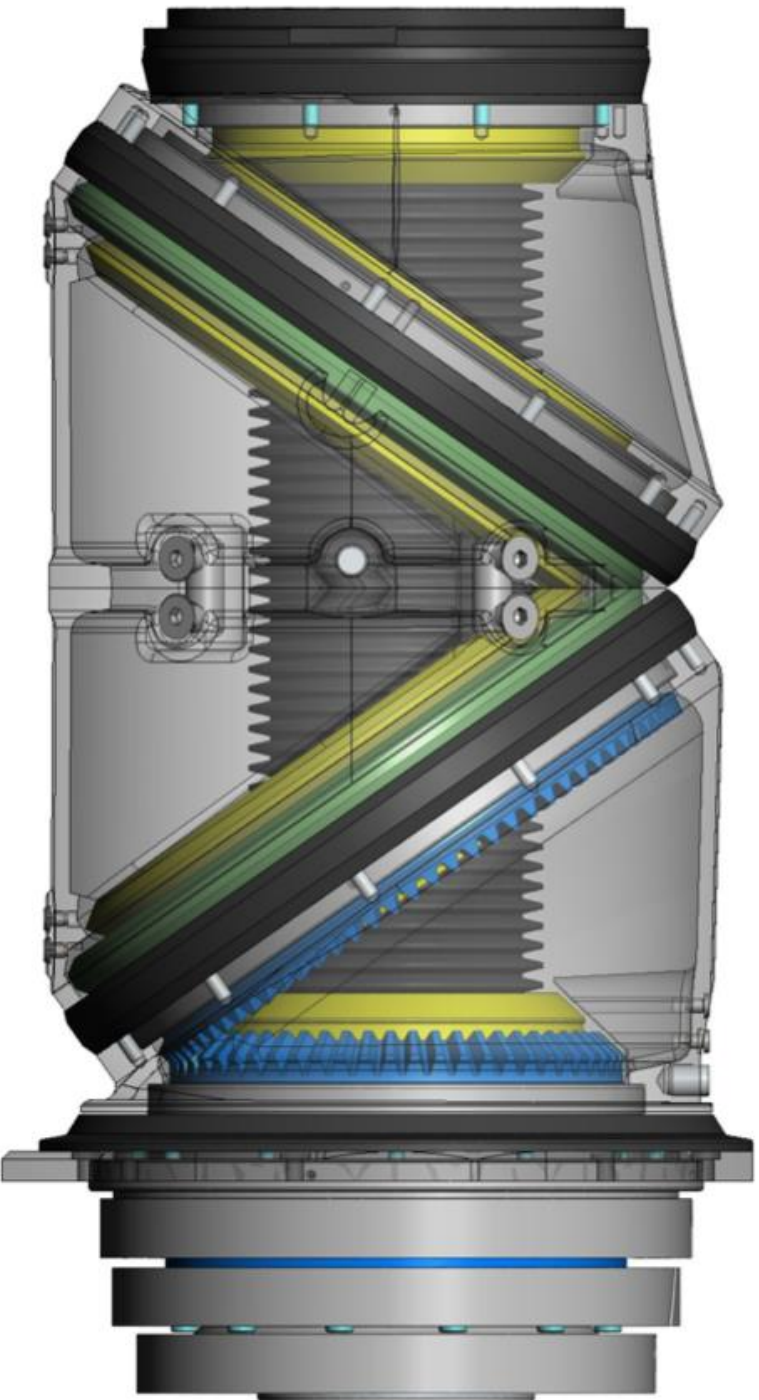
Q&T to 350 HB	RT	100°C	150°C	200°C	
R <sub>p0.2</sub>	870	810	770	730	MPa
R <sub>m</sub>	970	940	920	890	MPa

data without notice. This document is only valid for Ovako material. Other material, covering the same international specifications, does not necessarily comply with the properties presented in this document.

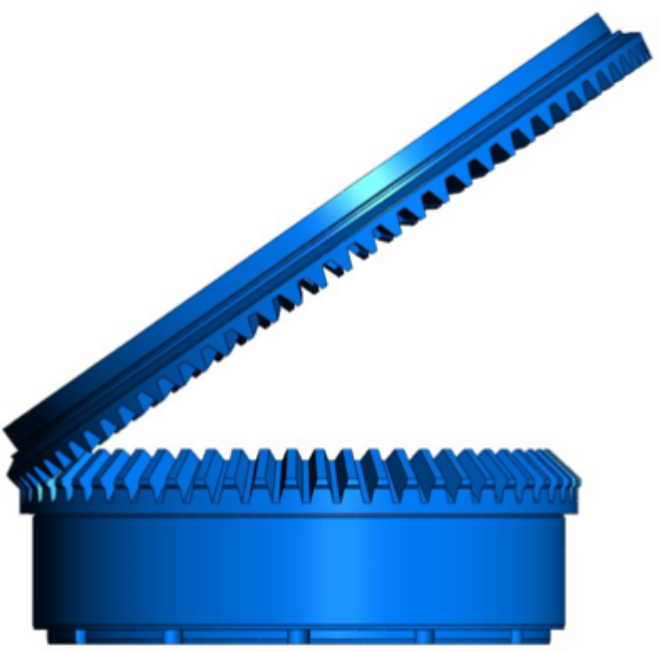
# **Appendix E**

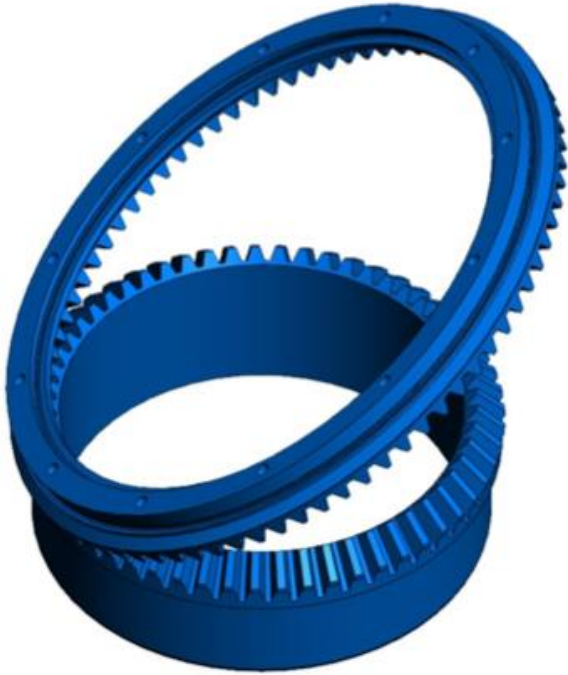
## **Technical Drawing**



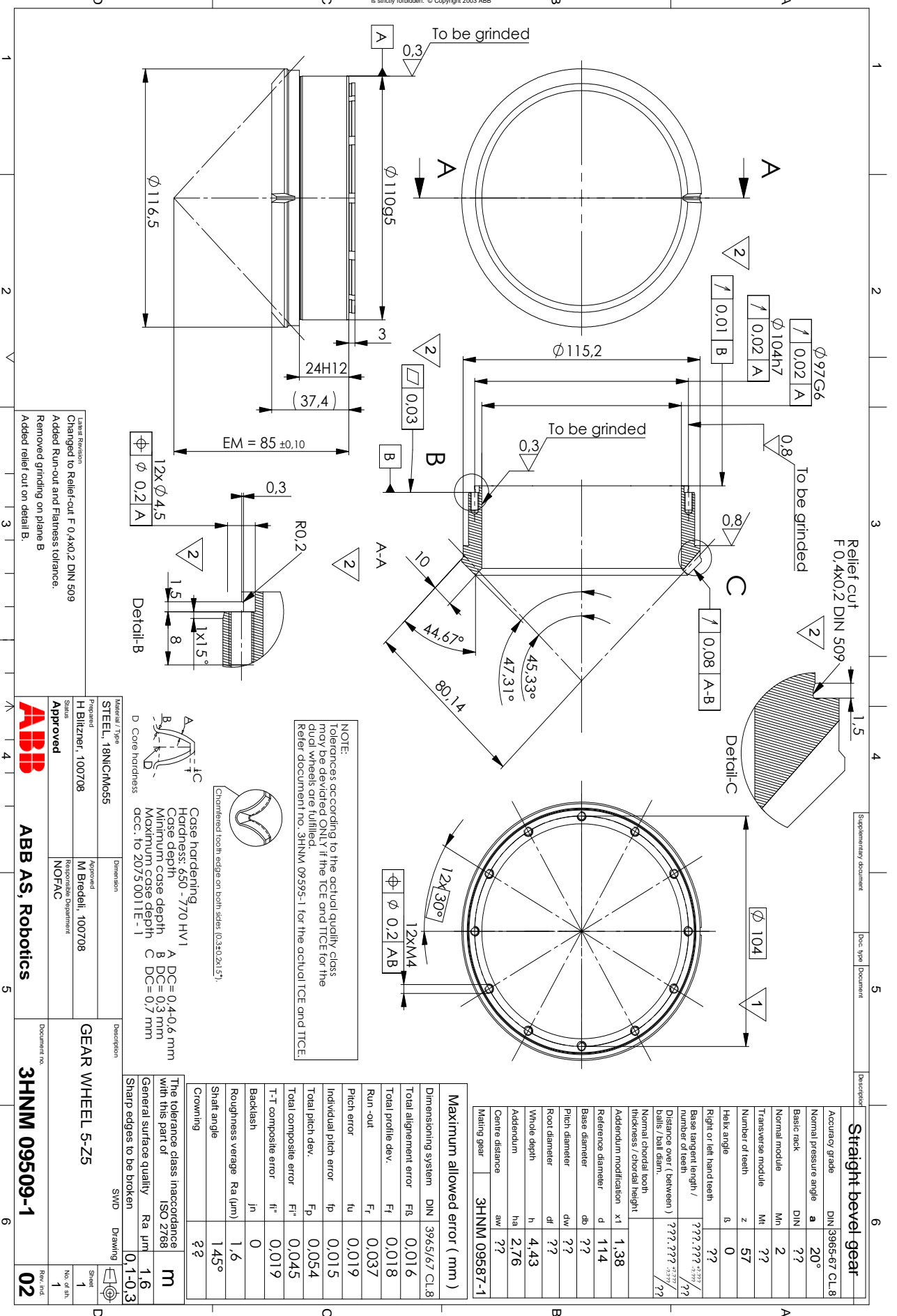


SOLIDWORKS Educational Product. For Instructional Use Only.





We reserve all rights in this document and in the information contained therein. Reproduction, use or disclosure to third parties without express authority is strictly forbidden. © Copyright 2003 ABB



**Straight bevel gear**

Accuracy grade	DIN 3965-67 CL.8
Normal pressure angle $\alpha$	20°
Basic rack	DIN $\phi$ $\phi$
Normal module	Mn 2
Transverse module	Mt $\phi$ $\phi$
Number of teeth	z 57
Helix angle	$\beta$ 0
Right or left hand teeth	$\phi$ $\phi$
Base tangent length / number of teeth	$\phi$ $\phi$ / $\phi$
Distance over (between) balls / ball diam.	$\phi$ $\phi$ / $\phi$
Normal chordal tooth thickness / chordal height	$\phi$ $\phi$ / $\phi$
Addendum modification	x1 1,38
Reference diameter	d 114
Base diameter	db $\phi$ $\phi$
Pitch diameter	d <sub>w</sub> $\phi$ $\phi$
Root diameter	d <sub>r</sub> $\phi$ $\phi$
Whole depth	h 4,43
Addendum	ha 2,76
Centre distance	aw $\phi$ $\phi$
Mating gear	3HNIM 09587-1

NOTE: Tolerances according to the actual quality class may be deviated ONLY if the TCE and TTCE for the Refer document no. 3HNIM 09595-1 for the actual TCE and TTCE.

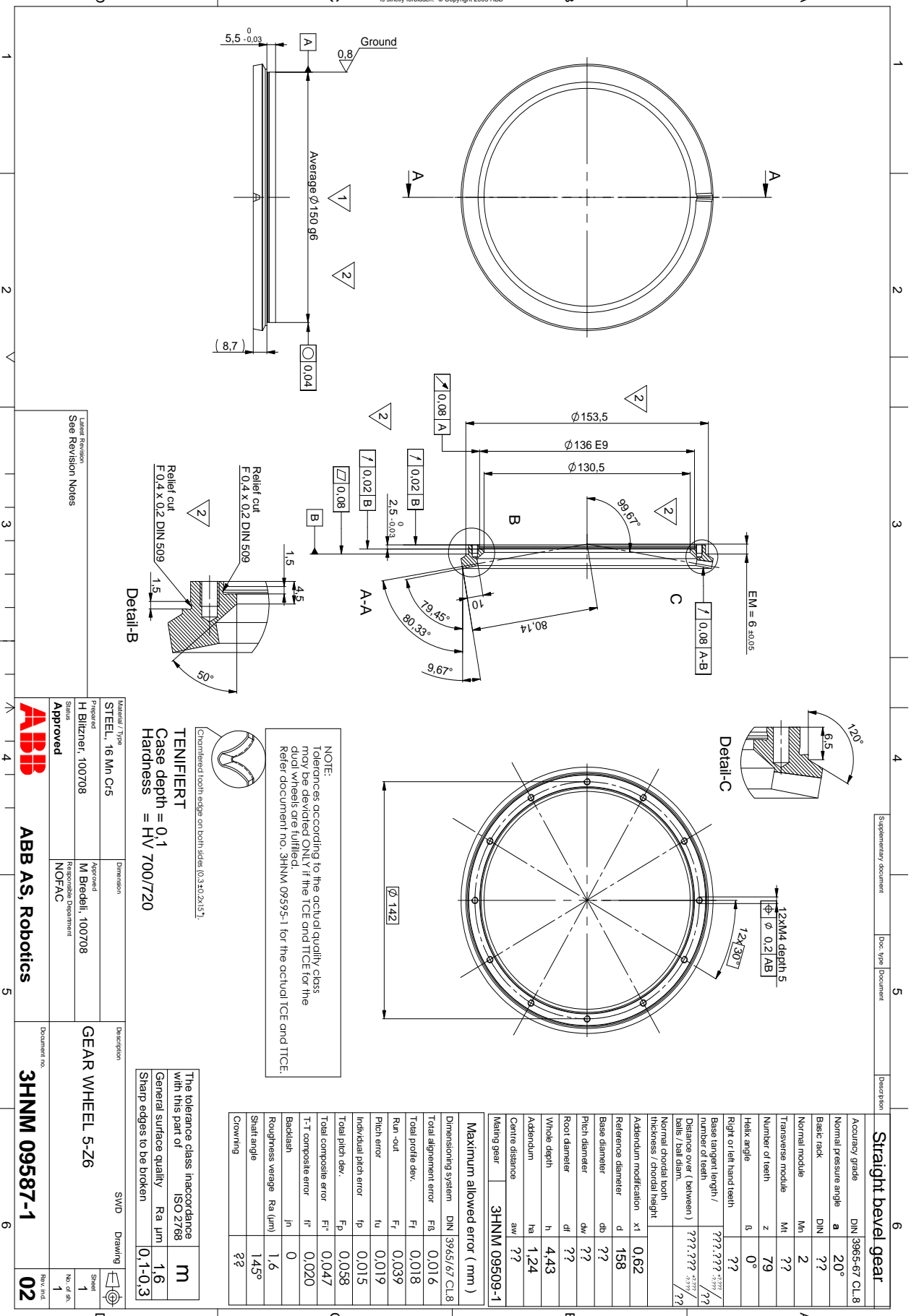
Case hardening  
 Hardness: 850 - 770 HV1  
 Case depth: A DC = 0.4±0.6 mm  
 Minimum case depth: B DC = 0.3 mm  
 Maximum case depth: C DC = 0.7 mm  
 Core hardness: D CC = 20.5 001 E - 1

Latest Revision  
 Changed to Relief-cut F 0.4x0.2 DIN 509  
 Added Run-out and Flatness tolerance.  
 Removed grinding on plane B  
 Added relief cut on detail B.

Material / Type	STEEL, 18NiCrMo55	Description	GEAR WHEEL 5-Z5
Prepared	H Blitzner, 100708	Approved	M Bredell, 100708
Status	Approved	Responsibility Department	NOFAC
ABB AS, Robotics		Document no.	3HNIM 09509-1
		Drawing	02



We reserve all rights in this document and in the information contained therein. Reproduction, use or disclosure to third parties without express authority is strictly forbidden. © Copyright 2003 ABB



**NOTE:**  
Tolerances according to the actual quantity class may be deviated ONLY if the TCE and TTCE for the dural wheels are fulfilled.  
Refer document no. 3HNM 09595-1 for the actual TCE and TTCE.

Chamfered tooth edge on both sides (0.250/2x1.5°)  
**TENIFIERT**  
Case depth = 0.1  
Hardness = HV 700/720

The tolerance class in accordance with this part of ISO 2/789	<b>M</b>
General surface quality Ra $\mu\text{m}$	1.6
Sharp edges to be broken	0.1-0.3

Maximum allowed error (mm)	
Dimensioning system	DIN 3965/67 CL8
Total alignment error	F8 0.016
Total profile dev.	F1 0.018
Run-out	F1 0.039
Pitch error	Iu 0.019
Individual pitch error	Ip 0.015
Total pitch dev.	Fp 0.058
Total composite error	Ft 0.047
T-T composite error	If 0.020
Backlash	Jr 0
Roughness average Ra ( $\mu\text{m}$ )	1.6
Shaft angle	14.5°
Crowning	???

Accuracy grade	DIN 3965-67 CL 8
Normal pressure angle $\alpha$	20°
Basic rack	DIN ???
Normal module	Mn 2
Transverse module	Mt ???
Number of teeth	z 79
Helix angle $\beta$	0°
Right or left hand teeth	???
Base tangent length / number of teeth	???.???.???.???
Distance over (between) balls / ball diam.	???.???.???.???
Normal chordal tooth thickness / chordal height	???
Addendum modification	xi 0.62
Reference diameter	d 158
Base diameter	db ???
Pitch diameter	d <sub>w</sub> ???
Root diameter	df ???
Whole depth	h 4.43
Addendum	ha 1.24
Centre distance	aw ???
Mating gear	3HNM 09509-1

Material / Type	STEEL, 16 Mn Cr5
Prepared	H Blitznier, 100708
Approved	M Bredell, 100708
Responsible Department	NOFAC
Status	Approved
Label Revision	See Revision Notes

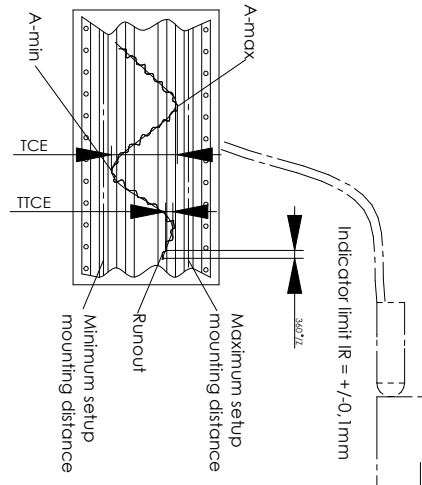
Dimension	
ABB AS, Robotics	

Description	GEAR WHEEL 5-Z6
Document no.	3HNM 09587-1
Sheet	1
No. of sh.	1
Rev. ind.	02

SWD Drawing

Principal illustration of setup for the wheel in dual test who shall be measured and shimmed.

Max. TCE (F<sub>1</sub>) = 0,12 mm  
 Max. TTCE (f<sub>1</sub>) = 0,05 mm



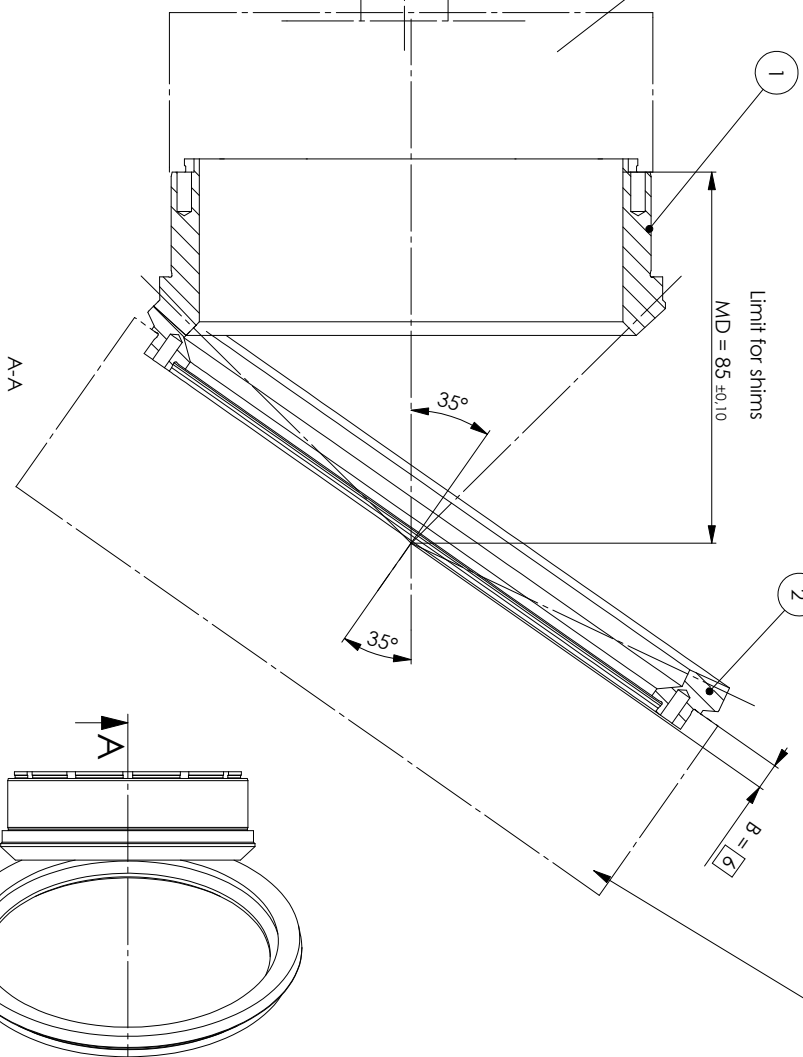
Max. TCE for dual wheels = 0,12  
 Max. TTCE for dual wheels = 0,05

5-75  
 1

Limit for shims  
 MD = 85 ±0,10

5-76  
 2

Principal illustration of support surface for the wheel in dual test who shall not be shimmed.

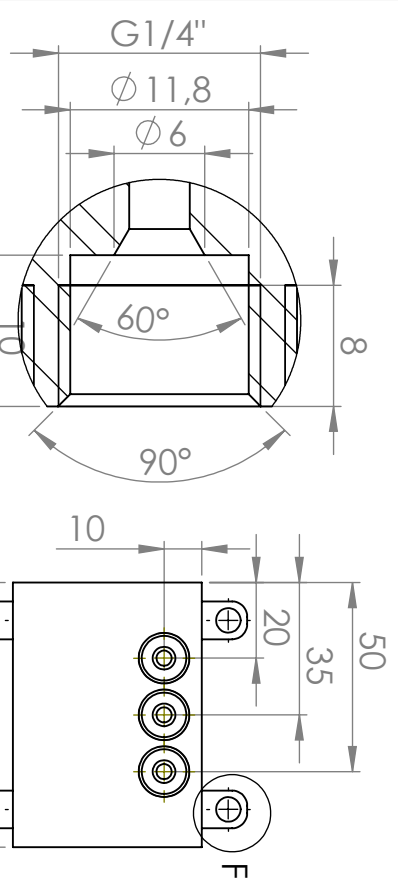


Material / Type		Dimension		Description		SWD Drawing	
Prepared	H Bilzner, 100708	Approved	M Bredell, 100708	GEAR WHEELS - COUPLE 1		Sheet	1
Status	Approved	Responsible Department	NOFAC	3HNM 09595-1		No. of sh.	1
Latest Revision Changed TCE from 0,074 and TTCE from 0,033				ABB AS, Robotics		Rev. ind.	01

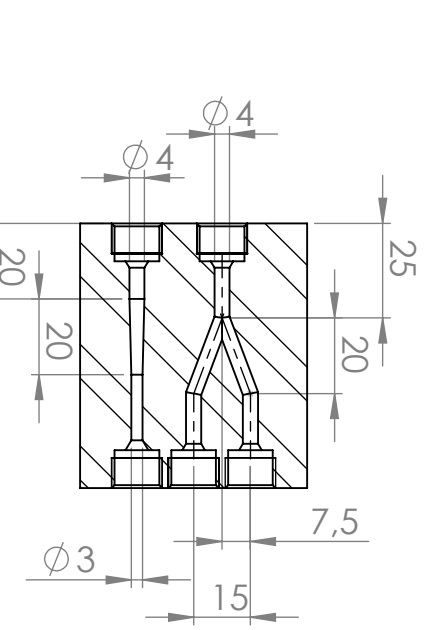
We reserve all rights in this document and in the information contained therein. Reproduction, use or disclosure to third parties without express authority is strictly forbidden. © Copyright 2003 ABB

# **Appendix F**

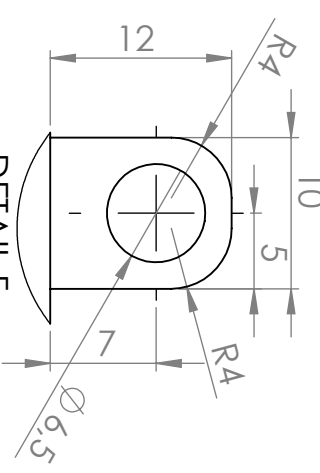
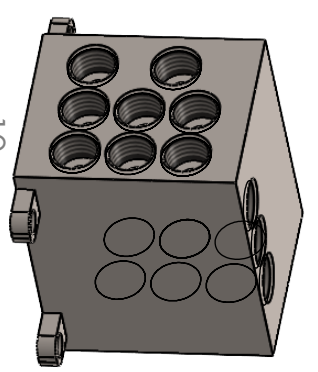
## **Technical Drawing Block**



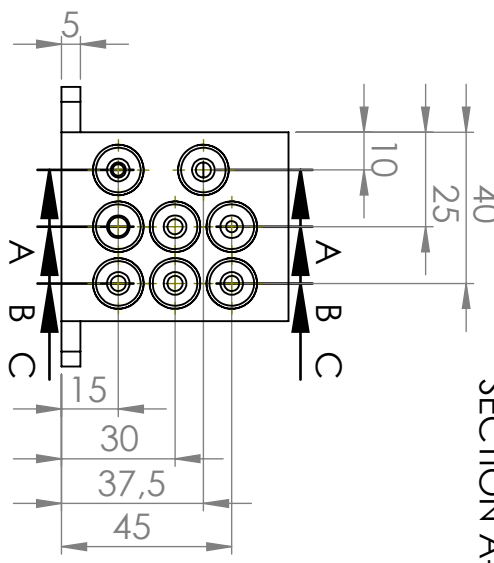
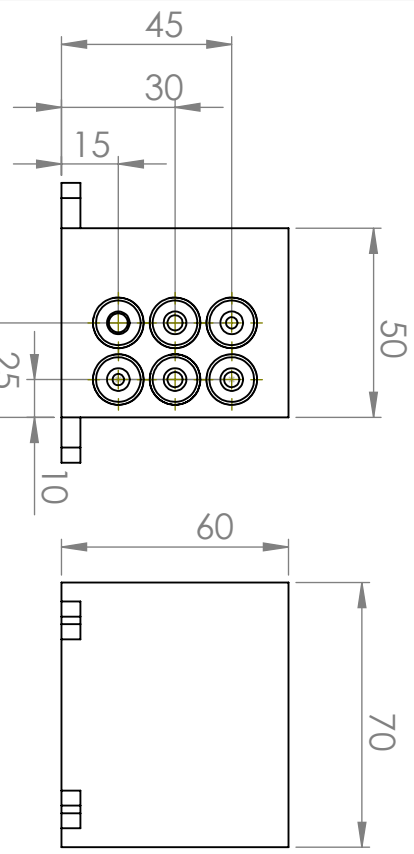
DETAIL D  
SCALE 2:1



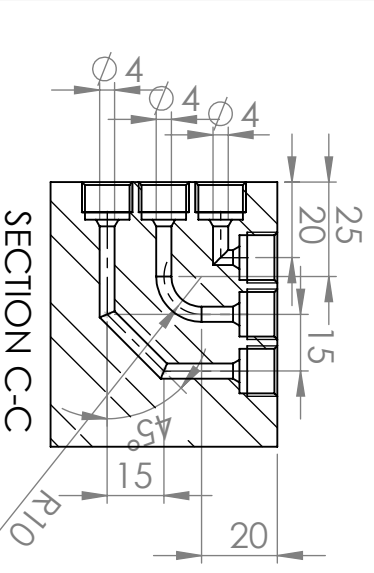
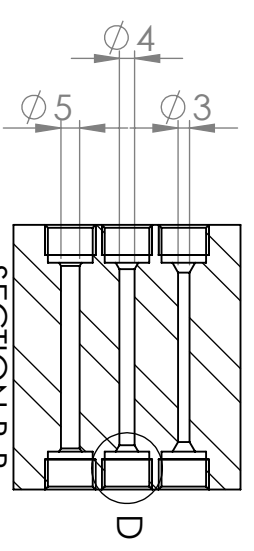
SECTION A-A



DETAIL F  
SCALE 2:1



SECTION B-B



SECTION C-C

UNLESS OTHERWISE SPECIFIED:  
DIMENSIONS ARE IN MILLIMETERS  
SURFACE FINISH:  
TOLERANCES:  
DIM: NS:ISO2768-1  
GEOMETRY: NS:ISO2768-2

FINISH: Ra = 0.8 - 1.6 After AFM

DEBURR AND  
BREAK SHARP  
EDGES

DO NOT SCALE DRAWING

REVISION

NAME	SIGNATURE	DATE
DRAWN Aksel Sørnareit		13.04.21
CHK'D Aksel Sørnareit		13.04.21
APP'VD Aksel Sørnareit		13.04.21
MFG Aksel Sørnareit		13.04.21
Q.A Aksel Sørnareit		13.04.21

31 6L stainless

WEIGHT: 1500 grams

ABB AFM Test Block

Block

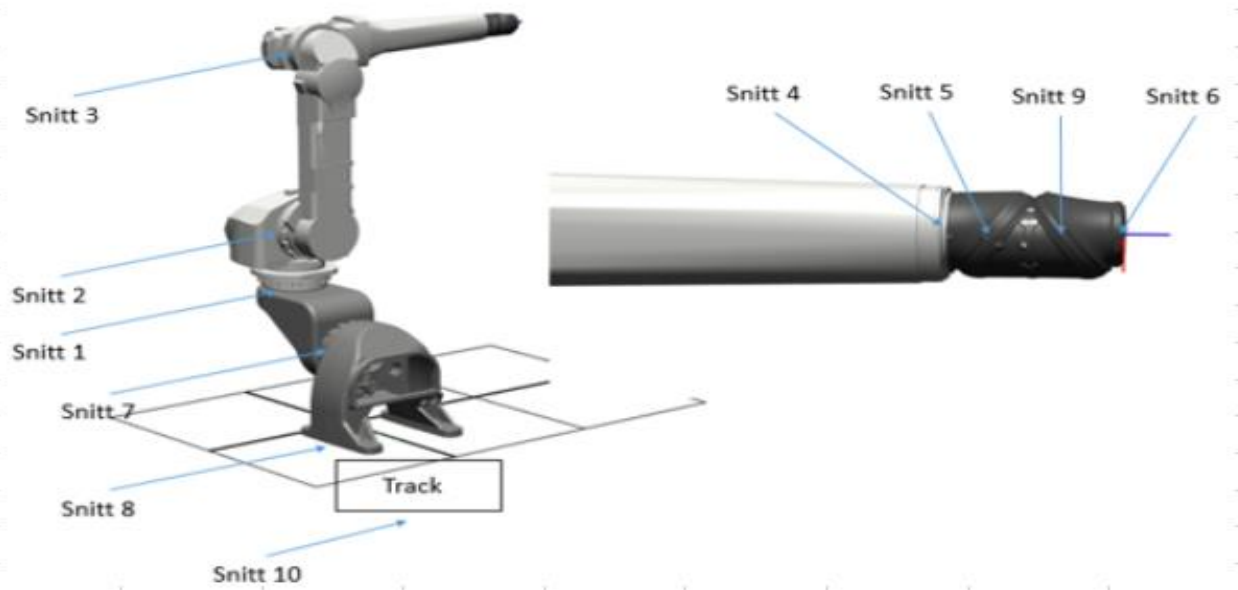
A4

DWG NO. SCALE: 1:2

SHEET 1 OF 1

# **Appendix G**

## **Data From ABB**



**Maximum motor torques for each axis**

**Normal operation**

Axis 4	2,78989	Nm
Axis 5	2,90023	Nm
Axis 6	2,54156	Nm

**Emergency stop**

Axis 4	5,35226	Nm
Axis 5	6,14602	Nm
Axis 6	7,08337	Nm

Section 4										
Normal operation										
		type	Fx[N]	Fy[N]	Fz[N]	Tx[Nm]	Ty[Nm]	Tz[Nm]	Fr[N]	Tr[Nm]
	section_4	Fx[N]	-858,773	181,287	300,322	73,2117	-4,54745	231,375	350,797	231,42
	section_4	Fy[N]	36,8915	752,578	167,251	-237,586	65,3133	81,376	770,938	104,345
	section_4	Fz[N]	-73,249	-113,762	-806,54	-213,243	-20,5283	-21,5435	814,523	29,7579
	section_4	Tx[Nm]	-591,784	592,43	-301,378	-242,491	-140,602	94,81	664,682	169,581
	section_4	Ty[Nm]	485,743	125,666	583,392	112,681	-277,142	-15,5205	596,774	277,577
	section_4	Tz[Nm]	-510,118	705,506	-455,654	-153,799	47,4948	293,893	839,857	297,706
	section_4	Fr[N]	-241,681	698,644	553,328	162,146	-22,2955	112,377	891,221	114,567
	section_4	Tr[Nm]	-519,278	-455,01	489,219	-52,459	-213,28	-267,819	668,109	342,367
Emergency stop										
		type	Fx[N]	Fy[N]	Fz[N]	Tx[Nm]	Ty[Nm]	Tz[Nm]	Fr[N]	Tr[Nm]
	section_4	Tr[Nm]	582,515	4888,29	4745,8	-6808,15	2680,83	1739,6	4922,87	7316,95
	section_4	Fx[N]	-3227,64	-340,002	1817,33	-248,721	-2894,33	-979,667	3704,1	1010,75
	section_4	Fy[N]	1137,8	-3042,25	1678,26	1651,07	286,54	-1248,63	2027,59	2070,05
	section_4	Fz[N]	-831,315	-1471,26	4216,8	-2306,6	-1548,91	-1268,26	4297,97	2632,28
	section_4	Tx[Nm]	1096,08	2786,06	1255,84	-4973,66	2003,71	1755,34	1666,89	5274,32
	section_4	Ty[Nm]	19,7819	501,573	2730,66	-128,582	-4240,28	1243,49	2730,73	1250,12
	section_4	Tz[Nm]	-110,496	-1995,53	1855,56	-8,6463	-2675,26	-3366,97	1858,84	3366,98
	section_4	Fr[N]	-1752,55	-1241,45	4134,11	-1675,85	-2211,71	-1554,65	4490,25	2285,92
Section 5										
Normal operation										
		type	Fx[N]	Fy[N]	Fz[N]	Tx[Nm]	Ty[Nm]	Tz[Nm]	Fr[N]	Tr[Nm]
	Section 5	Fx[N]	-782,685	-78,0993	-8,39761	20,6851	-194,003	-30,2303	78,5495	196,344
	Section 5	Fy[N]	-129,341	737,041	-207,929	208,868	29,7733	8,42454	765,81	30,9422
	Section 5	Fz[N]	56,5174	30,5331	-838,178	-193,081	215,168	9,58044	838,734	215,381
	Section 5	Tx[Nm]	-182,334	-478,68	-619,244	-266,734	117,14	-37,7358	782,686	123,068
	Section 5	Ty[Nm]	-47,571	149,56	-738,599	-108,639	272,252	66,3163	753,59	280,213
	Section 5	Tz[Nm]	-588,586	442,958	-174,424	-15,9845	93,4072	264,283	476,062	280,305
	Section 5	Fr[N]	56,5174	30,5331	-838,178	-193,081	215,168	9,58044	838,734	215,381
	Section 5	Tr[Nm]	-588,586	442,958	-174,424	-15,9845	93,4072	264,283	476,062	280,305
Emergency stop										
		type	Fx[N]	Fy[N]	Fz[N]	Tx[Nm]	Ty[Nm]	Tz[Nm]	Fr[N]	Tr[Nm]
	Section 5	Fx[N]	-2232,04	-56,4673	211,435	-6,13234	443,514	-396,775	218,846	595,092
	Section 5	Fy[N]	752,756	-2423,88	10,687	659,939	168,765	-744,793	2423,9	763,674
	Section 5	Fz[N]	4,19043	-380,644	-2775,19	-331,075	1006,2	31,9283	2801,17	1006,71
	Section 5	Tx[Nm]	-1048,34	-1718,14	-1090,61	-818,806	179,162	256,378	2035,05	312,776
	Section 5	Ty[Nm]	1060,78	87,1571	-2533,42	350,943	1067,71	31,3489	2534,92	1068,17
	Section 5	Tz[Nm]	-1753,82	1463,09	-80,5231	-154,406	-52,4612	857,287	1465,31	858,89
	Section 5	Fr[N]	4,19043	-380,644	-2775,19	-331,075	1006,2	31,9283	2801,17	1006,71
	Section 5	Tr[Nm]	1060,78	87,1571	-2533,42	350,943	1067,71	31,3489	2534,92	1068,17

Section 6											
Normal operation											
		type	Fx[N]	Fy[N]	Fz[N]	Tx[Nm]	Ty[Nm]	Tz[Nm]	Fr[N]	Tr[Nm]	
	section_6	Fx[N]	-544,037	6,91086	-154,546	-1,30181	-49,394	5,47204	154,7	49,6961	
	section_6	Fy[N]	28,2232	610,479	25,3235	75,979	-10,4889	151,499	611,004	151,862	
	section_6	Fz[N]	-281,347	44,5758	-604,249	-66,0255	185,29	41,1384	605,891	189,802	
	section_6	Tx[Nm]	-276,441	165,065	-561,202	-88,7898	128,666	86,8027	584,973	155,209	
	section_6	Ty[Nm]	-281,347	44,5758	-604,249	-66,0255	185,29	41,1384	605,891	189,802	
	section_6	Tz[Nm]	28,2232	610,479	25,3235	75,979	-10,4889	151,499	611,004	151,862	
	section_6	Fr[N]	47,0016	157,487	-592,249	-77,7107	152,228	32,9931	612,83	155,763	
	section_6	Tr[Nm]	-281,347	44,5758	-604,249	-66,0255	185,29	41,1384	605,891	189,802	
Emergency stop											
		type	Fx[N]	Fy[N]	Fz[N]	Tx[Nm]	Ty[Nm]	Tz[Nm]	Fr[N]	Tr[Nm]	
	section_6	Fx[N]	-1522,34	-189,916	-1008,58	-45,1031	513,048	-54,3669	1026,3	515,921	
	section_6	Fy[N]	-13,3922	-2101,57	-650,602	335,043	122,348	-497,296	2199,97	512,125	
	section_6	Fz[N]	-624,626	-104,475	-2212,57	153,707	615,498	-152,53	2215,03	634,116	
	section_6	Tx[Nm]	-12,9185	-2065,58	-806,515	339,019	164,391	-491,802	2217,45	518,549	
	section_6	Ty[Nm]	-1189,87	322,001	-1823,92	-6,24363	630,895	184,324	1852,13	657,27	
	section_6	Tz[Nm]	-847,304	1698,32	-1075,02	-279,005	139,871	526,707	2009,96	544,963	
	section_6	Fr[N]	727,046	1084,91	1963,01	-304,829	-437,426	408,4	2242,87	598,441	
	section_6	Tr[Nm]	-1189,87	322,001	-1823,92	-6,24363	630,895	184,324	1852,13	657,27	



# **Appendix H**

## **Material Standard for AM**

EOS StainlessSteel 316L  
Material Data Sheet

# EOS StainlessSteel 316L

EOS StainlessSteel 316L is a high performance marine-grade austenitic stainless steel that is molybdenum alloyed for enhanced corrosion resistance in chloride environments. 316L is a standard material for numerous applications in process, energy, paper, transportation and other industries.

## Main Characteristics:

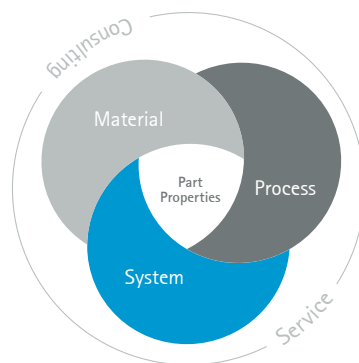
- High ductility and toughness
- High strength
- High corrosion resistance

## Typical Applications:

- Chemical industry
- Food processing
- Medical devices

## The EOS Quality Triangle

EOS uses an approach that is unique in the AM industry, taking each of the three central technical elements of the production process into account: the system, the material and the process – together simply described as the Quality Triangle. EOS focuses on delivering reproducible part properties for the customer.



All of the data stated in this material data sheet is produced according to EOS Quality Management System and international standards.

## Powder Properties

The chemical composition of EOS StainlessSteel 316L corresponds to ASTM F138 material standard for Surgical Implants (UNS S31673).

### Powder chemical composition (wt.-%)

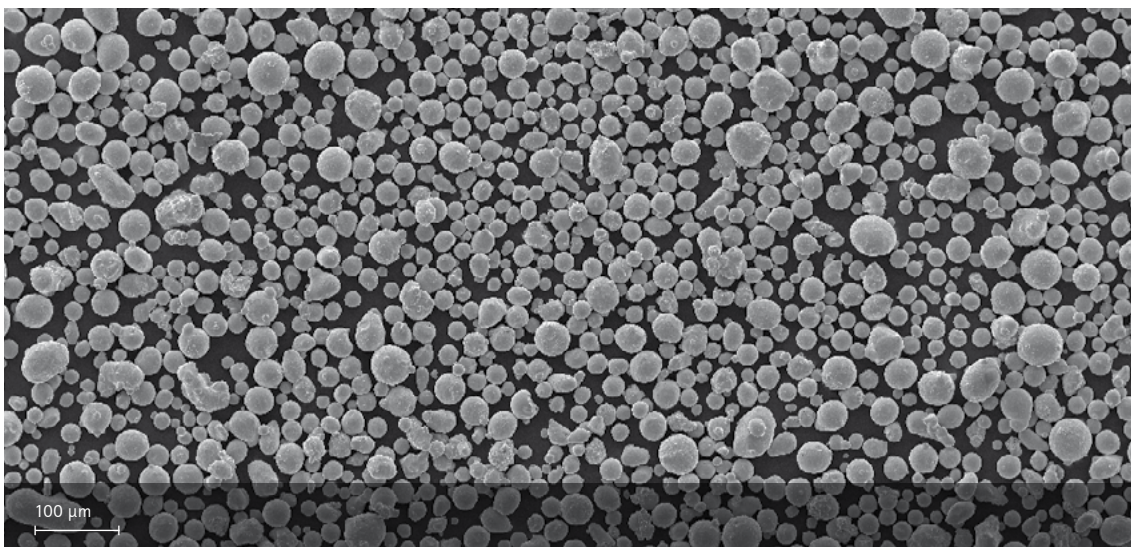
Element	Min.	Max.
Fe	Balance	
Cr	17.00	19.00
Ni	13.00	15.00
Mo	2.25	3.00
C	-	0.03
N	-	0.10

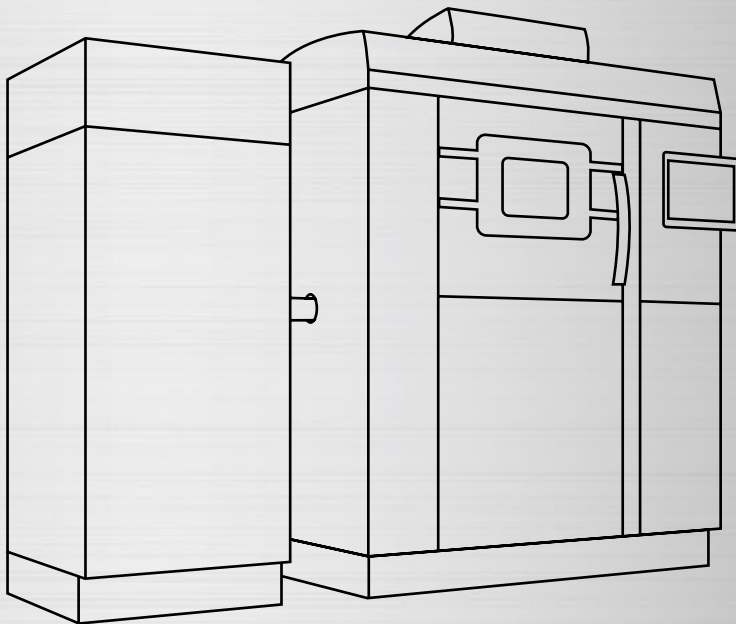
### Powder particle size

Generic particle size distribution

20 – 65  $\mu\text{m}$

*SEM picture of EOS StainlessSteel 316L powder.*





## EOS StainlessSteel 316L for EOS M 290 | 20 $\mu\text{m}$

Process Information

Chemical and Physical Part Properties

Heat Treatment

Mechanical Properties

Additional Data

## EOS StainlessSteel 316L for EOS M 290 | 20 µm

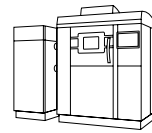
### Process Information

This process product is optimized for robustly building parts with EOS M 290 system using EOS StainlessSteel 316L. The mechanical properties have been validated to TRL8 level.

System set-up	EOS M 290
EOS ParameterSet	316L 20µm Surface M290/400W
EOSPAR name	316L_Surface_1.X
Software requirements	EOSPRINT 2.7 or newer EOSYSTEM 2.11 or newer
Powder part no.	9011-0032
Recoater blade	EOS HSS blade
Nozzle	Standard nozzle
Inert gas	Argon
Sieve	63 µm

#### Additional information

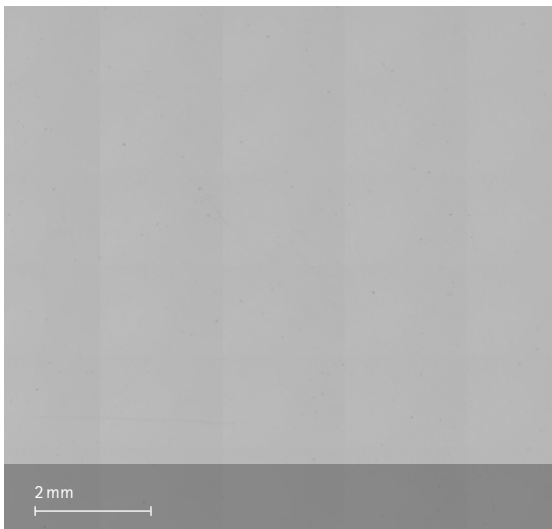
Layer thickness	20 µm
Min. wall thickness	0.3 - 0.4 mm
Typical dimensional change after HT	+0.02 %
Volume rate	2.0 mm <sup>3</sup> /s



## Chemical and Physical Properties of Parts

Chemical composition of built parts is compliant to EOS StainlessSteel 316L powder chemical composition.

Micrograph of polished surface



Microstructure solution annealed  
Etched with etchant Kallings 2



Defects	Result	Number of samples
Average defect percentage	0.018 %	45
Density, ISO3369	Result	Number of samples
Average density	$\geq 7.97 \text{ g/cm}^3$	45

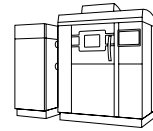
## Heat Treatment

Heat treatment according to AMS 2759 is optional.

Stress relief: Hold temperature 900 °C, hold time minimum 2 h when thoroughly heated, water quenching

Solution annealing: Hold temperature 1 150 °C, hold time minimum 1.5 h when thoroughly heated, water quenching

## Mechanical Properties as manufactured



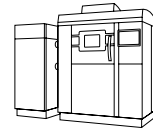
Mechanical properties ISO6892-1

	Yield strength $R_{p0.2}$ [MPa]	Tensile strength $R_m$ [MPa]	Elongation at break A [%]	Number of samples
Vertical	470	540	54	189
Horizontal	530	640	40	162

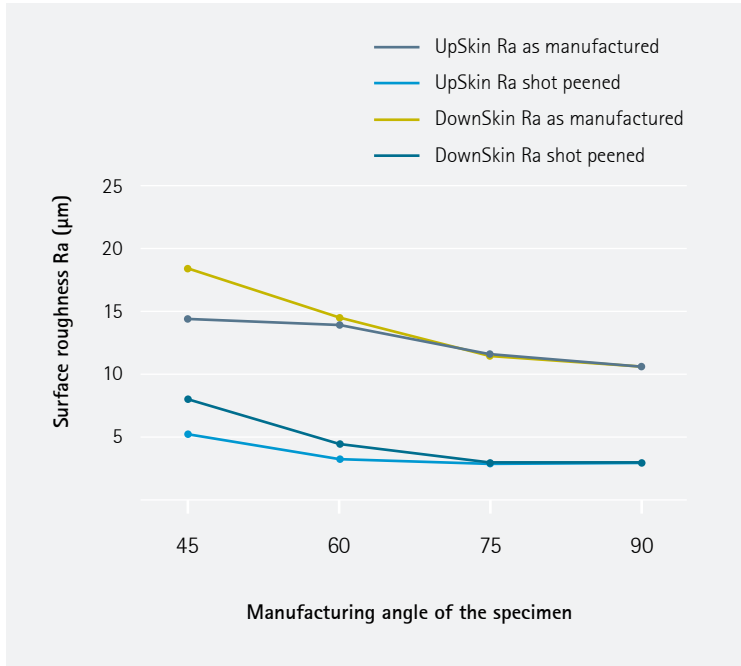




## Additional Data



### Surface Roughness



### Coefficient of Thermal Expansion ASTM E228

Temperature	25-100 °C	25-200 °C	25-300 °C	25-400 °C
CTE	15.72 *10 <sup>-6</sup> /K	16.75 *10 <sup>-6</sup> /K	17.27 *10 <sup>-6</sup> /K	17.70 *10 <sup>-6</sup> /K

# 316L Stainless Steel



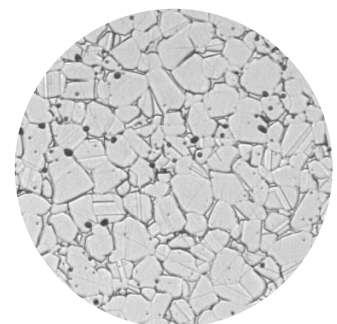
## Typical Material Properties

Material Properties	Test Method	316L
<b>Tensile Strength</b>		
Ultimate Strength	ASTM E8	X & Y: 450 - 580 MPa Z: 450 - 520 MPa
Yield Strength (0.2% offset)		X & Y: 140 - 220 MPa Z: 140 - 220 MPa
Elongation		X & Y: 40 - 55% Z: 40 - 50%
Elastic Modulus		X & Y: 190 - 220 GPa Z: 180 - 190 GPa
Hardness	ASTM E18	67 - 71 HRB
Impact	ASTM E23	55 - 75 J
Poisson's Ratio		0.28 - 0.30
Relative Density		96 - 99%
Density		7.6 - 7.9 g/cc
Surface Roughness		3 - 12 $\mu\text{m Ra}$



316L Printed Part

Material Composition			
Iron	bal	Molybdenum	2-3%
Nickel	10-14%	Manganese	2.0% max
Chromium	16-18%	Silicon	1.0% max
Carbon	0.03% max		

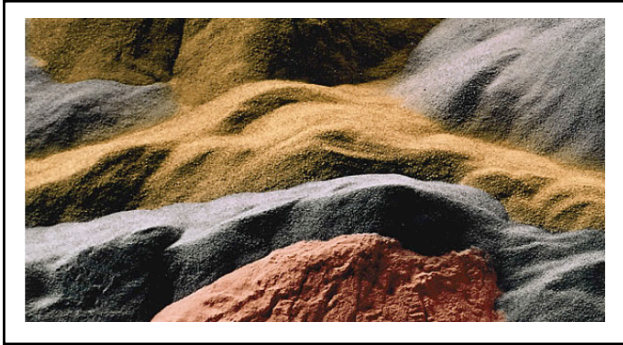


Microstructure

ExOne disclaims all warranties and liabilities for the content hereof and makes no representations as to its accuracy or fitness for use for any purpose. Any tradenames, trademarks, or service marks of others appearing herein are used strictly nominatively and are not to be construed as implying any affiliation, connection, association, sponsorship, or approval of the owners thereof for ExOne, its products, or the content hereof.



## LENS<sup>®</sup> MATERIALS FAQs



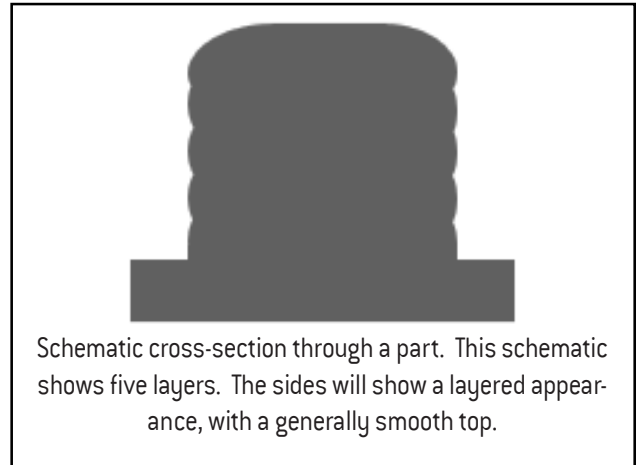
LENS systems process common engineering materials such as stainless steels, tool steels, titanium alloys, and cobalt alloys. LENS technology can also process other materials including Zirconium, Tantalum, Tungsten, Aluminum, Bronze, refractory metals and some ceramics. These materials are available in powder form from a variety of commercial suppliers.

### Printing Features of LENS Systems:

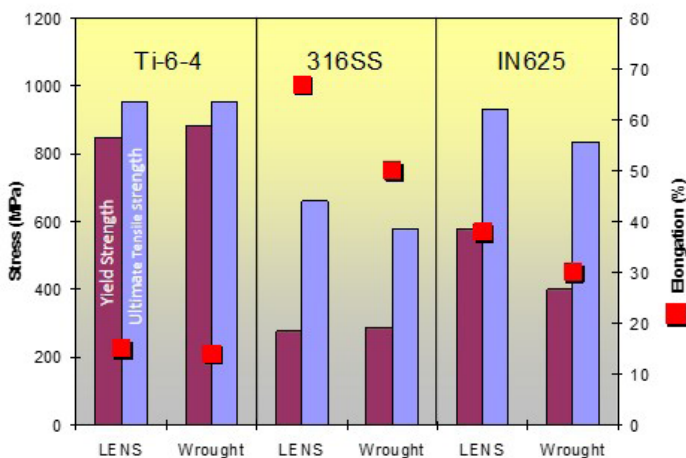
- Layer Thickness: 250 to 750 microns
- Melt Pool Diameter: 2,000 microns Typical
- Minimum Wall Thickness: 300 microns
- Deposition Rate Based on Laser Power: 2 kW = 0.5kg/hr.
- Surface Roughness: On the sides, 12- 25 microns Ra

### Printed Metal Properties

In general, the LENS process produces fully-dense material that has mechanical properties at least equal or better than cast material, and in some cases very similar to forged material.



Schematic cross-section through a part. This schematic shows five layers. The sides will show a layered appearance, with a generally smooth top.



### Powder Characteristics:

- **Size:** Powder particle size is -100/+325 mesh, equivalent to a powder diameter of 44 to 150 microns.
- **Shape:** Powder sufficiently spherical to flow.
- **Chemistry:** The LENS process does not alter powder chemistry.
- **Cleanliness:** Inert-Gas-Atomized or Plasma-Rotating-Electrode powders are normally of acceptable quality.

## MATERIALS FOR OPEN ATMOSPHERE

ALLOY CLASS	ALLOY
Stainless Steel	13-8
	17-4
	304
	316
	410
	420
	15-5PH
	AM 355
	309
	416
	420

ALLOY CLASS	ALLOY
Nickel	IN625
	IN718
	IN690
Copper	Pure Copper
	Bronze
	Cu-Ni
	GRCOP-84
Tool Steel	H13
	S7
	A-2
Cobalt	Stellite 6, 21
Carbide	Ni-WC
	Co-WC

## MATERIALS FOR CONTROLLED ATMOSPHERE

ALLOY CLASS	ALLOY
Titanium	CP-Ti
	Ti 6-4
	Ti 6-2-4-2
	Ti-6-2-4-6
	Ti-48-2-2
	Ti-22Al-23Nb
Ceramics	Alumina
Aluminum	4047

ALLOY CLASS	ALLOY
Nickel	Waspalloy
	Hastelloy X
	MarM 247
	Rene 41
	Rene 142
Refractories	W, Mo, Nb
Composites	TiC
	CrC

### ABOUT OPTOMEC

Optomec® is a privately-held, rapidly growing supplier of Additive Manufacturing systems. Optomec's patented Aerosol Jet Systems for printed electronics and LENS 3D Printers for metal components are used by industry to reduce product cost and improve performance. Together, these unique printing solutions work with the broadest spectrum of functional materials, ranging from electronic inks to structural metals and even biological matter. Optomec has more than 300 marquee customers around the world, targeting production applications in the Electronics, Energy, Life Sciences and Aerospace industries. For more information about Optomec, visit <http://www.optomec.com>.

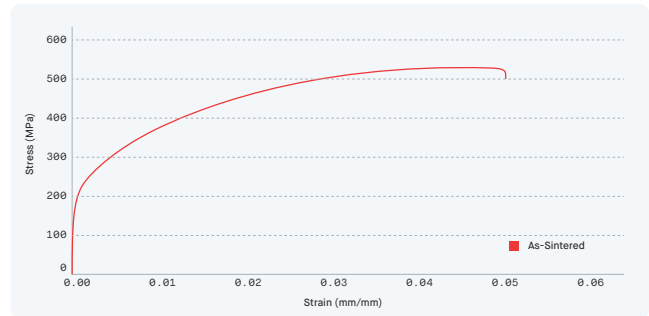


Optomec Inc.  
3911 Singer Blvd. NE  
Albuquerque, NM 87109 USA

Tel: 505-761-8250  
Fax: 505-761-6638  
E-mail: [sales@optomec.com](mailto:sales@optomec.com)

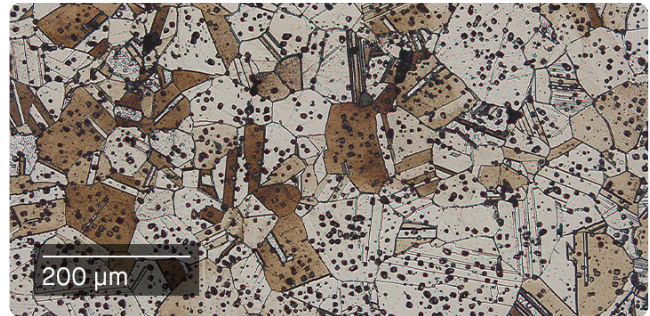
[Material Data Sheet]

# 316L v.2 Stainless Steel



**COMPOSITION %**

Fe	bal
Ni	10 - 14
Cr	16 - 18
Mo	2 - 3
Mn	2.0 (max)
Si	1.0 (max)
C	0.03 (max)



**MECHANICAL PROPERTIES**

	Standard	Studio System™ 2 As-Sintered	MIM - MPIF 35 Min As-Sintered	Wrought For reference
Ultimate tensile strength (MPa)	ASTM E8M	<b>533</b>	450	425
Yield strength (MPa)	ASTM E8M	<b>169</b>	140	170
Elongation (%)	ASTM E8M	<b>66</b>	40	40
Hardness (HRB)	ASTM E18	<b>66</b>	67 (typ)	95 (max)
Density (relative)	ASTM B311	<b>97%</b>	95%	100%

**PERFORMANCE**

	Standard	Studio System™ 2 As-Sintered
Boil test (corrosion)	ASTM F1089	<b>Pass</b>
Copper sulfate test (corrosion)	ASTM F1089	<b>Pass</b>

**OTHER STANDARD DESIGNATIONS**

UNS S31603  
EN 1.4404

- Per MPIF Standard 35, Materials Standards for Metal Injection Molded Parts (MPIF 35-MIM, 2018).
- Wrought values based on ASTM A240 standards.
- Prior to corrosion resistance testing, all test samples were machined and passivated in accordance with ASTM F1089.
- Listed designations are for reference purposes only. Composition and mechanical properties may vary.

End-use material performance is impacted (+/-) by certain factors including but not limited to part geometry and design, application and evaluation conditions, etc. Tensile properties and density data reported are mean values minus 1 sigma.

Due to the material's high elongation, strain values were obtained from crosshead displacement. In conformance with ASTM E8M, total elongation was obtained from scribed marks on the gage length and yield strength was calculated from extensometer measurements.